CORROSION SUSCEPTIBILITY OF CONCRETE EXPOSED TO A MARINE ENVIRONMENT

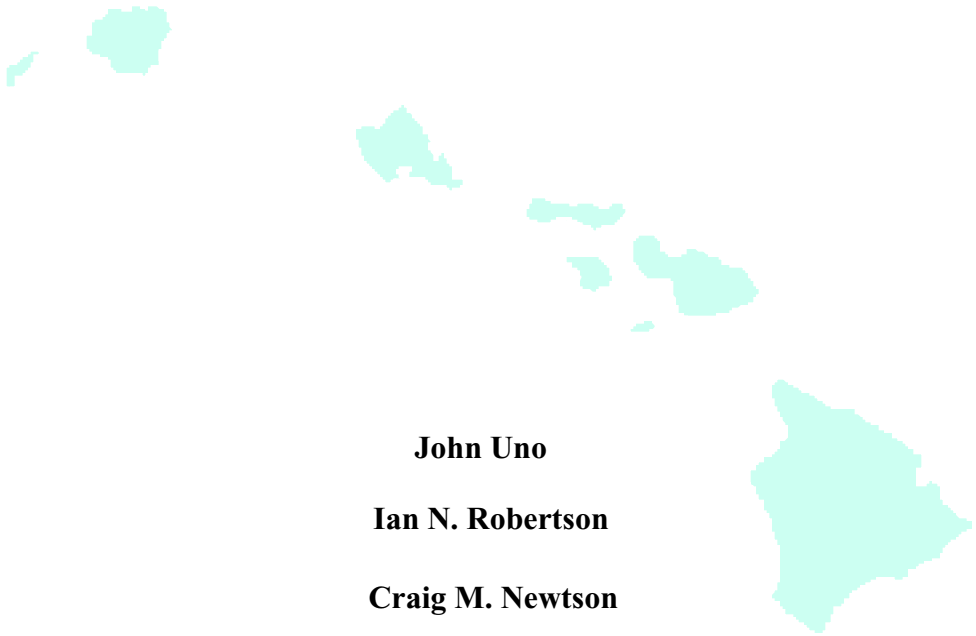

John Uno

Ian N. Robertson

Craig M. Newtson

Prepared in cooperation with the State of Hawaii Department of Transportation, Highways Division and U.S. Department of Transportation, Federal Highway Administration

UNIVERSITY OF HAWAII
COLLEGE OF ENGINEERING

DEPARTMENT OF CIVIL AND ENVIRONMENTAL ENGINEERING

Research Report UHM/CEE/04-09

December 2004

CORROSION SUSCEPTIBILITY OF CONCRETE EXPOSED TO A MARINE ENVIRONMENT

John Uno
Ian N. Robertson
Craig M. Newtson

Prepared in cooperation with the:

State of Hawaii
Department of Transportation
Highways Division
and
U.S. Department of Transportation
Federal Highway Administration

Research Report UHM/CEE/04-09
December 2004

ACKNOWLEDGEMENTS

This report is based on a Master of Science thesis prepared by John Uno under the direction of Dr. Ian Robertson of the Department of Civil and Environmental Engineering at the University of Hawaii at Manoa, and Dr. Craig Newtson of the Department of Civil and Environmental Engineering at New Mexico State University.

The authors acknowledge the considerable contributions made by The State of Hawaii Department of Transportation (HDOT), Ameron Hawaii, and Hawaiian Cement during this project. Funding for this project was provided by the HDOT. Aggregates and other constituents for the concrete mixtures were donated by Ameron Hawaii and Hawaiian Cement.

The authors are also grateful to Drs. Gregor Fischer and Si-Hwan Park for reviewing this report and providing valuable suggestions. Special thanks are also extended to laboratory technicians Andrew Oshita and Miles Wagner for their technical assistance. Appreciation is also extended to Grant Okunaga, Donn Kakuda, and Gaur Johnson for their help during fabrication and testing in the Structures Laboratory.

ABSTRACT

A study was conducted to evaluate the chloride concentrations of reinforced concrete panels placed in a marine environment and compare their performance to reinforced concrete specimens exposed to cyclic laboratory simulated marine conditions. The panels and specimens were proportioned using corrosion-inhibiting admixtures intended to slow the corrosion process. The corrosion-inhibiting admixtures included Darex Corrosion Inhibitor (DCI), Rheocrete CNI, Rheocrete 222+, FerroGard 901, Xypex Admix C-2000, latex, fly ash, silica fume, and Kryton KIM. The mixtures used to fabricate the field panels were based on the mixtures for the corresponding laboratory specimens. Relevant properties of the field panels are reported, including compressive strength, elastic modulus, Poisson's ratio, pH, air permeability, and half-cell potential. On average, based on chloride concentrations at 1.0 in. (25 mm), approximately 1.2 laboratory simulated cycles were equivalent to one year of field exposure for the control, DCI, FerroGard 901 and latex-modified panels. An average of 2.4 laboratory simulated cycles was equal to one year of field exposure for the silica fume panels. The chloride concentrations at various depths in the panel cover concrete were also predicted using the computer program Life-365. In most cases, the default values assumed by this program over-predicted the chloride concentrations in the panel concrete. Modified parameters are suggested to improve these predictions.

TABLE OF CONTENTS

LIST OF TABLES

LIST OF FIGURES

CHAPTER 1
INTRODUCTION

1.1 Introduction

Reinforced concrete is one of the most widely used construction materials because of its strength and durability. However, when reinforced concrete structures are exposed to a marine environment, deterioration can occur much quicker than normal. According to ACI Committee 222 (2003), approximately 173,000 bridges on the interstate highway system in the United States are structurally deficient or functionally obsolete, in part due to deterioration caused by corrosion of reinforcing steel. In 1998, a study by the Federal Highway Administration (FHWA 2001) estimated that the U.S. alone spent approximately 276 billion dollars on costs directly related to corrosion. These expenses demonstrate the necessity for cost-effective corrosion protection in reinforced concrete structures.

There are several methods used to prevent or decelerate the corrosion process. The methods include protective coatings, corrosion-resistant alloys, corrosion-inhibiting admixtures, engineering plastics and polymers, and cathodic and anodic protection. Of the aforementioned methods, corrosion-inhibiting admixtures were one of the most cost-effective solutions (FHWA 2001).

This report covers Phase III of a study on concrete durability. Phase I of the study evaluated the effectiveness of corrosion-inhibiting admixtures used in various piers at harbor facilities on the island of Oahu (Bola and Newtson 2000). Field evaluation procedures were conducted on-site to determine properties of the concrete and the extent of corrosion. The tests included pH, permeability, half-cell potential, linear polarization

resistance, and resistivity. Cores were also taken from each site to test the mechanical properties of the concrete and the chloride concentration at various depths below the concrete surface.

Phase II was an accelerated corrosion study, which involved cyclic testing of hundreds of specimens using 70 different concrete mixtures according to ASTM G 109 (Okunaga and Robertson 2004). Plastic dams were placed on the specimens and sealed with silicone glue. A salt-water solution was then poured into each plastic dam and left for two weeks. Voltage tests were taken one week after the salt-water solution was poured into the plastic dam. After two weeks of ponding, the plastic dams were removed and the specimens were allowed to dry for two weeks. Two weeks of the wet condition and two weeks of drying completed one ponding cycle. At the end of each cycle, tests were conducted to determine the corrosion activity of each specimen. The tests included half-cell potential, linear polarization, and resistivity. Chloride concentration, pH, and air permeability tests were performed on specimens following corrosion failure. These specimens were stored in the basement of the structures laboratory at Holmes Hall, where temperature and relative humidity are relatively constant at 73º F (27.8ºC) and 54%, respectively.

Phase III of the study involves the fabrication and deployment of twenty-five reinforced concrete field panels located at Pier 38 in Honolulu Harbor. Each field panel utilized one of the corrosion inhibiting admixtures evaluated in the Phase II study. Field tests on the panels included air permeability and half-cell potential. Laboratory tests on dust samples collected from each panel included chloride concentration and pH. The panels will be monitored continuously for five years.

1.2 Objective

The objective of this research was to investigate the effects of chloride concentrations in reinforced concrete specimens exposed to marine conditions and compare them to specimens exposed to accelerated laboratory corrosion testing. An effort will be made to develop a relationship between the time of exposure to field conditions and the number of cycles under laboratory conditions. Other properties of the concrete that were investigated include compressive strength, elastic modulus, Poisson's ratio, pH, air permeability, and half-cell potential. The corrosion inhibiting admixtures used in this study were DAREX Corrosion Inhibitor (DCI), Rheocrete CNI, Rheocrete 222+, FerroGard 901, Xypex Admix C-2000, latex modifier, silica fume, fly ash, and Kryton KIM. Thirteen different mixture designs were selected for Phase III based on results of Phase II of the study, reported by Pham and Newtson (2001) and Okunaga and Robertson (2004).

1.3 Scope

This report outlines the initiation of Phase III of this study. Chapter 2 provides information on the mechanisms of corrosion, the influence of chloride on corrosion, and chloride penetration. The concrete admixtures are introduced and their methodologies for protecting the reinforcing steel from corrosion are described. Descriptions are also given for all the tests performed in this study. Chapter 3 presents the materials, proportions, and experimental procedures for all the concrete mixtures. The fabrication of each field

panel is also described. The results from all the tests performed on the field panels are provided in Chapter 4. Chapter 5 provides a comparison of the chloride concentration results obtained from Phases II and III. Chapter 6 presents recommendations for improving the predictions calculated using the computer program Life-365. And finally, a summary of the entire study and conclusions drawn are presented in Chapter 7.

CHAPTER 2
BACKGROUND AND LITERATURE REVIEW

2.1 Introduction

Corrosion of the reinforcing steel in concrete is one of the main problems associated with structural deterioration in marine environments. One of the methods used to alleviate this problem is the addition of corrosion inhibiting admixtures to concrete mixtures. This chapter describes the principles and mechanisms of the corrosion process, the influence of chloride ions on corrosion, chloride penetration, and the corrosion-inhibiting admixtures used and their effects on the properties of concrete. A brief synopsis of the various tests used to determine slump, air entrainment, mechanical properties, chloride concentration, pH, air permeability, and half-cell potential is presented. A discussion is also provided for the computer program Life-365 used to predict service lives for the various concrete mixtures.

2.2 Mechanisms of corrosion of steel in concrete

Corrosion in reinforced concrete is an electrochemical process that involves the transfer of electrically charged ions between the anode and cathode through the pore fluid of the concrete (Al-Tayyib and Khan 1988). Reinforcing steel can also corrode by chemical means, such as an acid attack. However, electrochemical corrosion is the most common form in reinforced concrete structures (ACI Committee 222 1989).

The principles of electrochemical corrosion for a basic corrosion cell require the same components as the electrolytic cell, which must be established for corrosion to occur (Fraczek 1987). The components that encompass the electrolytic cell include the

anode, the cathode, and an electrolyte. In order for corrosion to occur, both the anode and cathode must be connected in a manner that permits electron flow.

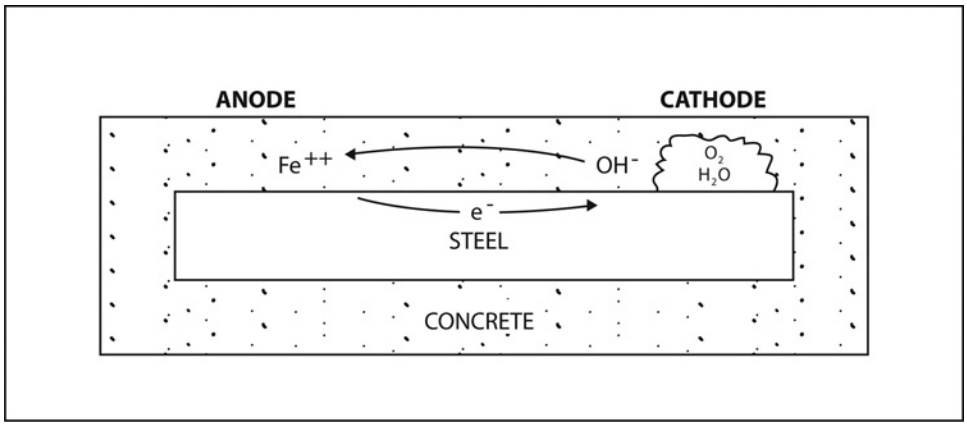

Figure 2.1. Corrosion cell in reinforced concrete (Hime and Erlin 1987).

The electrochemical process of corrosion involves oxidation at the anode and reduction at the cathode. The site where the reinforcing steel corrodes is called the anode (Hime and Erlin 1987). Metallic iron (Fe) from the steel is oxidized to produce ferrous ions and electrons are released according to Equation 2.1.

Anodic Reaction: $Fe \leftrightarrow Fe^{2+} + 2e^{-}$ (2.1)

The positively charged ions are called cations, and negatively charged ions are anions (Hime and Erlin 1987).

In order to maintain equilibrium of charges, an electrochemical reduction occurs at the cathode (Al-Tayyib and Khan 1988). In an acidic medium, the reaction taking place at the cathode is the reduction of hydrogen ions to hydrogen. However, concrete is highly basic (pH > 12-12.5) and usually has a sufficient supply of oxygen. The resulting

cathodic reaction combines oxygen and water to form hydroxyl ions, as displayed in Equation 2.2.

$$\text{Cathodic Reaction:} \quad O_2 + 2H_2O + 4e^- \leftrightarrow 4(OH)^- \tag{2.2}$$

The current that drives both the anodic and cathodic reactions flows through a medium termed the electrolyte. The electrolyte conducts current primarily through ionic diffusion, and must have a specific minimum ion content and a minimum water content to allow the flow of ions (Fraczek 1987). In the case of corrosion of reinforcing steel, the pore water in hardened concrete acts as the electrolyte.

The combination of the anode and cathode processes results in the equation that transforms the metallic iron (Fe) into iron hydroxides (rust).

$$Fe + \tfrac{1}{2}O_2 + H_2O + 2e^- \leftrightarrow Fe^{2+} + 2(OH)^- + 2e^- \tag{2.3}$$

Equation 2.3 simplifies to equation 2.4 as follows.

$$Fe + \tfrac{1}{2}O_2 + H_2O \leftrightarrow Fe^{2+} + 2(OH)^- \tag{2.4}$$

The Fe^{2+} cation combines with the hydroxyl ions [$(OH)^-$] to form a fairly soluble ferrous hydroxide, $Fe(OH)_2$, which is rust that possesses a whitish appearance. The reaction is shown in Equation 2.5. With sufficient oxygen, $Fe(OH)_2$ is further oxidized to

form $Fe(OH)_3$, which is the more common form of rust that has a reddish brown appearance.

$$Fe^{2+} + 2(OH)^- \leftrightarrow Fe(OH)_2 \quad (2.5)$$

For the transformation of metallic iron to rust to occur, all three of the following conditions must take place. Iron must be available in a metallic state at the surface of reinforcing steel during the anode process, oxygen and moisture must be available during the cathode process, and the electrical resistivity of concrete must be low to facilitate electron flow through the metal from anodic to cathodic areas (Mehta 1991).

2.3 Influence of chloride ions on corrosion

It has been recognized for many years that chloride ions play a major role in the corrosion of reinforcing steel in concrete. Most researchers agree that the chloride ion acts as an essential catalyst to the corrosion process (Fraczek 1987). However, many corrosion scientists do not agree on the mechanism for the depassivation reactions involving chloride ions.

According to ACI Committee 222 (1989), there are three modern theories that describe the effect that chloride ions have on the corrosion of reinforcing steel. The first theory is The Oxide Film Theory, which states that an oxide film on the metal surface is responsible for passivity, which provides protection against corrosion. The theory presumes that chloride ions penetrate the oxide film on the steel surface through pores or

defects in the film easier than other ions (e.g., SO_4^-). The chloride ions may also disperse the oxide film, making it easier to penetrate.

The second theory is The Adsorption Theory. It claims that chloride ions are adsorbed on the metal surface in competition with dissolved oxygen, O_2, or hydroxyl ions. The chloride ion facilitates hydration of the metal ions, which then advances the dissolution of the metal ions.

The third theory is The Transitory Complex Theory, which states that chloride ions compete with hydroxyl ions for the ferrous ions produced by corrosion. A soluble complex of iron chlorides forms which can diffuse away from the anode, destroying the protective layer of $Fe(OH)_2$. The disestablishment of the protective layer allows the corrosion process to continue.

Because the protective layer of $Fe(OH)_2$ is destroyed, iron ions continue to move into the concrete away from the site of corrosion. The iron ions react with oxygen to form higher oxides that result in a fourfold volume increase. As a result, internal stress is created and cracks in the concrete are formed. Iron chloride complexes can also be formed, which can lead to additional disruptive forces.

2.4 Chloride penetration

Chloride ions must first penetrate the concrete cover for any chloride-induced corrosion to occur. The porous microstructure of concrete created by the space between cement grains and aggregates constituents allows the transport of chlorides. However, if the pores of the concrete are saturated and the concrete element is thick, chloride

diffusion will be the main transport process. Chloride diffusion is the movement of chloride ions as a result of a concentration gradient (Yokota and Buenfeld 2004).

Concrete exposed near the top of the tidal zone experiences chloride-induced corrosion much quicker than when it is fully submerged (Yokota and Buenfeld 2004). While in the splash and tidal zones, concrete is wetted and then spends time drying. During the drying period, water that splashes onto the concrete is drawn in by capillary forces. This water absorption, along with the availability of oxygen required to sustain a significant corrosion rate, can lead to rapid chloride penetration in comparison to chloride diffusion (Yokota and Buenfeld 2004).

2.5 Corrosion-inhibiting admixtures

The admixtures DAREX Corrosion Inhibitor (DCI), Rheocrete CNI, Rheocrete 222+, FerroGard 901, Xypex Admix C-2000, latex, fly ash, silica fume, and Kryton KIM were added to the concrete mixtures for this study. These admixtures were chosen based on results from Phase II of this research study. The following sections provide a brief description of each admixture and the effects on the properties of concrete.

2.5.1 Calcium nitrite-based corrosion inhibitors

DAREX Corrosion Inhibitor (DCI), a product of W.R. Grace & Co., and Rheocrete CNI, a product of Master Builders, Inc., are both calcium nitrite-based corrosion-inhibitors that contain a minimum of 30% calcium nitrite by mass. A calcium nitrite-based corrosion-inhibitor performs two functions when used in concrete as an

admixture. It acts as a corrosion inhibitor by providing effective protection against chlorides and acts as a non-chloride accelerator (Master Builders, Inc. 2002). The level of corrosion protection increases in proportion to the dosage amount (Grace Construction Products 2003). Both admixtures also meet the requirements for ASTM C 494 as a type C accelerating admixture. Retarding or hydration control admixtures can be combined with calcium nitrite-based corrosion-inhibitors to reduce the accelerating effects.

Calcium nitrite-based corrosion inhibitors delay corrosion by preventing susceptible ferrous oxide ions in the passive layer from combining with chloride ions. The combination of ferrous and chloride ions forms a ferrous chloride complex (rust) that can initiate corrosion on the reinforcing steel. As corrosion progresses, the chloride ions continue to react with freshly exposed ferrous ions. If untreated, the natural passive ferric oxide layer on the surface of the reinforcing steel deteriorates, leading to cracking, spalling, and ultimately failure of the concrete (Master Builders, Inc. 2002).

In order for the calcium nitrate-based corrosion inhibitor to be effective, nitrite ions from the calcium nitrite must compete with chloride ions to react with the ferrous ions. Available nitrite ions surround defective ferrous oxide ions and combine to produce a ferric ion that is less susceptible to corrosion. The resulting oxidation reaction reestablishes the passive layer between the chlorides that initiate corrosion on the reinforcing steel.

2.5.2 Rheocrete 222+

Rheocrete 222+, a product of Master Builders, Inc., is an organic corrosion-inhibiting admixture (OCIA). The admixture is a combination of amines and esters in a

water medium (Master Builders, Inc. 2002). Rheocrete 222+ is dispersed consistently throughout the concrete matrix during the mixing process and becomes part of the cement paste (Nmai et al. 1992).

After the placement of concrete is complete, the admixture is physically and/or chemically adsorbed onto the surface of the reinforcing steel and a protective film is formed. The protective film reduces the vulnerability of the steel to chloride ion diffusion. The film also enhances the natural passive layer on the steel surface by providing additional resistance to the intrusion of chloride ions. Unlike calcium nitrite-based corrosion inhibitors, the organic corrosion inhibitor does not compete with chloride ions to maintain the natural passive layer near the surface of the reinforcing steel.

Organic corrosion inhibiting admixtures have insignificant effects on most of the plastic and hardened properties of concrete. There are marginal effects on compressive strength, but the elastic modulus and other stress-strain properties are unaffected (Nmai et al. 1992). Additional amounts of air-entraining admixture may be required to achieve a given air content.

2.5.3 FerroGard 901

FerroGard 901 is a liquid concrete admixture used for protecting reinforcing steel in concrete. It is a combination of organic and inorganic inhibitors that act as corrosion-proofing for reinforcing steel embedded in concrete. FerroGard 901 reacts to both the anodic and cathodic reactions of the steel electrochemical corrosion process. During placement of concrete, the admixture migrates to the reinforcing steel and develops a passivating film on the surface (cathode). The admixture also prevents steel from

decomposing by developing strong molecular bonds (anode) (Sika Corporation 1998). FerroGard 901 acts as a corrosion-preventing agent specifically against chloride attacks. The manufacturer also claims that it does not impair the properties of fresh or cured concrete.

2.5.4 Xypex Admix C-2000

Xypex Admix C-2000 is a chemical treatment used for waterproofing, protection, and improvement of concrete. It consists of Portland cement and various active proprietary chemicals. The active chemicals react with the moisture in fresh concrete and with the by-products of cement hydration to cause a catalytic reaction that generates a non-soluble crystalline formation throughout the pores and capillary tracts of the concrete (Xypex Chemical Corporation 2002). The result is a permanent seal around the concrete that prevents the penetration of water and other liquids.

2.5.5 Latex

Latex is a colloidal suspension of polymer in water (Pham and Newtson 2001). It is added to conventional concrete mixtures to produce latex-modified concrete. Latex-modified mixtures provide improved properties of high strength, extensibility, adhesion, waterproofing, and durability (Ohama 1987). The admixture forms a continuous polymer film within the cement paste that reduces the permeability and increases the flexibility of the concrete. The reduced permeability modifies the pore structure of the concrete and increases the corrosion resistance of the concrete. The high flexibility provided by the

latex increases the tensile strength and ductility of the concrete, which reduces cracking (Pham and Newtson 2001). The reduced cracking also increases the corrosion resisting capabilities of the concrete. Latex-modified mixtures provide no improvement in compressive strength when compared with concrete designed without any admixtures (Ohama 1987).

2.5.6 Fly ash

Fly ash is a pozzolonic material that results from the combustion of pulverized coal in electric power generating plants. It is primarily silicate glass containing silica, alumina, iron, and calcium. Other minor constituents include magnesium, sulfur, sodium, potassium, and carbon.

There are two classes of fly ash used as pozzolonic admixtures in concrete. ASTM C 618 Class F fly ash generally contains low amounts of calcium (less than 10% CaO) with carbon contents ranging from as low as 5% to as high as 10%. ASTM C 618 Class C fly ash contains high levels of calcium (10% to 30% CaO) with carbon contents lower than 2%.

Fly ash particles are solid spheres with some hollow cenospheres. There are also plenospheres, which are spheres containing smaller spheres. The particle sizes vary from less than 3.94×10^{-5} in. (1 μm) to more than 3.94×10^{-3} in. (100 μm) with typical particles sizes under 7.87×10^{-4} in. (20μm). Only 10% to 30% of the particles by weight are larger than 1.77×10^{-3} in. (45 μm) (Kosmatka and Panarese 1994).

The use of fly ash will affect the freshly mixed properties of concrete. Additional air-entraining admixtures will be required to obtain a specific air content level. The

workability improves when compared to concretes of equal slump and strength. Fly ash will generally retard the setting time, and as a result, accelerating admixtures can be used to speed up the setting process.

Fly ash can affect the hardened properties of concrete when used as an admixture. It increases the density of concrete by filling the voids within the concrete matrix. The chloride permeability is also reduced which results in a lower potential for corrosion induced damage (Keck 2001). The compressive strength at early ages will be less than that of a mixture that did not contain fly ash because of the lower rate of hydration. However, decreasing the water-cement plus pozzolan ratio, increasing the amount of cement, or using an accelerating admixture can significantly increase long term compressive strength. Fly ash also reacts chemically with the calcium hydroxide released by the hydration of Portland cement to provide additional cementitious properties.

2.5.7 Silica fume

Silica fume is a pozzolonic admixture that is also referred to as condensed silica fume. It is the result of the reduction of high-purity quartz with coal in an electric arc furnace in the manufacture of silicon or ferrosilicon alloy. Condensed silica fume is also processed to control particle size and remove any impurities.

Silica fume is essentially silicon dioxide in a noncrystalline form. It is a very fine material with particle sizes less than $0.04x10^{-3}$ in. (1μm) in diameter and an average diameter of $0.04x10^{-4}$ in. (0.1μm) (Kosmatka and Panarese 1994). The particles of silica fume are about 100 times smaller than particles of cement. The miniscule size helps to reduce concrete permeability by filling the voids between cement particles.

When silica fume is used as an admixture in concrete, it reacts with water and calcium hydroxide $Ca(OH)_2$, a product of the hydration reaction of cement and water. The result is calcium silicate hydrate (CSH), which enhances the bonding between the constituents of the concrete matrix.

2.5.8 Kryton KIM

Kryton KIM (Krystol Internal Membrane) is a chemical admixture used for treatment of concrete to protect against water intrusion, leakage and cracking, and corrosion of reinforcing steel. KIM enhances the concrete's natural hydration process by intensifying and prolonging the hydration of cementitious materials (Kryton 2003). The capillary pores are reduced in both size and number and as a result the concrete becomes less porous. The KIM also fills the remaining pores and capillaries with millions of long, needle-like crystals throughout the concrete. As a result, the concrete becomes impermeable to the migration of water or water-borne chemicals (Kryton 2003).

2.6 Other admixtures

In addition to the aforementioned corrosion inhibiting admixtures, other admixtures were added to the concrete mixtures to provide increased workability, air entrainment, and set retarding. These admixtures were Daracem 19, Darex II AEA, and Daratard HC respectively. All three admixtures are manufactured by Grace Construction Products.

2.6.1 Daracem 19

Daracem 19 is a high-range water-reducing admixture (HRWRA), also referred to as a superplasticizer. The admixture is an aqueous solution of a modified naphthalene sulfonate and contains no chloride (Grace Construction Products 2002). The addition of Daracem 19 to the concrete mixture provides increased workability of concrete, particularly for concrete mixtures with low water-cement ratios at low or normal slumps.

2.6.2 Darex II AEA

Darex II AEA is an air-entraining admixture which provides protection against freezing and thawing, severe weathering, or deicer chemicals by generating a highly stable air void system (Grace Construction Products 2003). The admixture is a complex mixture of organic acid salts in an aqueous solution. Darex II AEA provides improved workability while minimizing bleeding, segregation, and green shrinkage.

2.6.3 Daratard HC

Daratard HC is a set-retarding admixture. It is used to allow the setting time of fresh concrete to be controlled or delayed. Controlling or delaying the set of fresh concrete allows added time for placing, vibrating, and finishing the concrete.

2.7 Testing

Various tests were performed to determine the slump and air entrainment of fresh concrete as well as the mechanical, chemical, and electrical properties of hardened concrete and the reinforcing steel. The mechanical tests performed in this study were used to evaluate the properties of concrete. These properties include compressive strength, elastic modulus, and Poisson's ratio. Chloride concentration and pH tests were the chemical tests used to assess the corrosion-resistance properties of the concrete. The electrical test includes half-cell potential to evaluate the inhibiting properties of the various admixtures. The following sections describe each of these tests.

2.7.1 Slump, air entrainment, and mechanical tests

For each concrete panel mixture, slump, air entrainment, compressive strength, elastic modulus, and Poisson's ratio were determined. Air entrainment tests were performed according to ASTM C 231. Slump was determined according to ASTM C 143. Compressive strengths of each mixture were measured in accordance with ASTM C 39. The elastic modulus and Poisson's ratio were determined according to the standards described in ASTM C 469.

2.7.2 Chemical tests

Two chemical tests were performed on each field panel to measure chloride ion concentration in the concrete cover and pH at the level of the reinforcement. These tests

were conducted because chloride concentration and pH directly influence the corrosion of reinforcing steel in concrete.

2.7.2.1 Chloride concentration test

There are two basic methods for determining chloride ion content in concrete. The first involves dissolving concrete powder in water and the other involves digesting it in nitric acid. A portion of the chlorides in hardened concrete is combined chemically and only a fraction of the total amount of chloride ions is water-soluble and available to contribute to corrosion (Gaynor 1987).

The test for water-soluble chlorides involves collecting a concrete powder sample and boiling it in water for 5 minutes and then soaking in the water for 24 hours. The water is then used to determine the dissolved chloride. The results are reported as a percentage of the cement or concrete if the cement content is unknown (Gaynor 1987). The limits for water-soluble chloride content for concrete tested between 28 and 42 days after construction from ACI 318 are presented in Table 2.1.

Table 2.1. Maximum water-soluble chloride ion content in concrete (ACI 318).

Type of member	Maximum water-soluble chloride ion (Cl-) in concrete, percent by weight of cement
Prestressed concrete	0.06
Reinforced concrete exposed to chloride in service	0.15
Reinforced concrete that will be dry or protected from moisture in service	1.00
Other reinforced concrete construction	0.30

The other test is the total-chloride test or the acid-soluble chloride test. This test is faster and more reproducible than the water-soluble test (Gaynor 1987). For this test, a concrete powder sample is collected and dissolved in an extraction liquid such as nitric acid. The combined solution is tested to determine the chloride ion content. The results are reported as percent of the weight of the material being analyzed or as a weight per volume.

According to the ACI 318 Building Code, if the total or acid-soluble chloride ion content is less than the limits specified for water-soluble chloride ion content, then further tests are not required. Consequently, if the total or acid-soluble chloride ion content is higher than the water-soluble chloride ion content, then concrete powder samples would have to be collected and tested by the water-soluble method. However, a commonly accepted value for the corrosion threshold by the total chloride test method is 0.20 percent total chloride ion by weight of cement (Fraczek 1987). The limits for acid-soluble chloride content recommended by ACI Committee 222 (ACI Committee 201 1991) are presented in Table 2.2. These limits are for new construction tested between 28 and 42 days.

Table 2.2. Maximum acid-soluble chloride ion content in concrete.

Type of member	Maximum acid-soluble chloride ion (Cl^-) in concrete, percent by weight of cement
Prestressed concrete	0.08
Wet reinforced concrete	0.10
Dry reinforced concrete	0.20

2.7.2.2 pH test

The alkaline environment of concrete, pH greater than 12, acts a natural corrosion inhibitor for the reinforcing steel (Hope and Ip 1987). It is important to measure the pH of concrete to determine the actual alkalinity of the concrete and thus its ability to resist corrosion. Concrete dust samples collected near the reinforcing steel were mixed with 0.03 oz (1 gram) of distilled water per 0.03 oz. (1 gram) of concrete dust (EPA 2002). A pH probe was used to measure the pH of the concrete.

2.7.3 Air permeability test

The permeability of cover concrete is significant in assessing the durability of reinforced concrete. The cover concrete affords both the chemical and physical resistance against the ingress of deleterious elements, such as chloride ions. There are two tests for permeability, air and water permeability tests, but the air permeability test is preferred because of repeatability and because of its relevance to the rate of carbonation of concrete (Cather et al. 1984).

There are two methods to measure air permeability of concrete. The output methods measure the downstream flow rate through the specimen when the flow has attained a steady state (inlet flow rate = outlet flow rate). Darcy's equation is used to calculate the intrinsic permeability of the test material (Dhir et al. 1995). The output methods provide accurate results, but are time-consuming and cannot be used for in situ concrete.

The input method was first proposed by Figg (1973) and was later modified and improved by various researchers. The Figg method for determining air permeability is

based on applying low pressure with a hand vacuum to a drilled hole in the concrete through a hypodermic needle inserted through a silicone plug at the surface of the hole. The amount of time for the pressure to increase from 2.18 psi to 2.90 psi (15 kN/m^2 to 20 kN/m^2) absolute, or 12.33 psi to 11.60 psi (85 kN/m^2 to 80 kN/m^2) below atmospheric pressure, is used to determine the air permeability of the concrete. However, Cather et al. (1984) states that an alternative pressure range should be selected to account for certain test parameters.

There were several improvements to the Figg method proposed by Cather et al. (1984). A hole of larger dimensions is drilled to ease drilling on site, but still limit visual damage to the surface of the concrete. Larger pre-manufactured silicone rubber plugs are used to accommodate the change in test-hole dimensions. Lastly, the air permeability is determined from the time required for a pressure to increase from 7.98 psi to 7.25 psi (55 kN/m^2 to 50 kN/m^2) below atmospheric pressure. These changes were made to account for equipment restrictions and test parameters.

2.7.4 Half-cell potential test

The half-cell potential test is one of the most extensively used techniques used to assess corrosion of reinforced concrete structures. It follows the guidelines set out in ASTM C 876. The test measures the electrode potential of embedded steel in concrete against a reference electrode /cell placed on the surface of the concrete (Dhir et al. 1991). A damp sponge is usually used to obtain good electrical contact between the reference electrode and concrete (Manning 1992). Different types of reference electrodes include copper/copper sulfate (CSE), mercury/mercury chloride or saturated calomel (SCE), and

silver/silver chloride (Ag/AgCl). The potential is measured using a high impedance voltmeter (>10 mega ohm) to ensure low current conditions during testing. The test setup is shown in Figure 2.2.

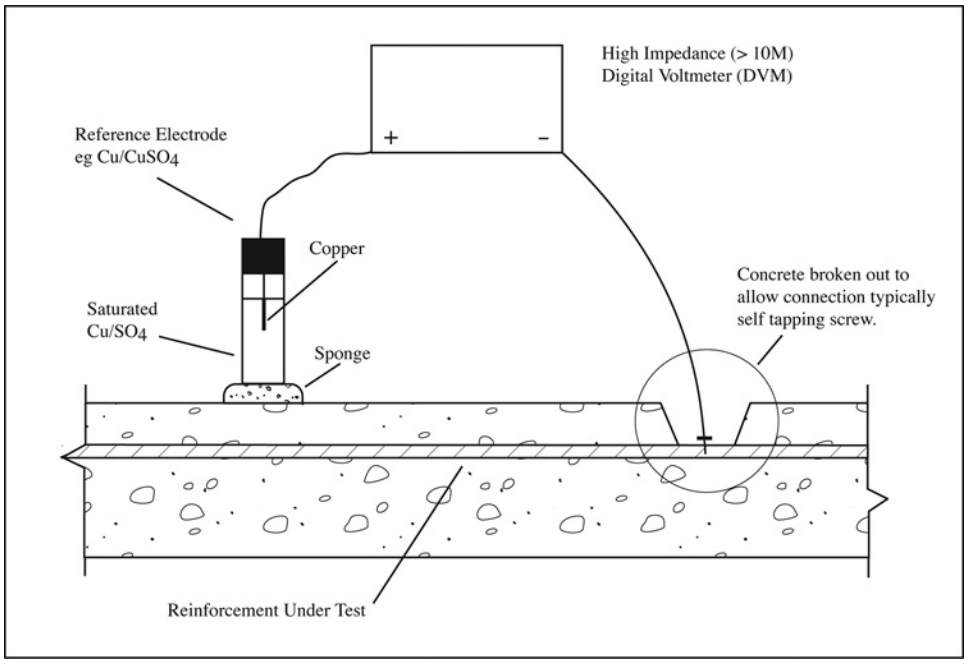

Figure 2.2. Setup for half-cell potential test (Dhir et al. 1991).

The measured half-cell potentials result in the variation of the potential of the steel in concrete because the potential in the reference electrode is constant. Electrode potentials can be measured at any location by simply moving the reference electrode along the surface of the concrete.

The half-cell potential test is inexpensive and simple to perform. Whole structures can be surveyed fairly quickly because of the test simplicity. The data produced is straightforward and easy to interpret using Table 2.3. Also, the type of reference electrode used is not critical provided that adequate contact with the concrete

surface is achieved (Sharp et al. 1988). A basic conversion can be done for data obtained using the different reference electrodes.

Table 2.3. Interpretation of half-cell test results using CSE (Dhir et al. 1991).

Measured Potential (mV)	Statistical risk of corrosion occurring
< -350	90%
Between -350 and -200	50%
> -200	10%

The main limitation of the half-cell potential test is that it does not provide information on the rate of corrosion or whether or not corrosion has already commenced (Bungey and Millard 1996). The test only provides a probability that corrosion is occurring at a specific location. Another limitation is the large range of uncertainty of the probability of corrosion for readings between -350 mV and -200 mV (Table 2.3). The statistical risk of corrosion for a potential measurement in this range is defined as uncertain in the standards set by ASTM C 876, which gives a probability of a 50% chance of corrosion. Furthermore, there must be continuous electrical contact with the reinforcing steel within the concrete for accurate readings. It is also difficult to perform the test if contaminants are present on or in the concrete.

2.8 Corrosion prediction

2.8.1 Life-365

Life-365 is a computer program designed to predict the service life and life-cycle cost of reinforced concrete structures. It is the first industry-sponsored computer model that engineers can use to help design more corrosion-resistant reinforced concrete

structures (Violetta 2002). The program conducts a life-cycle cost analysis (LCCA), which uses the initial costs and predicted repair costs of a structure to compute the costs over the entire life of the structure (Silica Fume Association 2001).

The analyses produced by Life-365 include predicting the initiation period, propagation period, determining repair schedules, and estimating life-cycle costs based on the initial concrete costs and future repair costs. The initiation period is the amount of time for sufficient chlorides to penetrate the concrete cover and initiate corrosion, and is based on Fick's law of diffusion. The propagation time is the time for corrosion to reach an unacceptable level.

Life-365 requires some general user inputs to analyze each structure. The inputs include geographic location, type of structure and exposure type, depth of clear concrete cover to the reinforcing steel, and some details of corrosion protection strategies. Some examples of corrosion protection strategies the program recognizes are water-cementitious material ratio (w/c ratio), corrosion inhibitors, coated or uncoated steel, and membranes or sealers. Life-365 also allows the user to analyze various combinations of corrosion protection systems.

2.9 Summary

This chapter presented a literature review of the principles and mechanisms of corrosion, chloride penetration, and the different admixtures that were added to concrete to protect reinforcing steel from corrosion. The admixtures included DCI, Rheocrete CNI, Rheocrete 222+, FerroGard 901, Xypex Admix C-2000, latex-modifier, fly ash, silica fume, and Kryton KIM. A description of the principles of the slump, air entrainment,

mechanical, chemical, pH, permeability and half-cell potential tests were presented as well as an introduction to the computer program Life-365.

CHAPTER 3
EXPERIMENTAL PROCEDURES

3.1 Introduction

This chapter describes the concrete mixtures for each field panel and how each mixture was proportioned. The process of preparing the materials, mixing and placing the concrete, and curing the panels are also presented. Test procedures for determining slump, air content, compressive strength, elastic modulus, Poisson's ratio, chloride concentration, pH, air permeability, and half-cell potential are presented in this chapter. The analyses performed with the computer program Life-365 are also described.

3.2 Mixtures

Twenty-five reinforced concrete panels were designed based on the thirteen different mixture designs from Phase II of this study. There are three control mixtures, three DCI mixtures, three Rheocrete CNI mixtures, four Rheocrete 222+ mixtures, three FerroGard 901 mixtures, one Xypex Admix C-2000 mixture, one latex-modified mixture, three silica fume mixtures, three fly ash mixtures, and one Kryton KIM mixture. The mixtures have varying admixture dosages, pozzolan content, aggregate source, and water-cement ratio. The aggregate sources are the Ameron Kapaa Quarry and the Halawa Quarry on the island of Oahu.

3.2.1 Control mixtures

There were six control mixture designs using each of the aggregate sources in Phase II of this study. These mixture proportions were modified from actual concrete mixture designed by Ameron and used for improvements on Pier 39 in Honolulu. The original mixture by Ameron was selected for Pier 39 improvements because it was considered an effective mixture for protecting the reinforcing steel (Pham and Newtson 2001).

For the Phase III study, there were two control mixtures using the Ameron aggregate source and one control mixture using the Halawa aggregate source. Panels 1 and 7 were based on Ameron mixture C2 and C1, respectively, of the Phase II study (Pham and Newtson 2001). Panel 2 was based on a Halawa mixture from the Phase II study (Okunaga and Robertson 2004).

Table 3.1. Mixture proportions for control mixtures.

Material or property	Panel 1 (C2 - Pham)	Panel 2 (Okunaga)	Panel 7 (C1 - Pham)
Aggregate source	Ameron	Halawa	Ameron
w/c	0.40	0.40	0.35
Paste volume (%)	31.2	31.2	31.2
Design slump (in.) (mm)	4 (102)	4 (102)	4 (102)
Coarse aggregate (lb/yd^3) (kg/m^3)	1576 (935.0)	1642 (974.2)	1576 (935.0)
Dune sand (lb/yd^3) (kg/m^3)	431 (255.7)	573 (340.0)	431 (255.7)
Concrete sand (lb/yd^3) (kg/m^3)	826.5 (490.4)	759.2 (450.4)	825.7 (489.9)
Cement (lb/yd^3) (kg/m^3)	733.3 (435.1)	733.3 (435.1)	786.2 (466.5)
Water (lb/yd^3) (kg/m^3)	292.1 (173.3)	292.1 (173.3)	275.1 (163.2)
Daratard (oz/sk) (ml/sk)	3 (88.7)	3 (88.7)	3 (88.7)
Darex (oz/sk) (ml/sk)	2 (59.1)	2 (59.1)	2 (59.1)
Design Air Content (%)	4	4	4

3.2.2 DCI mixtures

There were six DCI mixtures using Ameron aggregates in Phase II of this study. These mixtures were proportioned by replacing 2, 4, and 6 gallons of water with the DCI admixture for 1 cubic yard (9.9, 19.8, 29.7 $1/m^3$) of concrete. Ameron DCI mixtures D4, D5, and D6 were modified from Ameron control mixture C2.

For this study, panels 3 and 3A were fabricated using Ameron mixtures D4 and D5 respectively. Panel 3 replaces 2 gallons of water with DCI admixture and panel 3A

replaces 4 gallons of water with DCI admixture. Panel 4 was fabricated using a Halawa mixture from the Phase II study.

Table 3.2. Mixture proportions for DCI mixtures.

Material or property	Panel 3 (D4 - Pham)	Panel 3A (D5 - Pham)	Panel 4 (Okunaga)
Aggregate source	Ameron	Ameron	Halawa
w/c	0.40	0.40	0.40
Paste volume (%)	31.2	31.2	31.2
Design slump (in.) (mm)	4 (102)	4 (102)	4 (102)
Coarse aggregate (lb/yd^3) (kg/m^3)	1576 (935.0)	1576 (935.0)	1576 (935.0)
Dune sand (lb/yd^3) (kg/m^3)	431.5 (256.0)	431.5 (256.0)	431.5 (256.0)
Concrete sand (lb/yd^3) (kg/m^3)	826.5 (490.4)	826.5 (490.4)	826.5 (490.4)
Cement (lb/yd^3) (kg/m^3)	733.3 (435.1)	733.3 (435.1)	733.3 (435.1)
Water (lb/yd^3) (kg/m^3)	275.4 (163.4)	258.7 (153.5)	275.4 (163.4)
Liquid DCI (gal/yd^3) (l/m^3)	2 (9.9)	4 (19.8)	2 (9.9)
Daratard (oz/sk) (ml/sk)	3 (88.7)	3 (88.7)	3 (88.7)
Darex (oz/sk) (ml/sk)	2 (59.1)	2 (59.1)	2 (59.1)
Design Air Content (%)	4	4	4

3.2.3 Rheocrete CNI

Rheocrete CNI mixtures were designed by replacing DCI with Rheocrete CNI since both are calcium nitrite-based corrosion inhibitors that contain 30% calcium nitrite.

In Phase II, There were six Rheocrete CNI mixtures using Ameron aggregates denoted as CNI1 to CNI6.

For this study, panels 5 and 6 were fabricated using Ameron mixtures CNI4 and panel 5A was fabricated using CNI5. Panel 5 and 6 replaces 2 gallons of water with Rheocrete CNI admixture and panel 5A replaces 4 gallons of water with Rheocrete CNI admixture.

Table 3.3. Mixture proportions for Rheocrete CNI mixtures.

Material or property	Panel 5 (CNI4 - Pham)	Panel 5A (CNI5 - Pham)	Panel 6 (CNI4 - Pham)
Aggregate source	Ameron	Ameron	Ameron
w/c	0.40	0.40	0.40
Paste volume (%)	31.2	31.2	31.2
Design slump (in.) (mm)	4 (102)	4 (102)	4 (102)
Coarse aggregate (lb/yd^3) (kg/m^3)	1576 (935.0)	1576 (935.0)	1641.9 (974.1)
Dune sand (lb/yd^3) (kg/m^3)	431.5 (256.0)	431.5 (256.0)	572.7 (339.8)
Concrete sand (lb/yd^3) (kg/m^3)	826.5 (490.4)	826.5 (490.4)	759.2 (450.4)
Cement (lb/yd^3) (kg/m^3)	733.3 (435.1)	733.3 (435.1)	733.3 (435.1)
Water (lb/yd^3) (kg/m^3)	275.4 (163.4)	258.7 (153.5)	275.4 (163.4)
Liquid CNI (gal/yd^3) (l/m^3)	2 (9.9)	4 (19.8)	2 (9.9)
Daratard (oz/sk) (ml/sk)	3 (88.7)	3 (88.7)	3 (88.7)
Darex (oz/sk) (ml/sk)	2 (59.1)	2 (59.1)	2 (59.1)
Design Air Content (%)	4	4	4

3.2.4 Rheocrete 222+ mixtures

Rheocrete 222+ mixtures were proportioned by adding 1 gallon of Rheocrete 222+ per cubic yard (4.95 l/m^3) of concrete to the control mixture designs. There were six Rheocrete 222+ mixtures using Ameron aggregates denoted as RHE1 to RHE6. For this study, panels 15 and 16 were based on Ameron mixture RHE2. Panels 17 and 17A were fabricated using a Halawa mixture from the Phase II study.

Table 3.4. Mixture proportions for Rheocrete 222+ mixtures.

Material or property	Panel 15 (RHE2 - Pham)	Panel 16 (RHE2 - Pham)	Panel 17 & 17A (Okunaga)
Aggregate source	Ameron	Ameron	Halawa
w/c	0.40	0.40	0.40
Paste volume (%)	31.2	31.2	31.2
Design slump (in.) (mm)	4 (102)	4 (102)	4 (102)
Coarse aggregate (lb/yd^3) (kg/m^3)	1576 (935.0)	1576 (935.0)	1642 (974.2)
Dune sand (lb/yd^3) (kg/m^3)	431.5 (256.0)	431.5 (256.0)	572.7 (339.8)
Concrete sand (lb/yd^3) (kg/m^3)	826.5 (490.4)	826.5 (490.4)	759.2 (450.4)
Cement (lb/yd^3) (kg/m^3)	733.3 (435.1)	733.3 (435.1)	733.3 (435.1)
Water (lb/yd^3) (kg/m^3)	292.1 (173.3)	292.1 (173.3)	292.1 (173.3)
Rheocrete 222+ (gal/yd^3) (l/m^3)	1 (4.95)	1 (4.95)	1 (4.95)
Daratard (oz/sk) (ml/sk)	3 (88.7)	3 (88.7)	3 (88.7)
Darex (oz/sk) (ml/sk)	2 (59.1)	2 (59.1)	2 (59.1)
Design Air Content (%)	4	4	4

3.2.5 FerroGard 901 mixtures

FerroGard 901 mixtures were designed by replacing a portion of water in the control mixtures with the same amount of FerroGard 901. The mixtures were designed by using 3 gallons of admixture per cubic yard (14.85 l/m^3) of concrete. In Phase II, there were six FerroGard 901 mixture designs using Ameron aggregates denoted as FER1 to FER6. For this study, panel 20 was designed using Ameron mixture FER2. Panels 18 and 19 were fabricated using a Halawa mixture from the Phase II study.

Table 3.5. Mixture proportions for FerroGard 901 mixtures.

Material or property	Panel 18 & 19 (Okunaga)	Panel 20 (FER2 - Pham)
Aggregate source	Halawa	Ameron
w/c	0.40	0.40
Paste volume (%)	31.2	31.2
Design slump (in.) (mm)	4 (102)	4 (102)
Coarse aggregate (lb/yd^3) (kg/m^3)	1642 (974.2)	1576 (935.0)
Dune sand (lb/yd^3) (kg/m^3)	759.2 (450.4)	431 (255.7)
Concrete sand (lb/yd^3) (kg/m^3)	572.7 (339.8)	826.5 (490.4)
Cement (lb/yd^3) (kg/m^3)	733.3 (435.1)	733.3 (435.1)
Water (lb/yd^3) (kg/m^3)	292.1 (173.3)	292.1 (173.3)
FerroGard 901 (gal/yd^3) (l/m^3)	3 (14.85)	3 (14.85)
Daratard (oz/sk) (ml/sk)	3 (88.7)	3 (88.7)
Darex (oz/sk) (ml/sk)	2 (59.1)	2 (59.1)
Design Air Content (%)	4	4

3.2.6 Xypex Admix C-2000 mixture

There were six Xypex Admix C-2000 mixtures using Ameron aggregates in Phase II. The mixtures were proportioned by replacing 2% of cement by mass from the control mixtures with Xypex Admix C-2000 admixture. The mix design for Panel 21 was proportioned based on Ameron mixture XYP2.

Table 3.6. Mixture proportions for Xypex Admix C-2000 mixture.

Material or property	Panel 21 (XYP2 - Pham)
Aggregate source	XYP2
w/c	0.40
Paste volume (%)	31.2
Design slump (in.) (mm)	4 (100)
Coarse aggregate (lb/yd^3) (kg/m^3)	1576 (935.0)
Dune sand (lb/yd^3) (kg/m^3)	431 (255.7)
Concrete sand (lb/yd^3) (kg/m^3)	825.6 (489.8)
Cement (lb/yd^3) (kg/m^3)	718.5 (426.3)
Water (lb/yd^3) (kg/m^3)	292.1 (173.3)
Xypex (lb/yd^3) (kg/m^3)	14.7 (8.72)
Daratard (oz/sk) (ml/sk)	3 (88.7)
Darex (oz/sk) (ml/sk)	2 (59.1)
Design Air Content (%)	4

3.2.7 Latex-modified mixture

For the Phase II study, latex-modified mixtures were designed by adding latex admixture to the Ameron aggregate control mixtures. The amounts added were 2.5, 5.0, and 7.5 percent of the mass of the cement. There were six latex-modified mixtures labeled L1 to L6. For this study, mixture L5 was used to design panel 14. Mixture L5 was modified from control mixture C2 with a latex content of 5%.

Table 3.7. Mixture proportions for latex-modified mixture.

Material or property	Panel 14 (L5 - Pham)
Aggregate source	Ameron
w/c	0.40
Paste volume (%)	31.2
Design slump (in.) (mm)	4 (102)
Coarse aggregate (lb/yd^3) (kg/m^3)	1576 (935.0)
Dune sand (lb/yd^3) (kg/m^3)	399.5 (237.0)
Concrete sand (lb/yd^3) (kg/m^3)	765.2 (454.0)
Cement (lb/yd^3) (kg/m^3)	733.2 (435.0)
Water (lb/yd^3) (kg/m^3)	182.1 (108.0)
Latex Liquid (lb/yd^3) (kg/m^3)	146.6 (87.0)
Design Air Content (%)	4

3.2.8 Fly ash mixtures

The fly ash used in both Phase II and III of this study was obtained from a coal power plant on the island of Oahu. The specification of the locally produced fly ash does not meet the ASTM requirements for class C or class F fly ash. The chemical composition is shown in Table 3.8.

Table 3.8. Fly ash chemical composition (Pham and Newtson 2001).

Chemical composition (%)		ASTM C 618 Specifications	
	Hawaiian fly ash	Class C	Class F
Total silica, aluminum, iron	56.09	70.0 Min	50.0 Min
Sulfur trioxide	9.85	5.0 Max	5.0 Max
Calcium oxide	25.99		
Moisture content	0.10	3.0 Max	3.0 Max
Loss on ignition	2.81	6.0 Max	6.0 Max
Available alkalis (as Na_2O)	1.26	1.5 Max	1.5 Max

Because silica fume and fly ash are pozzolans, the mixture designs for both are similar. The only difference affecting the mixture design using silica fume and fly ash is the difference in specific gravity. For the fly ash mixture, cement was replaced by an equal mass of fly ash and the sand content was adjusted to account for the difference in specific gravity. Panel 11 was fabricated using the design for mixture FA4. Panels 12 and 13 were fabricated using a Halawa mix design from the Phase II study.

Table 3.9. Mixture proportions for fly ash mixtures.

Material or property	Panel 11 (FA4 - Pham)	Panel 12 (Okunaga)	Panel 13 (Okunaga)
Aggregate source	Ameron	Halawa	Halawa
w/(c+p)	0.36	0.36	0.36
Paste volume (%)	33	33	33
Design slump (in.) (mm)	8-10 (200-250)	8-10 (200-250)	8-10 (200-250)
Coarse aggregate (lb/yd^3) (kg/m^3)	1668 (989.6)	1737 (1030.6)	1737 (1030.6)
Dune sand (lb/yd^3) (kg/m^3)	526.5 (312.4)	548.9 (325.7)	548.9 (325.7)
Concrete sand (lb/yd^3) (kg/m^3)	698 (414.1)	727.4 (431.6)	727.4 (431.6)
Cement (lb/yd^3) (kg/m^3)	689.3 (409.0)	689.3 (409.0)	689.3 (409.0)
Water (lb/yd^3) (kg/m^3)	291.9 (173.2)	291.9 (173.2)	291.9 (173.2)
Fly Ash (lb/yd^3) (kg/m^3)	121.77 (72.2)	121.77 (72.2)	121.77 (72.2)
Design Air Content (%)	1	1	1

3.2.9 Silica fume mixtures

There were eleven silica fume mixtures with water cement ratios of 0.36 and 0.45 using Ameron aggregates in Phase II of this study. Modifying the concrete mixtures that were used in the Ford Island Bridge Project proportioned the first six mixtures, SF1 to SF6. These mixtures were considered to be effective in protecting the reinforcing steel. The other five mixtures were based on the design recommendations of the Portland Cement Association.

For this study, silica fume from two different manufacturers was used. The first is from Master Builders Inc. and the other is from W.R. Grace & Co. Panels 8 and 9 were fabricated using the Master Builders silica fume and panel 10 was fabricated using the Grace silica fume. All three mixtures were designed using mixture SF2.

Table 3.10. Mixture proportions for silica fume mixtures.

Material or property	Panel 8 & 9 (M.B.) (SF2 - Pham)	Panel 10 (Grace) (SF2 - Pham)
Aggregate source	Ameron	Ameron
w/(c+p)	0.36	0.36
Paste volume (%)	32.9	32.9
Design slump (in.) (mm)	8-10 (200-250)	8-10 (200-250)
Coarse aggregate (lb/yd^3) (kg/m^3)	1668 (989.6)	1668 (989.6)
Dune sand (lb/yd^3) (kg/m^3)	521.1 (309.2)	521.1 (309.2)
Concrete sand (lb/yd^3) (kg/m^3)	679.3 (403.0)	679.3 (403.0)
Cement (lb/yd^3) (kg/m^3)	771.1 (457.5)	771.1 (457.5)
Water (lb/yd^3) (kg/m^3)	291.9 (173.2)	291.9 (173.2)
Silica Fume (lb/yd^3) (kg/m^3)	40 (23.7)	40 (23.7)
Design Air Content (%)	4	4

3.2.10 Kryton KIM mixtures

The Kryton mixtures were proportioned by adding 2% by weight of the cementitious content of Kryton KIM up to a maximum of 13.5 pounds per cubic yard (8.0 kg/m^3) of concrete. The water content is also reduced by 5-10% depending on the slump requirement. For the mixture design of panel 22, approximately 5% of water was removed. Kryton KIM was not used in any of the mixtures in Phase II.

Table 3.11. Mixture proportion for Kryton Kim mixture.

Material or property	Panel 22
Aggregate source	Ameron
w/c	0.40
Paste volume (%)	31.2
Design slump (in.) (mm)	4 (102)
Coarse aggregate (lb/yd^3) (kg/m^3)	1576 (935.0)
Dune sand (lb/yd^3) (kg/m^3)	431.5 (256.0)
Concrete sand (lb/yd^3) (kg/m^3)	826.47 (490.3)
Cement (lb/yd^3) (kg/m^3)	733.3 (435.1)
Water (lb/yd^3) (kg/m^3)	278.6 (165.3)
Kryton Kim (lb/yd^3) (kg/m^3)	13.50 (6.1)
Design Air Content (%)	4

3.2.11 Other admixtures

Three additional admixtures used in this study were Daracem 19, Darex II AEA, and Daratard HC for providing workability, air-entrainment, and set-retarding respectively. The manufacturer's recommended addition rate for Daracem 19 is 6 to 20 fl oz per 100 lbs of cement (390 to 1300 ml per 100 kg of cement). For mixtures that required a superplasticizer, the amount of Daracem 19 added was determined by the desired slump. The recommended range for Darex II AEA usage was from 0.5 to 5.0 fl oz per 100 lbs of cement (30 to 320 ml per 100 kg of cement). For mixtures that included Darex II AEA, the amount used was 3.0 fl oz (88.7 ml). The amount of Daratard HC used for mixtures requiring a controlled setting was 2.0 fl oz (59.1 ml).

It should be noted that the previous three admixtures were not used for all twenty-five mixtures in this study. According to the manufacturers, certain admixtures could not be used together due to potential chemical reactions that could have adverse effects on the properties of the concrete. Some of these admixtures were also omitted from some mixtures to control the workability of the mixture.

3.3 Concrete panel specimens

Twenty-five specimens, 6 by 21 by 59.5 in. (152 by 533 by 1511 mm) reinforced with No. 4 steel bars, were made for testing corrosion resistance. The specimen length was selected so that a portion of the panel was still submerged during low tide while high tide would not reach the top of the panel. The panel thickness was selected to encase two layers of reinforcing steel and provide adequate cover on all sides.

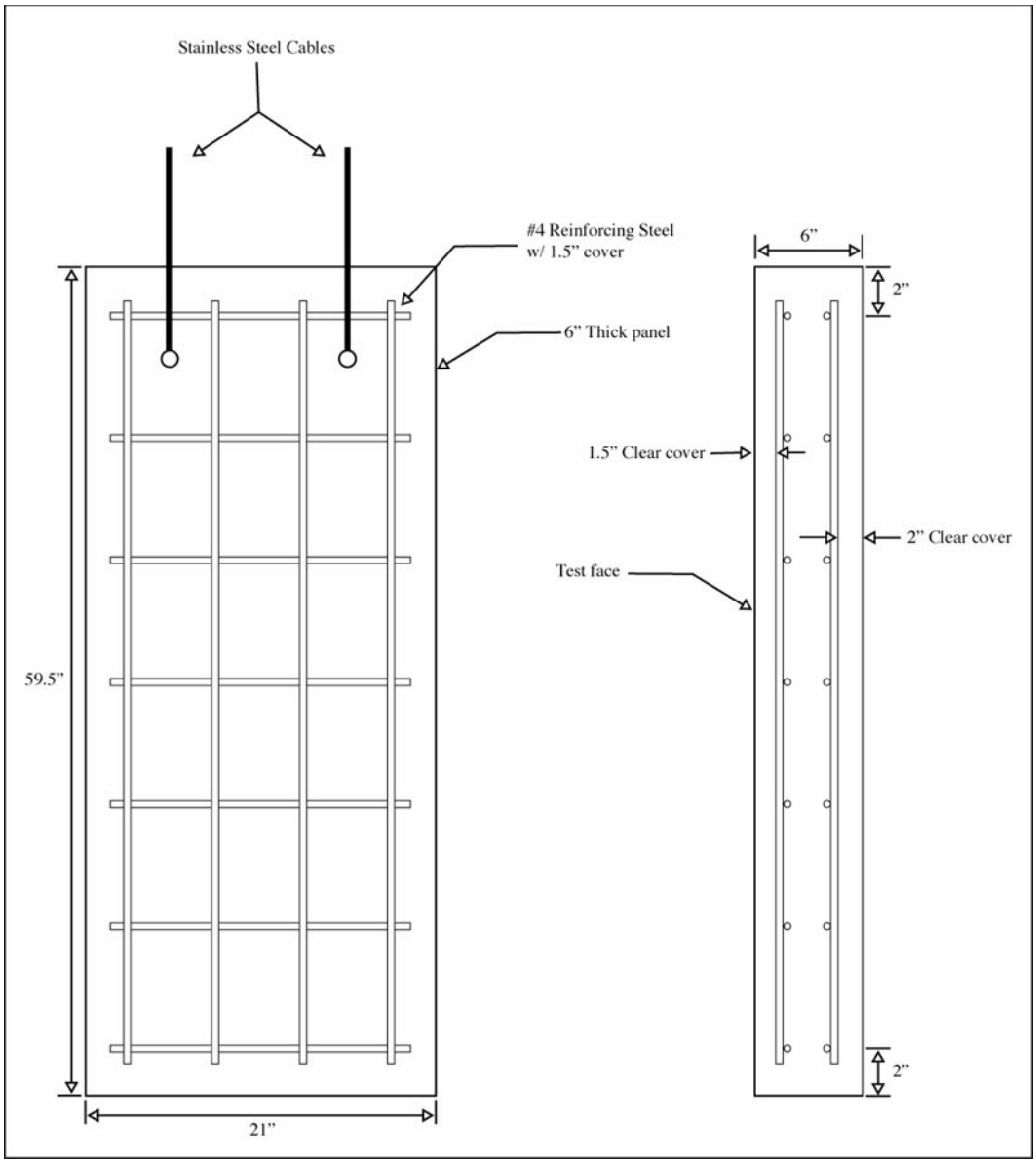

Figure 3.1. Diagram of concrete panel.

3.3.1 Preparation

Prior to the mixing process, samples of the coarse aggregate, Maui dune sand and basalt sand were collected in a steel pan. Each pan was weighed with and without the constituents and then placed in an oven at 110ºC for 24 hours to determine the moisture

content. Then, the constituents were weighed and the adsorption of the materials is calculated.

The steel reinforcing bars used in the specimens were pickled in a 10% sulfuric acid solution for 30 minutes to an hour, depending on the amount of rust on the bars. The bars were then removed and scrubbed with a wire brush to remove all rust. If the rust was not removed after scrubbing, the bars were soaked for another 10 to 20 minutes and then scrubbed again.

Each panel had two layers of reinforcing steel placed with the longitudinal bars closest to the panel top and bottom surfaces. The panels were constructed with exactly 1.5 in. (38 mm) clear cover on the bottom surface, and at least 2.0 in. (51 mm) on all edges and top surface. The off-formwork bottom surface was intended as the test surface in the field condition, so the panels were inverted for installation at Pier 38. Each layer of steel reinforcement consisted of four No. 4 longitudinal bars cut to approximately 54.5 in. (1384 mm) and seven No. 4 transverse bars cut to approximately 16 in. (406 mm). The reinforcing steel in each layer was connected using steel tie-wire. Five PVC conduit spacers with plastic cable ties were used to separate the two reinforcing layers physically and electrically.

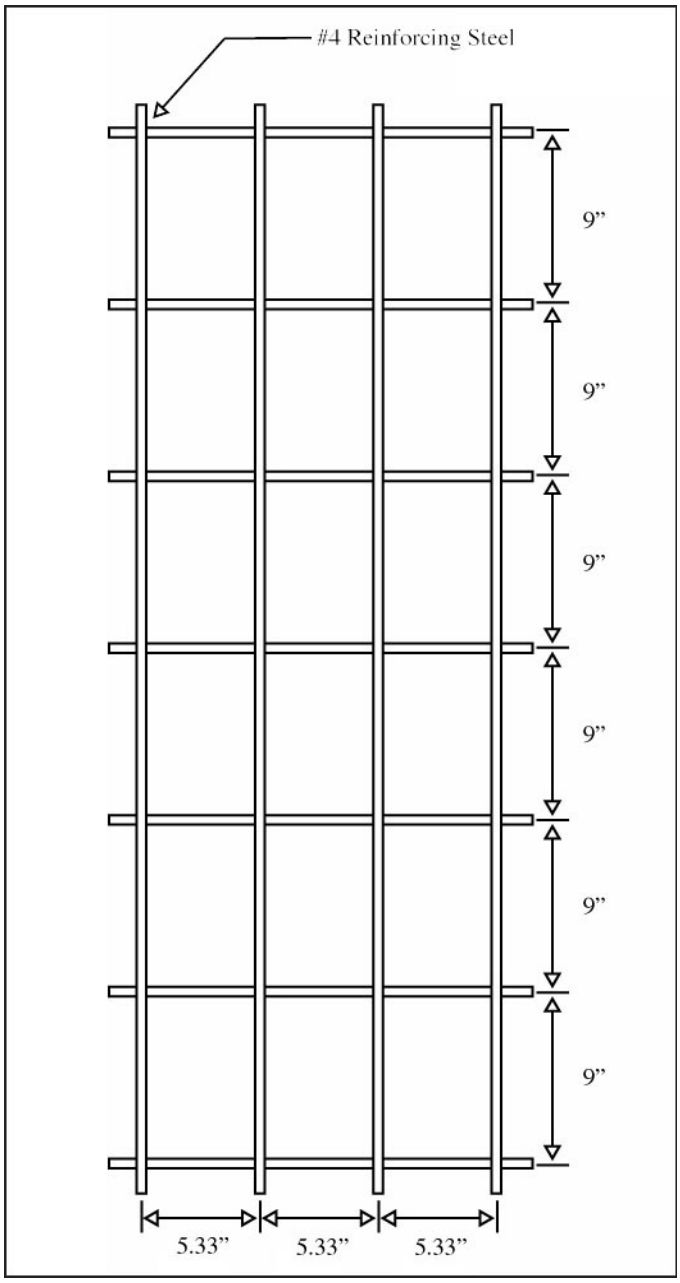

Figure 3.2. Reinforcing steel layout.

Reinforcing chairs were not used to support the steel reinforcing bars so as to avoid creating pathways for water ingress on the test surface. Instead the reinforcing cage was hung from the formwork as shown in Figure 3.3. The hanger wires passing through the non-test surface of the panel were cut off and epoxy was used to seal the area

against wire ingress. A 0.75 in. (19 mm) diameter PVC conduit was placed at the top edge of the panel as a sleeve to access the reinforcing steel after the concrete is poured.

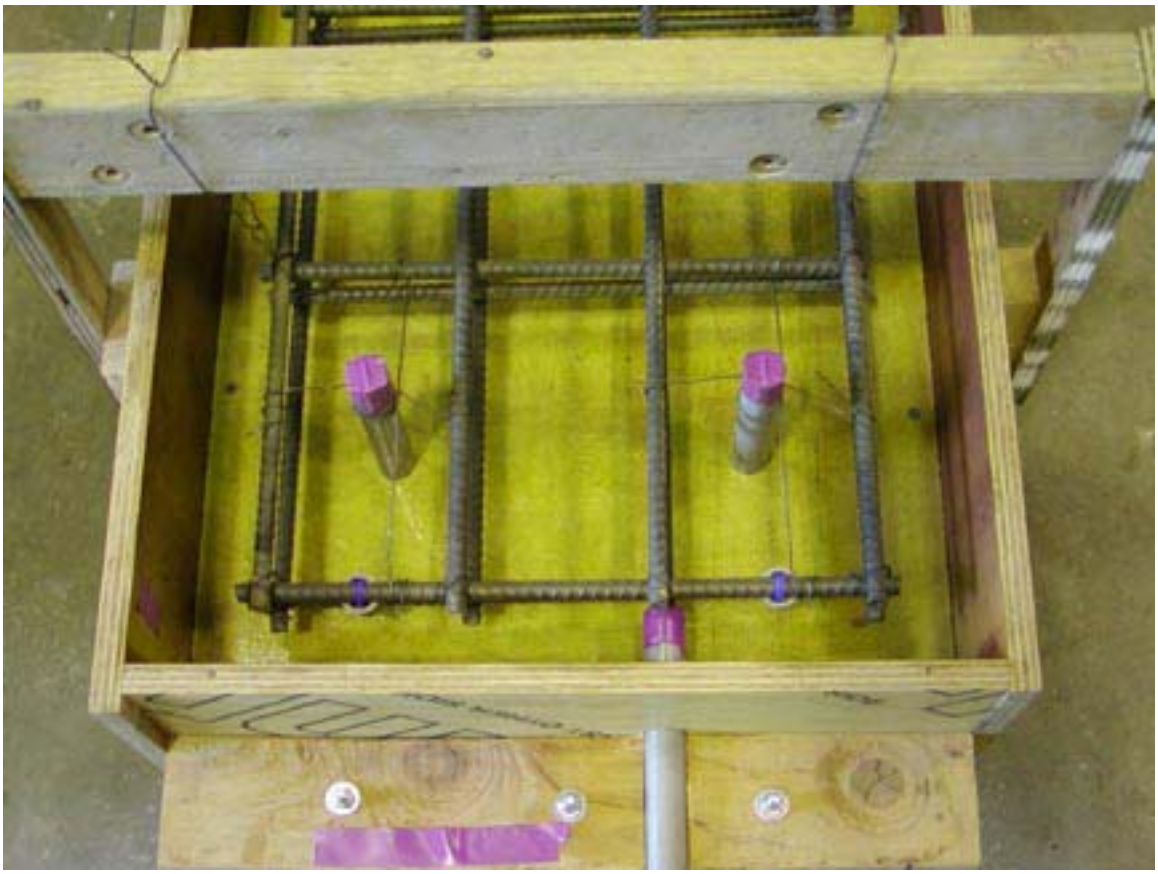

Figure 3.3. Reinforcing steel hanging from formwork.

3.3.2 Mixing process

The original mix designs were modified to account for the various moisture contents of each constituent. Coarse and fine aggregates, basalt sand, cement, water and admixtures were all pre-weighed for both the butter batch and main batch and placed in buckets prior to mixing. Mixing was conducted according to ASTM C 192.

3.3.3 Casting specimens

Fresh concrete was placed in the panel forms and consolidated with a vibrator. Caution was taken during vibrating to avoid over-consolidation. Fresh concrete was also placed in prepared cylinder molds with three equal layers of concrete. Each layer was rodded 25 times with a 0.625 in. (16 mm) diameter steel rod.

3.3.4 Curing process

Approximately 24 hours after casting, the panel specimens were taken out of the forms and the cylinder specimens were taken out of the molds. The panels were wet cured for 7 days and then taken out to the test site. The cylinders were wet cured for approximately 28 days. After the curing period, the cylinder specimens were removed from the curing bath for determination of compressive strength, elastic modulus, and Poisson's ratio.

3.4 Placement

The concrete panels were placed at Pier 38 in Honolulu Harbor off Nimitz Highway on the island of Oahu. Prior to panel placement, concrete anchor blocks were poured at various locations along the pier to provide an anchor for the concrete panels. The panels were then secured to the concrete anchors with stainless steel cables (Figure 3.4). The panels were located so that mean sea level was slightly below mid-height of the panel.

Figure 3.4. Panels hanging along Pier 38 rip-rap.

3.5 Laboratory test procedures

3.5.1 Slump

Slump tests were performed on both the butter batch and the main batch in accordance with ASTM C 143. The slump tests were conducted on the butter batch to get a rough estimation of the amount of high-range water reducer or superplasticizer that would be needed for the main batch in order to achieve a predetermined target slump. The predetermined target slump was based on mix designs and recommendations presented by Pham and Newtson (2001) and Okunaga and Robertson (2004).

3.5.2 Air content

Air content tests were performed during placement of concrete for all specimens. The method used was the ASTM C 231 standard test method for air content of freshly mixed concrete by the pressure method. The test was conducted to measure the percentage of air voids in the concrete.

3.5.3 Compressive strength, elastic modulus, and Poisson's Ratio

Compressive strength, elastic modulus, and Poisson's Ratio tests were performed at approximately 28 days for each mixture. Compressive strength tests were performed in accordance with ASTM C 39, and elastic modulus and Poisson's ratio were measured according to ASTM C 469. Three concrete cylinders 6 in. (152 mm) in diameter and 12 in. (305 mm) long were used for these tests according to ASTM C 470 mold requirements.

After 28 days of curing in water according ASTM C 192, all three cylinders were capped with a sulfur-capping compound in accordance with ASTM C 617 requirements. Compression strength tests were then conducted on two of the cylinders. The mean fracture load of the two cylinders was used to perform the elastic modulus and Poisson's ratio test on the third cylinder. Finally, the compression strength test was performed on the third cylinder. The average compressive strength of all three cylinders was used as the compressive strength of the mixture.

3.6 Field test procedures

3.6.1 Chloride concentration

Chloride concentrations were determined using the CL-2000 Chloride Field Test System by James Instruments, Inc. Approximately 0.11 oz (3 grams) of concrete dust samples were collected at 3 different locations from each panel by drilling perpendicular to the top face to depths of 0.5 in. (13 mm), 1.0 in. (25 mm), and 1.5 in. (38 mm) on the top face of each panel using a ¾ in. (19 mm) diameter bit as shown in Figure 3.5. The first test hole was located in an area in the upper half of the tidal zone. The second is in an area that is in the tidal zone. And the third test hole is located in the lower half of the tidal zone.

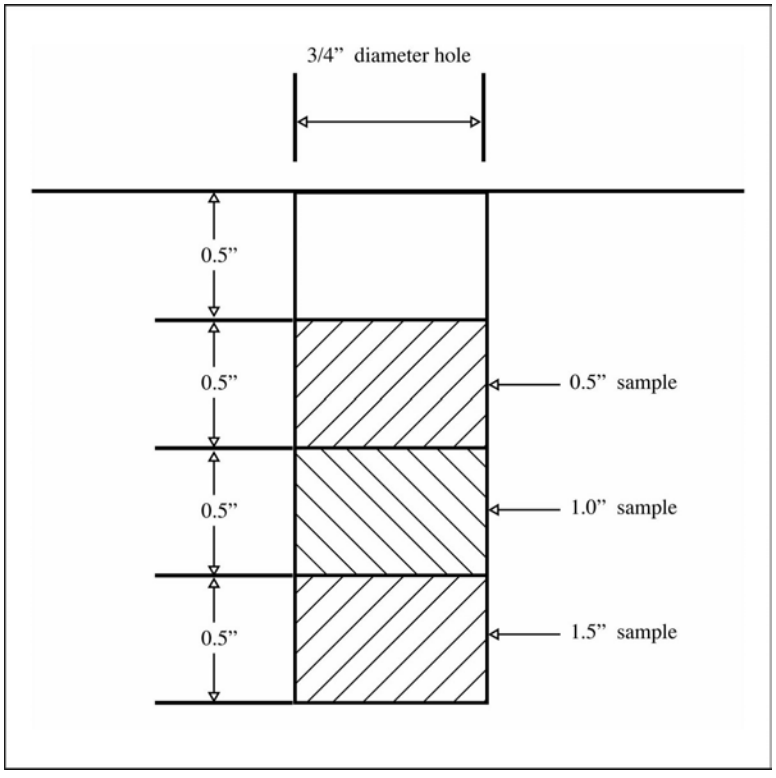

Figure 3.5. Depths of dust samples for chloride concentration test.

Prior to testing for chloride content, the CL-2000 was calibrated using the calibration liquids according to the instruction manual provided. The dust samples are dissolved in 0.67 fl oz (20 ml) of extraction liquid. The concrete dust and liquid are then shaken for one minute to allow time to react before taking the measurement. Chloride concentrations were measured in percentage by weight of concrete and converted to percentage by weight of cement using the cement content from the mixture proportions.

3.6.2 pH

The pH of each concrete panel was measured using the HI 8424 portable microprocessor pH meter by Hanna Instruments. Dust samples of approximately 0.11 oz (3 grams) were collected by drilling into the concrete at a depth of 1.5 in. (38 mm). The dust was then weighed and mixed with 0.03 oz (1 gram) of distilled water per 0.03 oz. (1 gram) of concrete dust and then stirred for one minute. The pH meter was dipped into the mixture of concrete dust and distilled water and the measurement was recorded. The meter was rinsed with distilled water and dried between measurements to ensure accurate readings.

3.6.3 Air permeability

The air permeability test was performed using the Poroscope Plus P-6000 (James Instruments, Inc. 1998). A 0.39 in. (10 mm) diameter hole was drilled to a depth of 1.57 in. (40 mm) on the top surface of the concrete panel. All loose dust was blown out of the hole and a 0.79 in. (20 mm) long molded silicon rubber plug was inserted into the hole,

leaving a cylindrical test void 0.39 in. (10 mm) in diameter and 0.79 in. long (20 mm) in length. A hypodermic needle was then inserted through the silicon rubber plug so that the tip of the needle was positioned in the void between the bottom of the plug and the bottom of hole. The air in the void was then vacuumed out through the needle in the plug using a hand-operated vacuum pump. The time in seconds required for a pressure change within the test hole from –7.98 psi to –7.25 psi (-55 kPa to –50kPa) determines the Figg number, which is a measure of the air permeability of the concrete.

3.6.4 Half-cell potential test

The half-cell potential test was performed using a saturated calomel electrode (SCE) and a voltmeter. Prior to testing, the epoxy filled access hole located at the top end of each concrete panel was drilled out to expose a single longitudinal reinforcing steel bar. A steel screw was drilled into the exposed steel bar to establish an electrical connection. Half-cell potential tests were conducted at ten locations on the front face of each panel as shown in Table 3.12.

Table 3.12. Test locations of half-cell measurements.

Location	Distance from left side, in. (mm)		Distance from top, in. (mm)	
1	2.5	(64)	7.25	(184)
2	18.5	(470)	7.25	(184)
3	2.5	(64)	16.25	(413)
4	18.5	(470)	16.25	(413)
5	2.5	(64)	25.25	(641)
6	18.5	(470)	25.25	(641)
7	2.5	(64)	34.25	(870)
8	18.5	(470)	34.25	(870)
9	2.5	(64)	43.25	(1099)
10	18.5	(470)	43.25	(1099)

3.7 Corrosion prediction

3.7.1 Life-365

An analysis of each concrete panel to predict chloride concentrations was performed using the computer program Life-365. The program required user inputs to define input and output units, water-cement ratios, types of corrosion-inhibiting products, structure type, percentage of steel, and level of exposure. US units were used for all analysis and the water-cement ratios used for each panel can be found in the Mixtures section of this chapter.

Commercial product names were used for the corrosion-inhibiting admixtures DCI, Rheocrete CNI, Rheocrete 222+, fly ash, and silica fume. Analyses on FerroGard 901, Xypex Admix C-2000, latex, and Kryton KIM were not performed because they were not included in the program.

One-dimensional chloride loading (slabs and walls) was used to represent the type of structure used in this study. Since there was no long term exposure location for Hawaii, San Juan in Puerto Rico was used as it has similar climate conditions. The exposure used was marine tidal zone. A complete listing of monthly temperature values and month of first exposure can be found in Appendix D.

According to the user's manual, Life-365 assumed 0.80% chloride concentration by weight of concrete for the maximum surface concentration for marine tidal zone exposures. The input for time to build up to this chloride concentration level was 0, because the maximum surface concentration occurred on each panel instantaneously upon submersion. Inputs for a cost-benefit analysis were not used for this study.

3.8 Summary

This chapter presented the experimental procedures for all the tests performed in this study. The tests include slump, air entrainment, compressive strength, elastic modulus, Poisson's ratio, chloride concentration, pH, air permeability, and half-cell potential. The mixture proportions used in this study were also included. A complete description of the preparation of the reinforcing steel, concrete constituents, and formwork were provided as well as the mixing process and casting, curing and placement of each panel. All the inputs and procedures used for the computer program Life-365 were also presented.

CHAPTER 4
RESULTS FROM FIELD SPECIMENS

4.1 Introduction

This chapter describes the orientation of each panel in the field, the location of each test hole along the face of each panel, the orientation, and the location of mean sea level with respect to each panel based on data from NOAA (2004). Also presented are the results for the slump, air entrainment, mechanical tests, chemical tests, air permeability tests, and half-cell potential tests conducted for the concrete mixtures presented in Chapter 3. Compressive strength values for each cylinder can be found in Appendix A. Raw data for the chloride concentrations, pH, and half-cell potential tests are provided in Appendix B, Appendix C, and Appendix D respectively.

4.2 Panel measurements

All twenty-five panels were placed along the rip-rap at Pier 38 lie at different vertical angles. As a result, the test holes along the panels were exposed to different sea water exposures. Mean sea level (MSL), mean higher high water (MHHW), and mean lower low water (MLLW) also occur at a different location along the front face of each panel.

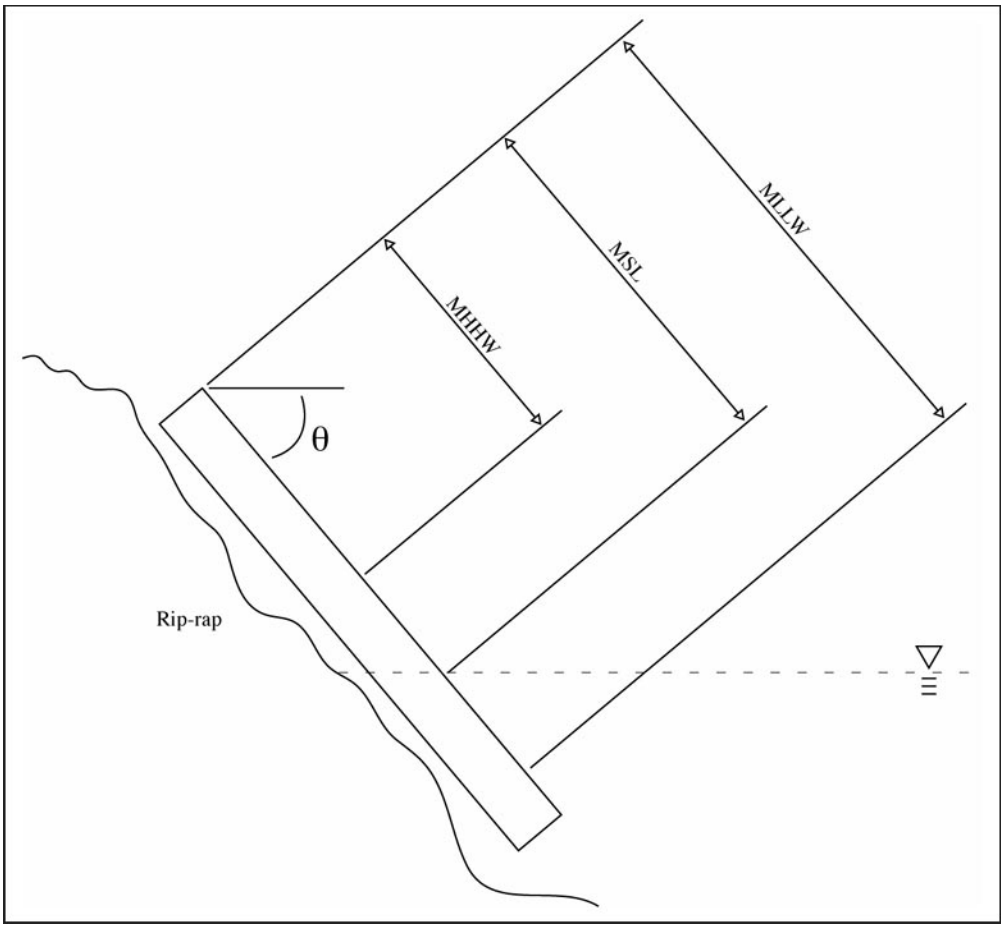

Figure 4.1. Panel orientation and tide levels.

4.2.1 Panel orientation

The vertical angle of each panel was determined using a spirit level and measuring tape. The angle measured, θ, is shown in Figure 4.1. The vertical angles relative to the horizontal plane for each panel are provided in Table 4.1.

Table 4.1. Vertical angles of field panels.

Specimen	Vertical angle (degrees)
Control panel 1	43.9
Control panel 2	43.0
Control panel 7	38.6
DCI panel 3	40.3
DCI panel 3A	38.6
DCI panel 4	41.0
Rheocrete CNI panel 5	40.7
Rheocrete CNI panel 5A	45.4
Rheocrete CNI panel 6	46.6
Rheocrete 222+ panel 15	37.1
Rheocrete 222+ panel 16	39.3
Rheocrete 222+ panel 17	45.4
Rheocrete 222+ panel 17A	46.6
FerroGard 901 panel 18	41.0
FerroGard 901 panel 19	46.0
FerroGard 901 panel 20	42.0
Xypex Admix C-2000 panel 21	40.7
Latex panel 14	43.9
Fly ash panel 11	43.9
Fly ash panel 12	39.6
Fly ash panel 13	42.0
M.B. Silica fume panel 8	49.0
M.B. Silica fume panel 9	48.7
W.R. Grace Silica fume panel 10	45.4
Kryton KIM panel 22	45.1

4.2.2 Test hole locations

Three test holes are located down the center of each panel designated as top, middle, and bottom. The location of each test hole is presented in Table 4.2 as the distance from the top of the panel measured along the front face of the panel.

Table 4.2. Test hole locations.

	Top		Middle		Bottom	
Specimen	in.	(mm)	in.	(mm)	in.	(mm)
Control panel 1	16.8	(427)	27.4	(697)	37.7	(957)
Control panel 2	15.2	(386)	25.8	(656)	37.5	(953)
Control panel 7	16.8	(425)	27.3	(694)	37.5	(953)
DCI panel 3	17.0	(432)	27.6	(702)	37.3	(948)
DCI panel 3A	16.3	(413)	24.7	(627)	36.4	(926)
DCI panel 4	17.3	(438)	27.9	(708)	37.8	(959)
Rheocrete CNI panel 5	17.2	(437)	28.2	(716)	37.3	(946)
Rheocrete CNI panel 5A	6.8	(171)	26.2	(665)	37.1	(943)
Rheocrete CNI panel 6	15.0	(381)	26.4	(670)	38.0	(965)
Rheocrete 222+ panel 15	7.8	(197)	25.3	(643)	36.5	(927)
Rheocrete 222+ panel 16	15.8	(402)	27.2	(691)	37.3	(946)
Rheocrete 222+ panel 17	7.8	(197)	25.8	(654)	37.6	(954)
Rheocrete 222+ panel 17A	15.4	(391)	25.9	(657)	36.9	(937)
FerroGard 901 panel 18	14.8	(376)	27.4	(697)	37.8	(959)
FerroGard 901 panel 19	15.1	(384)	26.3	(667)	37.8	(959)
FerroGard 901 panel 20	17.0	(432)	28.5	(724)	38.3	(972)
Xypex Admix C-2000 panel 21	16.3	(413)	28.0	(711)	37.3	(946)
Latex panel 14	7.5	(191)	28.0	(711)	38.0	(965)
Fly ash panel 11	16.4	(416)	26.9	(683)	37.8	(959)
Fly ash panel 12	15.2	(386)	26.4	(672)	38.4	(976)
Fly ash panel 13	15.8	(400)	27.0	(686)	38.0	(965)
M.B. Silica fume panel 8	7.6	(194)	26.3	(667)	37.6	(956)
M.B. Silica fume panel 9	14.4	(367)	25.5	(648)	36.3	(921)
Grace Silica fume panel 10	15.9	(403)	27.1	(689)	43.7	(1110)
Kryton KIM panel 22	16.3	(414)	27.4	(695)	43.3	(1100)

4.2.3 Tide information

For this study, mean sea level (MSL) was used as the zero datum for the tide level. On June 22, 2004 between 9:00 AM and 11:00 AM, the distance from the top of the panel to the water level was measured along the front face of each panel. Tide information for that day was collected from NOAA (2004) and used to determine the

location of mean sea level with respect to the top of each individual panel. NOAA defines the tidal datum by reference to a mean lower low water (MLLW) level and a mean higher high water (MHHW) level averaged over a 19-year period. At Honolulu Harbor, the MHHW is 12.95 in. (329 mm) above mean sea level. MLLW is 9.88 in. (251 mm) below mean sea level. Between the dates of July 24, 2002 and August 9, 2004, the highest observed water level was 27.12 in. (689 mm) above mean sea level and the lowest observed water level was 15.72 in. (400 mm) below mean sea level. The distances from the top of each panel to mean sea level, mean higher high water, and mean lower low water are presented in Table 4.3.

Table 4.3. Distance from top of panel to MSL, MHHW, and MLLW.

	MSL		MHHW		MLLW	
Specimen	in.	(mm)	in.	(mm)	in.	(mm)
Control panel 1	42.1	(1069)	29.1	(740)	52.0	(1320)
Control panel 2	40.7	(1035)	27.8	(706)	50.6	(1286)
Control panel 7	42.1	(1069)	29.1	(740)	52.0	(1320)
DCI panel 3	46.7	(1186)	33.7	(857)	56.6	(1437)
DCI panel 3A	40.0	(1015)	27.0	(686)	49.8	(1266)
DCI panel 4	32.5	(825)	19.5	(496)	42.4	(1076)
Rheocrete CNI panel 5	47.2	(1199)	34.3	(870)	57.1	(1450)
Rheocrete CNI panel 5A	46.6	(1183)	33.6	(854)	56.4	(1434)
Rheocrete CNI panel 6	39.9	(1013)	26.9	(684)	49.8	(1264)
Rheocrete 222+ panel 15	43.3	(1099)	30.3	(770)	53.1	(1350)
Rheocrete 222+ panel 16	42.4	(1078)	29.5	(749)	52.3	(1329)
Rheocrete 222+ panel 17	56.6	(1438)	43.7	(1109)	66.5	(1689)
Rheocrete 222+ panel 17A	37.9	(964)	25.0	(635)	47.8	(1215)
FerroGard 901 panel 18	39.8	(1010)	26.8	(681)	49.6	(1261)
FerroGard 901 panel 19	41.4	(1053)	28.5	(724)	51.3	(1304)
FerroGard 901 panel 20	39.3	(998)	26.3	(669)	49.2	(1249)
Xypex Admix C-2000 panel 21	42.2	(1072)	29.3	(743)	52.1	(1323)
Latex panel 14	33.9	(862)	21.0	(533)	43.8	(1113)
Fly ash panel 11	42.4	(1076)	29.4	(747)	52.2	(1327)
Fly ash panel 12	47.4	(1205)	34.5	(876)	57.3	(1456)
Fly ash panel 13	42.3	(1073)	29.3	(744)	52.1	(1324)
M.B. Silica fume panel 8	44.8	(1138)	31.9	(809)	54.7	(1389)
M.B. Silica fume panel 9	43.7	(1110)	30.8	(781)	53.6	(1361)
Grace Silica fume panel 10	37.4	(951)	24.5	(622)	47.3	(1202)
Kryton KIM panel 22	47.5	(1206)	34.5	(877)	57.4	(1457)

4.3 Mechanical tests

Tests for slump, compressive strength, elastic modulus, Poisson's ratio, and air content were performed for all of the concrete mixtures described in Chapter 3. This section presents the results and a discussion of how each mixture varied based on aggregate source and admixture amount. The results of the mechanical tests in this study

were also compared to the results obtained for the same mixtures in Phase II. The compressive strength values reported in this chapter are the average of three cylinder compressive strengths for the mixture. Results for the compressive strength of each individual test cylinder from every mixture are provided in Appendix A.

4.3.1 Control mixtures

Mechanical test results for the control mixtures and mixture C2 from the Phase II study are provided in Table 4.4. The average compressive strengths for panels 1 and 7 were lower than the average value for Ameron mixture C2 by about 18% and 5% respectively. The elastic modulus of panel 1 and 7 were higher than that of mixture C2. Poisson's ratio was also higher in panels 1 and 7 than mixture C2.

Table 4.4. Slump, air content, and mechanical test results of control mixtures.

	Panel 1	C2 (Pham)	Panel 2	HCON1 (Okunaga)	Panel 7	C1 (Pham)
Aggregate source	Ameron	Ameron	Halawa	Halawa	Ameron	Ameron
w/c	0.40	0.40	0.40	0.40	0.35	0.35
Paste content (%)	31.2	31.2	31.2	31.2	31.2	31.2
Slump (in.) (mm)	5.50 (140)	4.25 (108)	4.50 (114)	3.00 (76)	7.00 (178)	3.75 (95)
Compressive strength (psi) (MPa)	5789 (39.9)	7050 (48.6)	5312 (36.6)	5270 (36.3)	6727 (46.4)	7620 (52.5)
Elastic modulus (ksi) (GPa)	3547 (24.5)	3200 (22.1)	3604 (24.8)	3862 (26.6)	3934 (27.1)	3900 (26.9)
Poisson's ratio	0.21	0.17	0.13	0.30	0.25	0.17
Air Content (%)	7.0		7.5	5.0	6.0	

4.3.2 DCI mixtures

Mechanical test results for DCI mixtures and mixtures D4 and D5 from the Phase II study are provided in Table 4.5. The mixture for panel 3 and mixture D4 contain the same amount of DCI admixture. The mixture for panel 3A and mixture D5 also contain the same dosage of DCI admixture.

Panel 3 had an average compressive strength about 22% higher than mixture D4. Panel 3 and mixture D4 had similar elastic modulus and Poisson's ratio. Panel 3A had a similar average compressive strength, lower elastic modulus, and higher Poisson's ratio than mixture D5. Mechanical test results for DCI mixtures proportioned with Halawa aggregates from the Phase II study were not available.

Table 4.5. Slump, air content, and mechanical test results of DCI mixtures.

	Panel 3	D4 (Pham)	Panel 3A	D5 (Pham)	Panel 4
Aggregate source	Ameron	Ameron	Ameron	Ameron	Halawa
w/c	0.40	0.40	0.40	0.40	0.40
DCI (gal/yd^3) (l/m^3)	2.0 (9.9)	2.0 (9.9)	4.0 (19.8)	4.0 (19.8)	2.0 (9.9)
Paste content (%)	31.15	31.15	31.15	31.15	31.15
Slump (in.) (mm)	5.50 (140)	6.00 (152)	4.50 (114)	5.75 (146)	5.00 (127)
Compressive strength (psi) (MPa)	8843 (61.0)	7260 (50.1)	8077 (55.7)	8040 (55.4)	6809 (46.9)
Elastic modulus (ksi) (GPa)	4043 (27.9)	4100 (28.3)	4088 (28.2)	4350 (30.0)	3997 (27.6)
Poisson's ratio	0.20	0.20	0.33	0.15	0.10
Air Content (%)	2.5		4.2		5.0

4.3.3 Rheocrete CNI mixtures

Mechanical test results for Rheocrete CNI mixtures and mixtures CNI4 and CNI5 from the Phase II study are provided in Table 4.6. The mixture for panels 5 and 6 and mixture CNI5 contain the same amount of admixture. Panel 5A and mixture CNI5 have the same dosage of admixture.

Panels 5 and 6 had average compressive strengths that were similar to that of mixture CNI4. The elastic modulus for both panels 5 and 6 were higher than the value from mixture CNI4. Poisson's ratio for panel 5 was significantly lower than mixture CNI4, while the value for panel 6 was very close.

The mixture for panel 5A provided a compressive strength that was about 8% higher than mixture CNI5. The elastic modulus of panel 5A was higher than mixture CNI5. Poisson's ratio was lower than the value for mixture CNI5.

Table 4.6. Slump, air content, mechanical test results of Rheocrete CNI mixtures.

	Panel 5	Panel 6	CNI4 (Pham)	Panel 5A	CNI5 (Pham)
Aggregate source	Ameron	Ameron	Ameron	Ameron	Ameron
w/c	0.40	0.40	0.40	0.40	0.40
Rheocrete CNI (gal/yd^3) (l/m^3)	2.0 (9.9)	2.0 (9.9)	2.0 (9.9)	4.0 (19.8)	4.0 (19.8)
Paste content (%)	31.2	31.2	31.2	31.2	31.2
Slump (in.) (mm)	8.50 (216)	6.50 (165)	6.25 (159)	4.00 (102)	8.50 (216)
Compressive strength (psi) (MPa)	7508 (51.8)	7977 (55.0)	7590 (52.3)	8177 (56.4)	7560 (52.1)
Elastic modulus (ksi) (GPa)	4091 (28.2)	4292 (29.6)	3900 (26.9)	4415 (30.4)	3800 (26.2)
Poisson's ratio	0.08	0.21	0.24	0.10	0.18
Air Content (%)	3.5	7.0	3.6	4.0	3.5

4.3.4 Rheocrete 222+ mixtures

Mechanical test results for Rheocrete 222+ mixtures and mixture RHE2 from the Phase II study are provided in Table 4.7. In terms of compressive strength, the Rheocrete 222+ mixtures performed poorly. The average compressive strengths for panels 15 and 16 were about 35% and 52% lower than mixture RHE2 respectively. Results for elastic modulus and Poisson's ratio were also lower than the results from mixture RHE2.

Table 4.7. Slump, air content, and mechanical test results of Rheocrete 222+ mixtures.

	Panel 15	Panel 16	RHE2 (Pham)	Panel 17	Panel 17A	HRHE1 (Okunaga)
Aggregate source	Ameron	Ameron	Ameron	Halawa	Halawa	Halawa
w/c	0.40	0.40	0.40	0.40	0.40	0.40
Rheocrete 222+ (gal/yd^3) (l/m^3)	1.0 (5.0)	1.0 (5.0)	1.0 (5.0)	1.0 (5.0)	1.0 (5.0)	1.0 (5.0)
Paste content (%)	31.2	31.2	31.2	31.2	31.2	31.2
Slump (in.) (mm)	8.00 (203)	7.00 (178)	4.25 (108)	5.50 (140)	5.50 (140)	4.50 (114)
Compressive strength (psi) (MPa)	4218 (29.1)	3148 (21.7)	6530 (45.0)	1576 (10.9)	2010 (13.9)	5980 (41.2)
Elastic modulus (ksi) (GPa)	3234 (22.3)	2967 (20.5)	3650 (25.2)	2154 (14.9)	2547 (17.6)	3591 (24.8)
Poisson's ratio	0.12	0.12	0.22	0.06	0.11	0.19
Air Content (%)	8.0	10.0	6.5	6.0	11.0	4.3

4.3.5 FerroGard 901 mixtures

Mechanical test results for FerroGard 901 mixtures and mixture FER2 from the Phase II study are provided in Table 4.8. Panel 20 had an average compressive strength that was about 15% higher than mixture FER2. The elastic modulus for this mixture was higher than the results of mixture FER2, and slightly lower for Poisson's ratio.

Mechanical test results for FerroGard 901 mixtures proportioned with Halawa aggregates from the Phase II study were not available.

Table 4.8. Slump, air content, and mechanical test results of FerroGard 901 mixtures.

	Panel 18	Panel 19	Panel 20	FER2 (Pham)
Aggregate source	Halawa	Halawa	Ameron	Ameron
w/c	0.40	0.40	0.40	0.40
FerroGard 901 (gal/yd^3) (l/m^3)	3.0 (14.9)	3.0 (14.9)	3.0 (14.9)	3.0 (14.9)
Paste content (%)	31.2	31.2	31.2	31.2
Slump (in.) (mm)	8.00 (203)	5.00 (127)	6.50 (165)	7.50 (191)
Compressive strength (psi) (MPa)	5789 (39.9)	6267 (43.2)	7547 (52.0)	6540 (45.1)
Elastic modulus (ksi) (GPa)	4121 (28.4)	4038 (27.8)	3852 (26.6)	3500 (24.1)
Poisson's ratio	0.14	0.19	0.21	0.22
Air Content (%)	6.5	4.8	5.5	

4.3.6 Xypex Admix C-2000 mixtures

Mechanical test results for the Xypex Admix C-2000 mixture and mixture XYP2 of the Phase II study are provided in Table 4.9. Panel 21 provided an average compressive strength that was about 3% higher that mixture XYP2. Panel 21 had a higher elastic modulus and a lower Poisson's ratio than mixture XYP2.

Table 4.9. Slump, air content, and mechanical test results of Xypex mixtures.

	Panel 21	XYP2 (Pham)
Aggregate source	Ameron	Ameron
w/c	0.40	0.40
Xypex (% of cement wt.)	2.0	2.0
Paste content (%)	31.2	31.2
Slump (in.) (mm)	7.00 (178)	6.00 (152)
Compressive strength (psi) (MPa)	5642 (38.9)	5460 (37.6)
Elastic modulus (ksi) (GPa)	3720 (25.6)	3150 (21.7)
Poisson's ratio	0.09	0.19
Air Content (%)	7.0	4.8

4.3.7 Latex-modified mixtures

The mechanical test results for the latex-modified mixture and mixture L5 of the Phase II study are provided in Table 4.10. The mixture for panel 14 provided a higher compressive strength than mixture L5 by about 16%. Panel 14 had a higher elastic modulus and lower Poisson's ratio than mixture L5.

Table 4.10. Slump, air content, and mechanical test results of latex-modified mixtures.

	Panel 14	L5 (Pham)
Aggregate source	Ameron	Ameron
w/c	0.40	0.40
Latex (% of cement wt.)	5.0	5.0
Paste content (%)	33.3	33.3
Slump (in.) (mm)	8.50 (216)	9.75 (248)
Compressive strength (psi) (MPa)	5200 (35.9)	4490 (31.0)
Elastic modulus (ksi) (GPa)	3339 (23.0)	3025 (20.9)
Poisson's ratio	0.12	0.24
Air Content (%)	5.5	

4.3.8 Fly ash mixtures

Mechanical test results for fly ash mixtures and mixture FA4 from the Phase II study are provided in Table 4.11. The average compressive strength for the mixture of Panel 11 was about 27% higher than that of mixture FA4. The elastic modulus was higher than mixture FA4 and Poisson's ratio was lower. Mechanical test results for fly ash mixtures proportioned with Halawa aggregates from the Phase II study were not available.

4.3.9 Silica fume mixtures

Mechanical test results for silica fume mixtures and mixture SF2 from the Phase II study are provided in Table 4.12. Panel 8 had an average compressive strength that is about 1% lower than mixture SF2. Panel 9 and 10 provided an average compressive strength that was about 1% and 2% higher than mixture SF2. All three panel mixtures

had a lower elastic modulus than mixture SF2. Panels 8 and 10 have higher values of Poisson's ratio than mixture SF2, while Panel 9 had a lower value.

Table 4.11. Slump, air content, and mechanical test results of fly ash mixtures.

	Panel 11	Panel 12	FA4 (Pham)	Panel 13
Aggregate source	Ameron	Halawa	Ameron	Halawa
w/c	0.36	0.36	0.36	0.36
Fly ash (%)	15.0	15.0	15.0	15.0
Paste content (%)	33.2		33.2	
Slump (in.) (mm)	8.00 (203)	3.00 (76)	8.75 (222)	3.00 (76)
Compressive strength (psi) (MPa)	9633 (66.4)	8336 (57.5)	7610 (52.5)	7853 (54.1)
Elastic modulus (ksi) (GPa)	4490 (31.0)	4522 (31.2)	4100 (28.3)	4366 (30.1)
Poisson's ratio	0.20	0.16	0.25	0.10
Air Content (%)	1.0	1.5		1.0

Table 4.12. Slump, air content, and mechanical test results of silica fume mixtures.

	Panel 8	Panel 9	Panel 10	SF2 (Pham)
Aggregate source	Ameron	Ameron	Ameron	Ameron
w/c	0.36	0.36	0.36	0.36
Silica fume content (%)	5.0	5.0	5.0	5.0
Paste content (%)	32.9	32.9	32.9	32.9
Slump (in.) (mm)	7.00 (178)	6.75 (171)	6.00 (152)	8.00 (203)
Compressive strength (psi) (MPa)	9131 (63.0)	9297 (64.1)	9410 (64.9)	9210 (63.5)
Elastic modulus (ksi) (GPa)	4520 (31.2)	4669 (32.2)	4360 (30.1)	4700 (32.4)
Poisson's ratio	0.19	0.12	0.25	0.17
Air Content (%)	1.0	1.5	1.0	

4.3.10 Kryton KIM mixture

Mechanical test results for the Kryton KIM mixture is provided in Table 4.13. Because Kryton KIM was used for the first time in the Phase III study, there were no previous results for comparison.

Table 4.13. Slump, air content, and mechanical test results of Kryton KIM mixture.

	Kryton
	Panel 22
Aggregate source	Ameron
w/c	0.40
Kryton Kim (lb/yd^3) (kg/m^3)	13.50 (6.1)
Paste content (%)	32.9
Slump (in.) (mm)	2.00 (51)
Compressive strength (psi) (MPa)	8036 (55.4)
Elastic modulus (ksi) (GPa)	4176 (28.8)
Poisson's ratio	0.03
Air Content (%)	2.0

4.3.11 Compressive strength comparison

A comparison of the average compressive strength of all the mixtures shows that the Ameron mixtures provided higher average compressive strengths than the Halawa mixtures. The water-cement ratios were 0.40 for all the mixtures except control 7, which had a water-cement ratio of 0.35, and all the fly ash and silica fume mixtures had water-cement ratios of 0.36.

Fly ash and silica fume provided the highest average compressive strengths. The next highest strengths were provided by DCI, Rheocrete CNI, and Kryton KIM.

FerroGard 901, Xypex Admix C-2000, and latex provided similar average compressive strengths to the control mixtures, indicating that there was little influence on compressive strength. The Rheocrete 222+ mixtures had significantly lower average compressive strengths than the control mixtures. Because mixture 17 provided a low average compressive strength, a duplicate, mixture 17A, was created to rule out any errors.

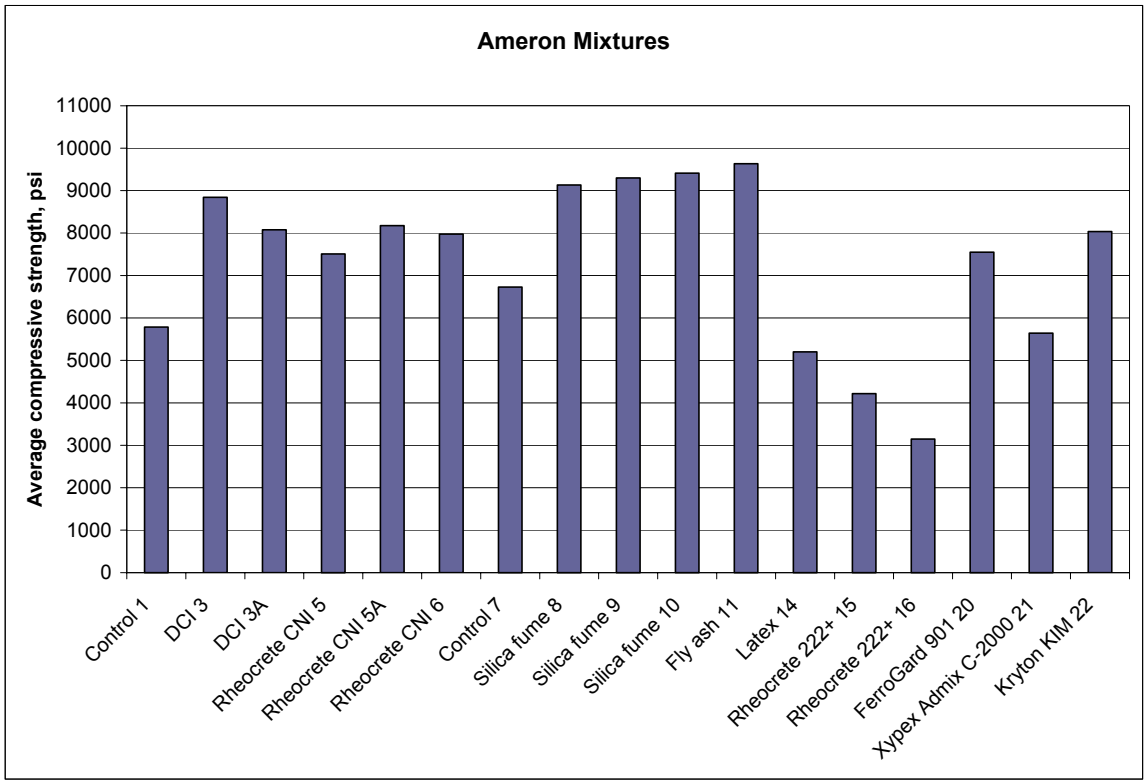

Figure 4.2. Average compressive strength of Ameron mixtures.

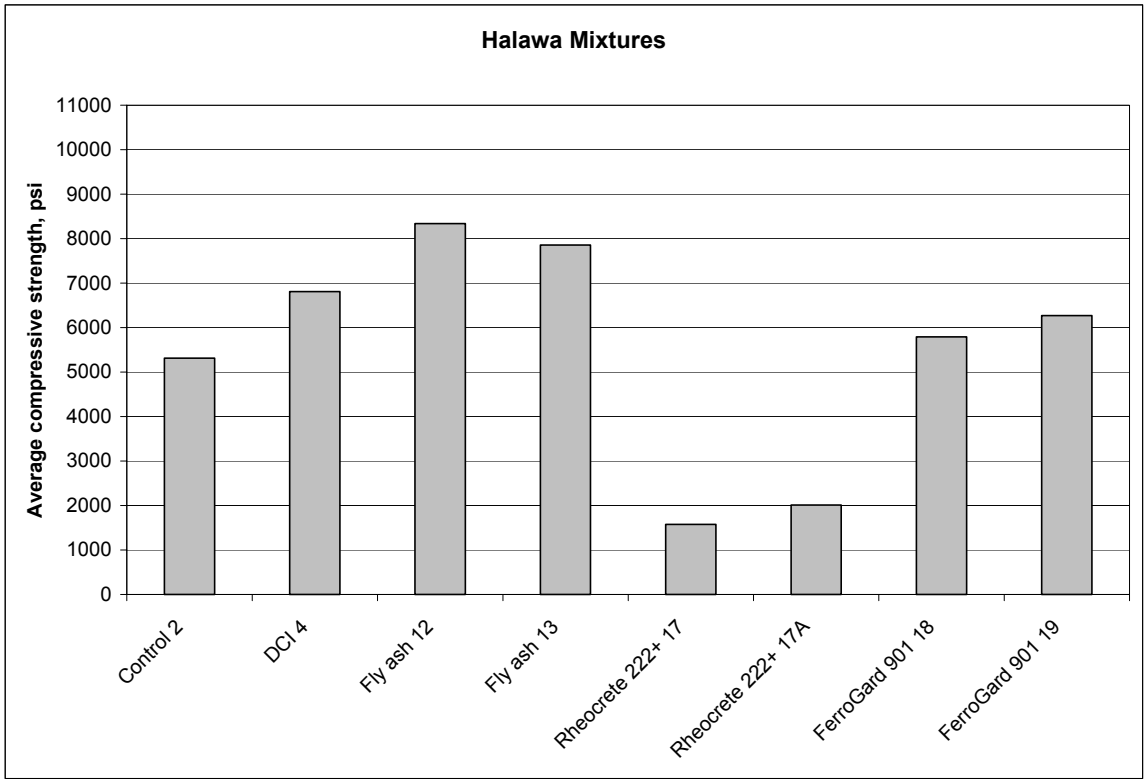

Figure 4.3. Average compressive strength of Halawa mixtures.

4.4 Chloride concentration

Chloride concentration tests were performed to determine the acid-soluble chloride concentration of each panel. The concrete dust sample collected at a depth of 0.5 in. (13 mm) represent concrete dust from a depth of 0.5 (13 mm) in to 1.0 in (25 mm). Dust samples from a depth of 1.0 in. (25 mm) represent concrete dust from 1.0 in. (25 mm) to 1.5 in. (38 mm), and samples from 1.5 in. (38 mm) actually represent concrete dust from a depth of 1.5 in. (38 mm) to 2.0 in. (51 mm). The duration of exposure, in days, of each individual sample is reported in each figure. Results of the chloride concentration tests were converted from percentage by mass of concrete to percentage by mass of cement using the cement content from the mixture proportions and can be found

in Appendix B. The ACI threshold reported in each figure represents the threshold for new concrete tested between 28 and 42 days.

4.4.1 Control mixtures

The results of the chloride concentration tests for the control panels are provided in Figure 4.4, Figure 4.5, and Figure 4.6. The chloride concentrations decrease at increasing depths for panel 1. The top test hole had the highest concentrations at each depth, followed by the bottom hole and the middle hole. Concentrations at a depth of 1.5 in. (38 mm) were near or below the 0.20% ACI threshold, which indicates that corrosion probably was not taking place at the level of the steel for panel 1.

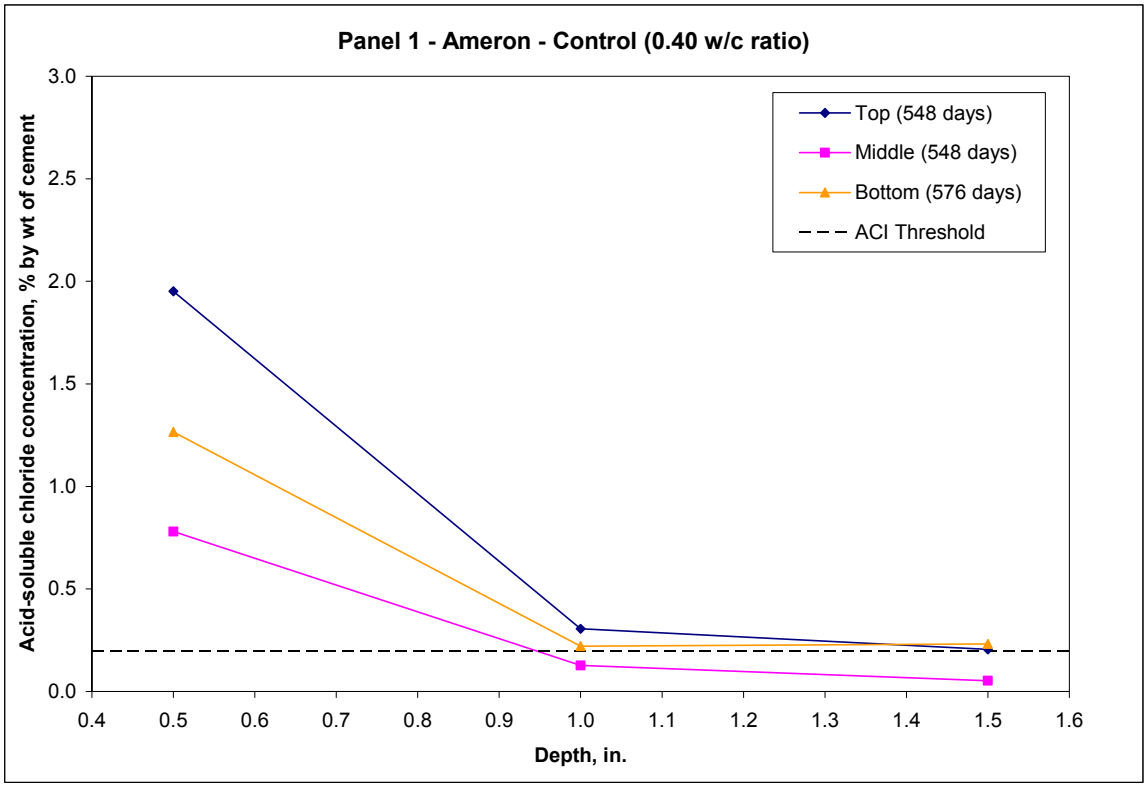

Figure 4.4. Acid-soluble chloride concentration vs. depth for panel 1.

Chloride concentrations for panel 2 were generally lower than panel 1. The chloride concentrations were higher near the surface of the concrete and decreased near the reinforcing steel. The top test hole had the highest concentrations at each depth, followed by the middle hole and the bottom hole. Concentrations at depths of 1.0 in. (25 mm) and 1.5 in. (38 mm) for all three test holes were below the 0.20% ACI threshold, which denotes that corrosion probably was not occurring at the depth of the steel for panel 2.

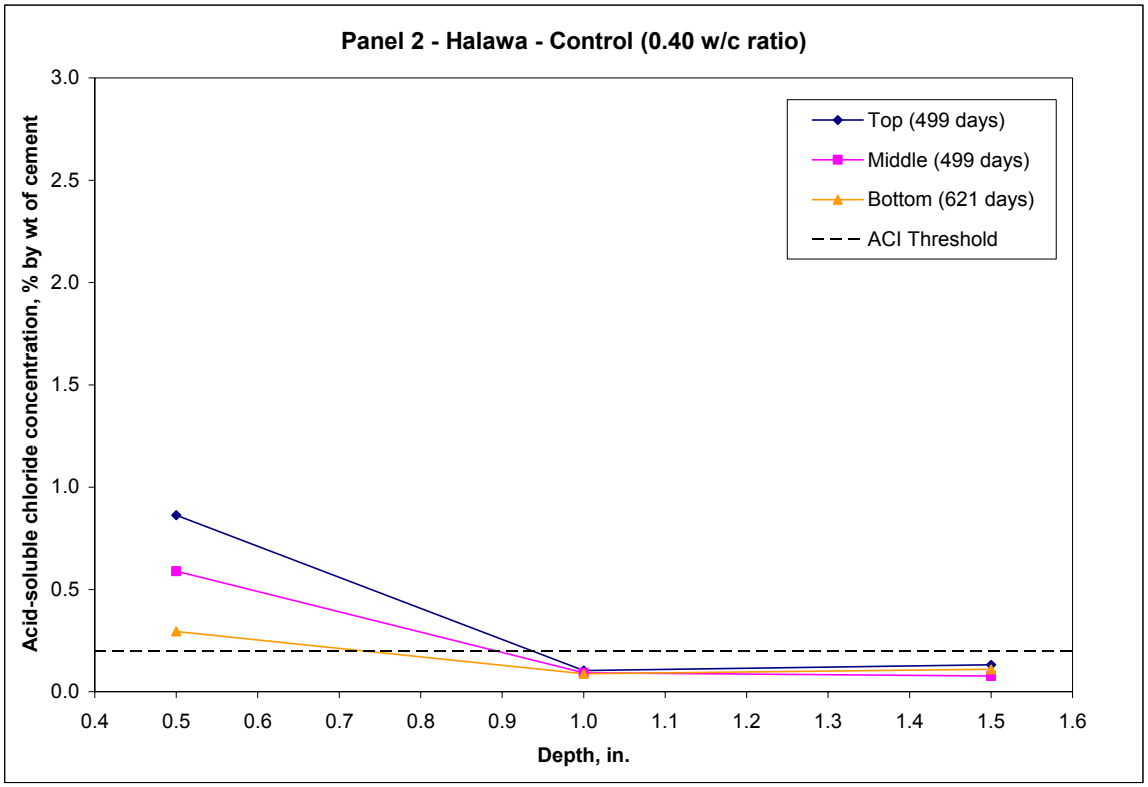

Figure 4.5. Acid-soluble chloride concentration vs. depth for panel 2.

Chloride concentrations for panel 7 were also collectively lower than panel 1. The chloride concentrations were higher near the surface of the concrete and decreased

near the reinforcing steel. The bottom test hole had the highest concentrations at each depth, followed by the middle hole and the top hole. Concentrations at depths of 1.0 in. (25 mm) and 1.5 in. (38 mm) for the middle and bottom test holes were below the 0.20% ACI threshold, which suggests that corrosion probably was not taking place at the level of the steel for panel 7.

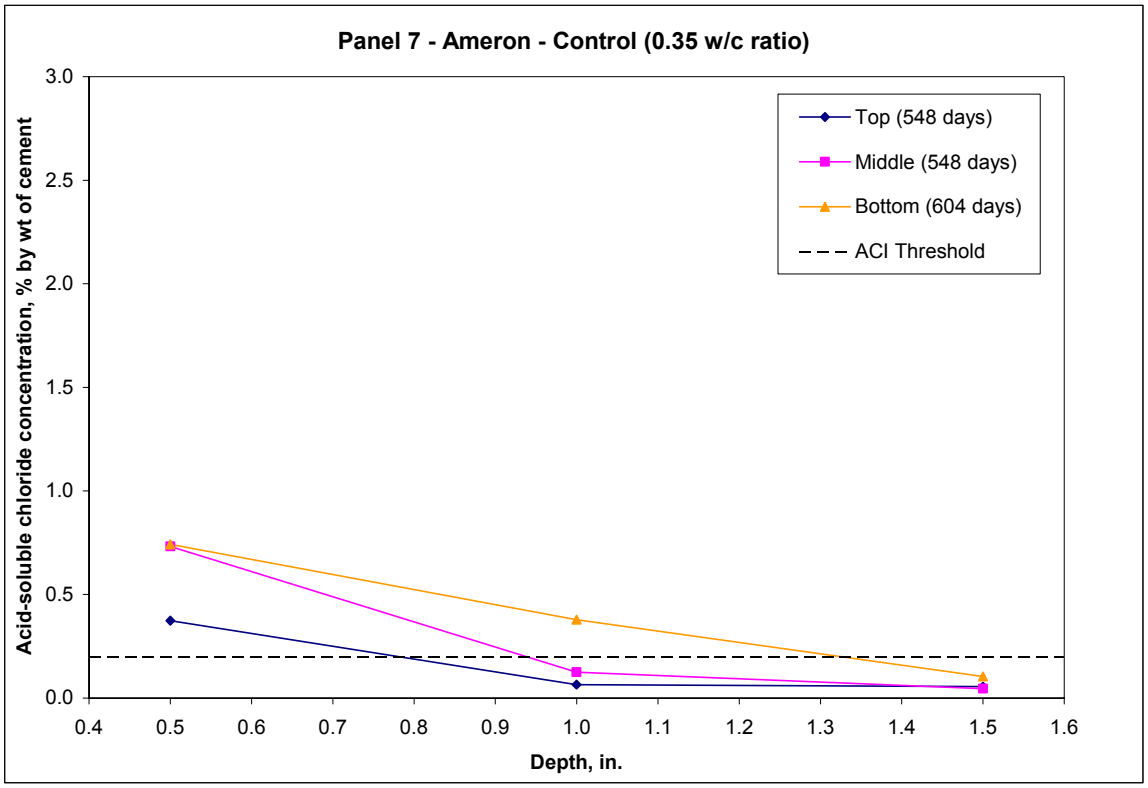

Figure 4.6. Acid-soluble chloride concentration vs. depth for panel 7.

4.4.2 DCI mixtures

Chloride concentration results for the DCI panels are presented in Figure 4.7, Figure 4.8, and Figure 4.9. The chloride concentrations decreased at increasing depths for panel 3. The chloride concentration at a depth of 0.5 in. (13 mm) for the bottom test hole was slightly lower than the same depth at the top hole, but the bottom hole had the highest overall concentrations, followed by the top hole and the middle hole. Concentrations at a depth of 1.5 in. (38 mm) were below the 0.20% ACI threshold for all three test holes, which indicates that corrosion probably was not occurring at the level of the steel.

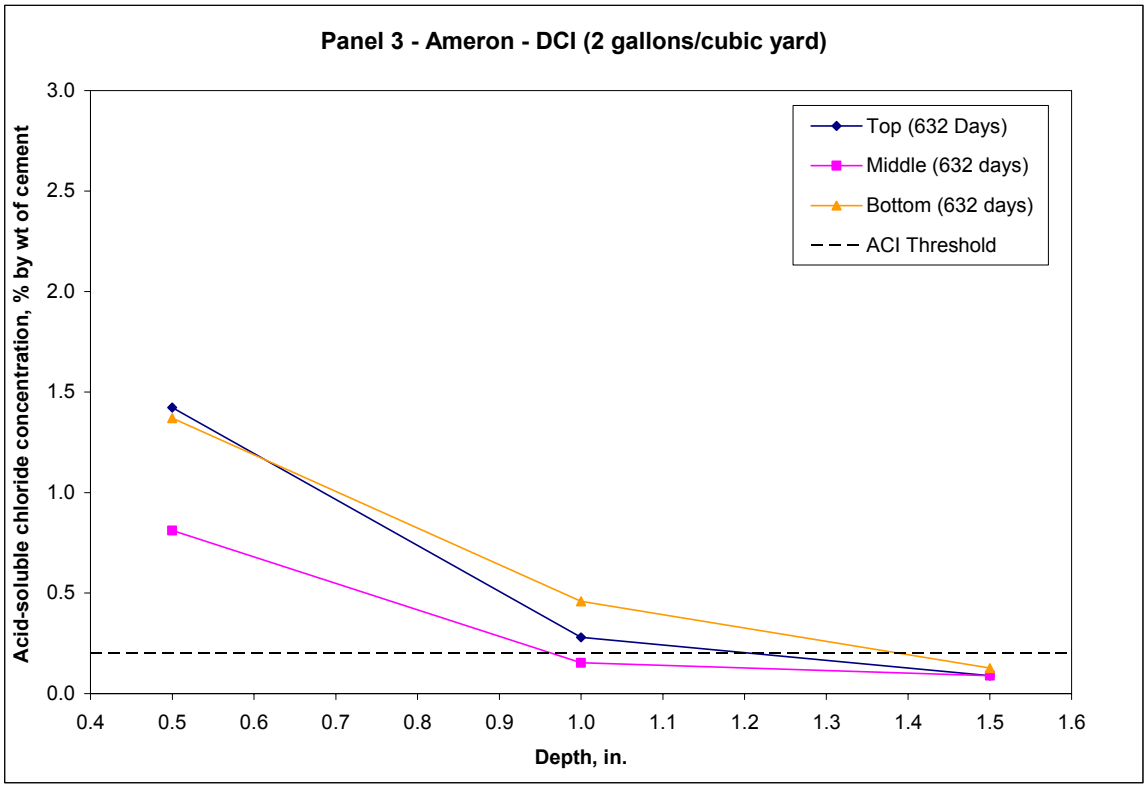

Figure 4.7. Acid-soluble chloride concentration vs. depth for panel 3.

Chloride concentrations for panel 3A were collectively lower than panel 3. Panel 3A had twice the amount of DCI as panel 3, and according to the manufacturer, Grace Construction, increasing the dosage increases the corrosion protection. The chloride concentrations for all three tests holes were higher near the surface of the concrete and decreased near the reinforcing steel. The bottom hole had the highest concentrations at each depth, followed by the middle hole and the top hole. Concentrations at depths of 1.0 in. (25 mm) and 1.5 in. (38 mm) for all three test holes are below the 0.20% ACI threshold, which denotes that corrosion probably is not taking place at the depth of the steel.

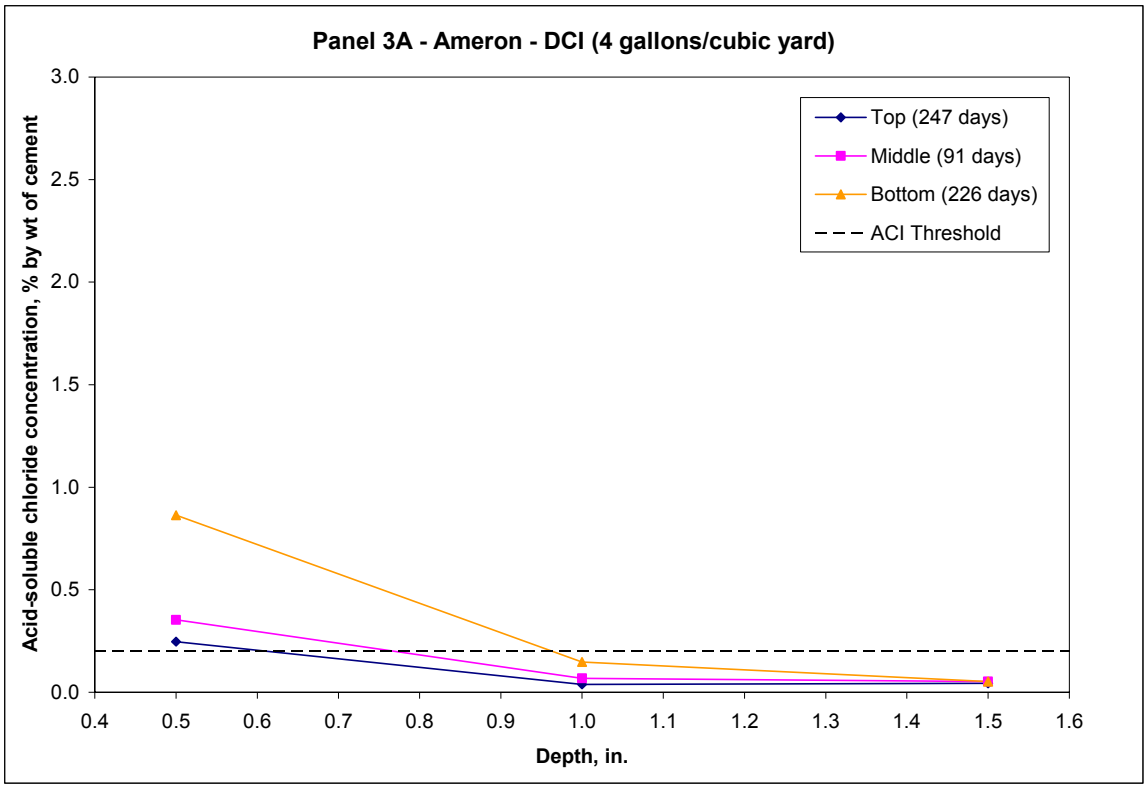

Figure 4.8. Acid-soluble chloride concentration vs. depth for panel 3A.

Chloride concentrations for panel 4 were also generally lower than panel 3, with the exception of the concentrations in the top test hole. The low concentrations can be attributed to the difference in age between the two panels. Overall, the chloride concentrations are higher near the surface of the concrete and decrease near the reinforcing steel. The top test hole has the highest concentrations at each depth, followed by the bottom and middle hole. Test results from the top hole at a depth of 1.0 in. (25 mm) were higher than the results from the middle and bottom holes at a depth of 0.5 in. (13 mm). Concentrations at depths of 1.0 in. (25 mm) and 1.5 in. (38 mm) for the middle and bottom test holes are below the 0.20% ACI threshold, which indicates that corrosion probably is not occurring at the level of the steel.

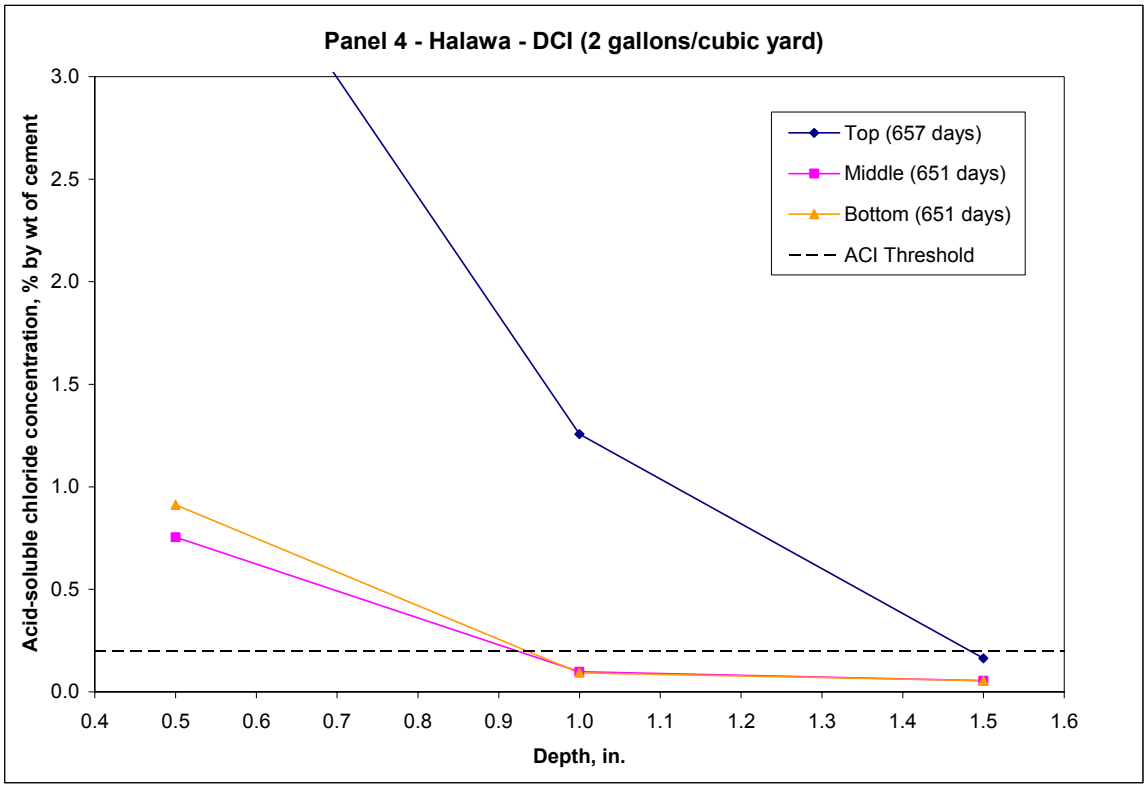

Figure 4.9. Acid-soluble chloride concentration vs. depth for panel 4.

4.4.3 Rheocrete CNI mixtures

The results of the chloride concentration tests for the Rheocrete CNI panels are provided in Figure 4.10, Figure 4.11, and Figure 4.12. Chloride concentrations decrease at increasing depths for panel 5. The bottom test hole has concentrations that are significantly higher than the middle and top holes. The middle test hole has the next highest concentrations followed by the top test. The middle test hole has a slightly lower concentration at the depth of 0.5 in. (13 mm) than the top test hole. Concentrations at a depth of 1.5 in. (38 mm) are near or below the 0.20% ACI threshold at the top and middle test holes, which indicates that corrosion probably is not taking place at the depth of the steel.

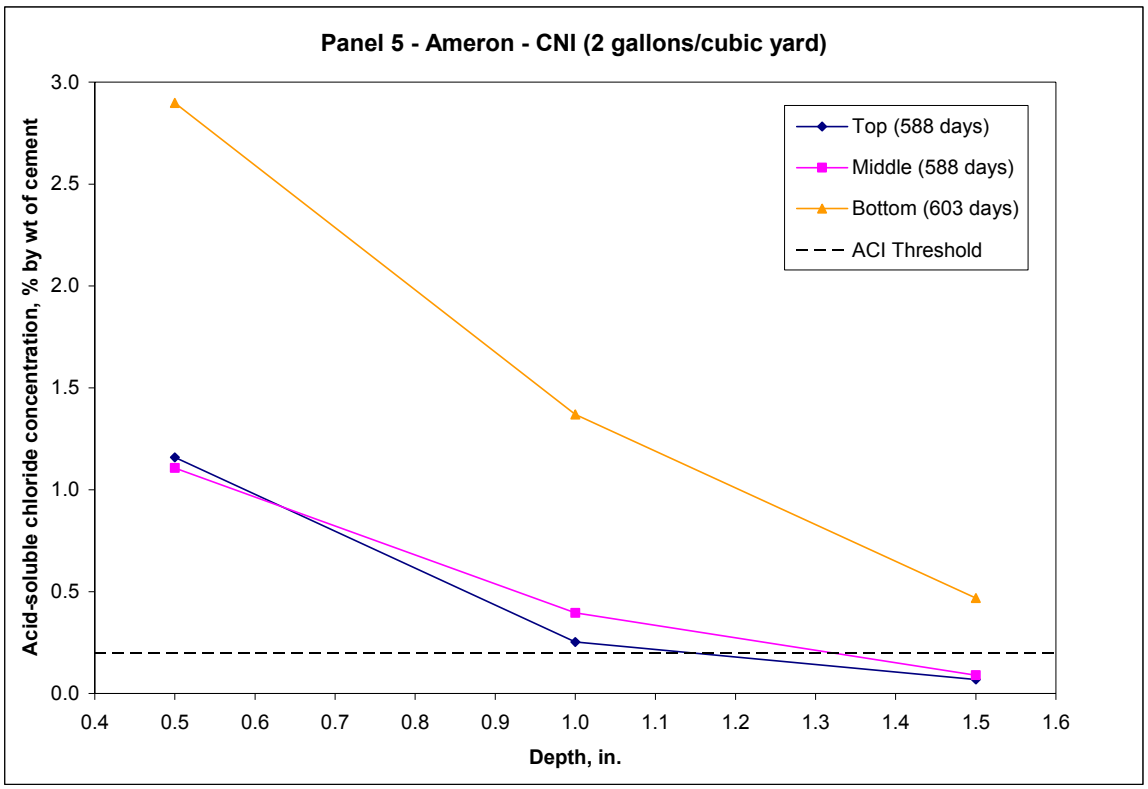

Figure 4.10. Acid-soluble chloride concentration vs. depth for panel 5.

Chloride concentrations for panel 5A are collectively lower than panel 5. The low concentrations can be attributed to the difference in age between the two panels. Panel 5A has twice the amount of Rheocrete CNI as panel 5, and according to the manufacturer, Master Builders, Inc., increasing the dosage increases the corrosion protection. The chloride concentrations for all three tests holes are higher near the surface of the concrete and decrease near the reinforcing steel. The bottom hole has the highest concentrations at a depth of 0.5 in. (13 mm), followed by the middle hole and the top hole. All three have similar concentrations at depths of 1.0 in. (25 mm) and 1.5 in. (38 mm), which are below the 0.20% ACI threshold.

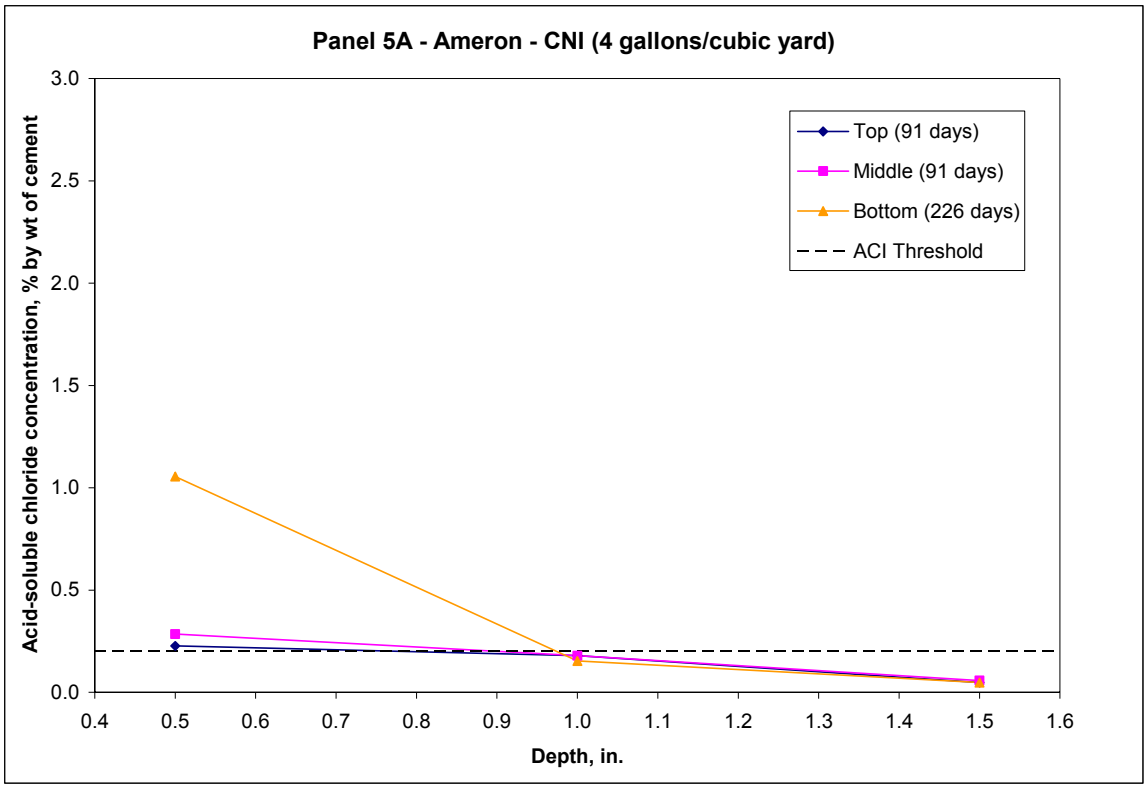

Figure 4.11. Acid-soluble chloride concentration vs. depth for panel 5A.

Chloride concentrations for panel 6 are also generally lower than panel 5. Overall, the chloride concentrations are higher near the surface of the concrete and decrease near the reinforcing steel. The bottom test hole has the highest concentrations at each depth, followed by the top and middle hole. The chloride concentration increased slightly for the middle hole from a depth of 1.0 in. (25 mm) to the depth of 1.5 in. (38 mm). Concentrations at depths of 1.0 in. (25 mm) and 1.5 in. (38 mm) for all three test holes are below the 0.20% ACI threshold, with the exception of the result from the middle hole at the 1.5 in. (38 mm) depth.

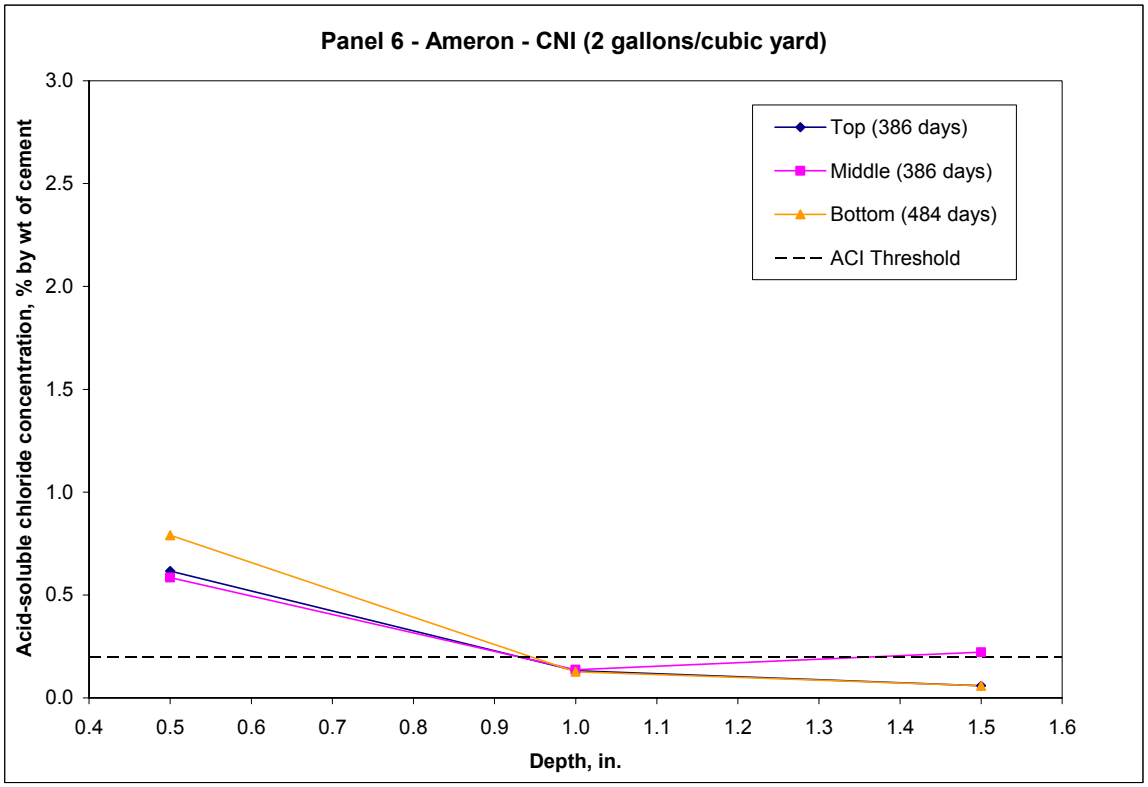

Figure 4.12. Acid-soluble chloride concentration vs. depth for panel 6.

4.4.4 Rheocrete 222+ mixtures

Chloride concentration results for the Rheocrete 222+ panels are presented in Figure 4.13, Figure 4.14, Figure 4.15, and Figure 4.16. The chloride concentrations decrease at increasing depths for panel 15. The chloride concentration at a depth of 0.5 in. (13 mm) for the bottom hole is slightly lower than the same depth at the top hole, but the bottom hole has the highest overall concentrations, followed by the top hole and the middle hole. Concentrations at a depth of 1.5 in. (38 mm) are below the 0.20% ACI threshold for all three test holes, which indicates that corrosion probably is not occurring at the level of the steel for panel 15.

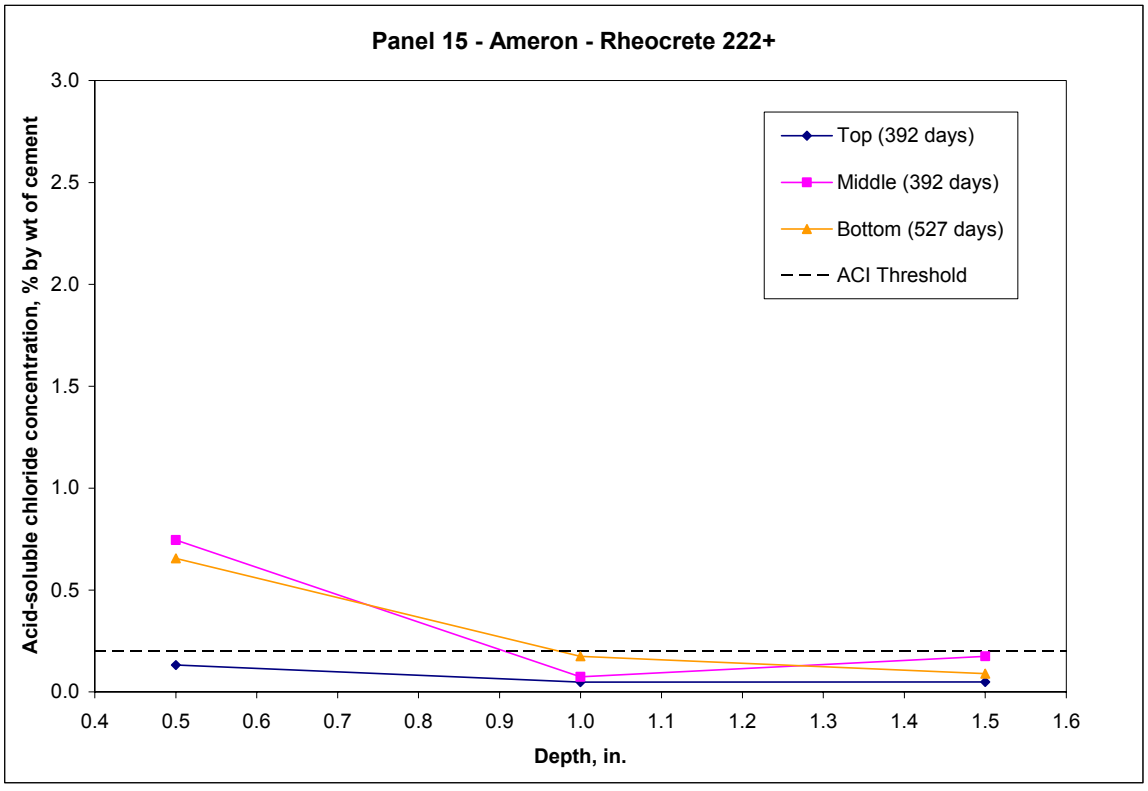

Figure 4.13. Acid-soluble chloride concentration vs. depth for panel 15.

Chloride concentrations for panel 16 are collectively higher than panel 15. The chloride concentrations for all three tests holes are higher near the surface of the concrete and decrease near the reinforcing steel. The bottom hole has the highest concentrations at a depth of 0.5 in. (13 mm), followed by the middle hole and the top hole. All three have similar concentrations at a depth of 1.5 in. (38 mm), which are below the 0.20% ACI threshold.

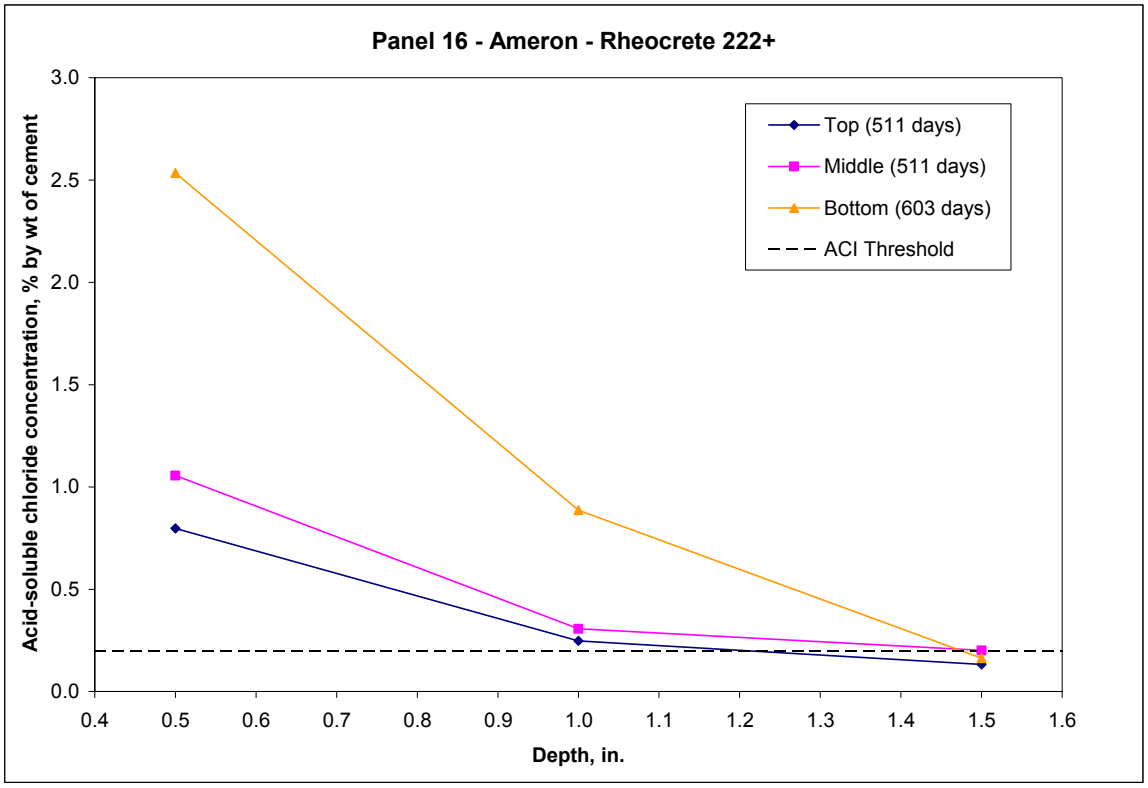

Figure 4.14. Acid-soluble chloride concentration vs. depth for panel 16.

Chloride concentrations for panel 17 are similar to panel 15. Overall, the chloride concentrations are higher near the surface of the concrete and decrease near the reinforcing steel. The middle test hole has the highest concentrations at each depth, followed by the top and bottom hole. Concentrations at depths of 1.0 in. (25 mm) and 1.5 in. (38 mm) for all three test holes are below the 0.20% ACI threshold, which indicates that corrosion probably has not reached the depth of the steel for panel 17.

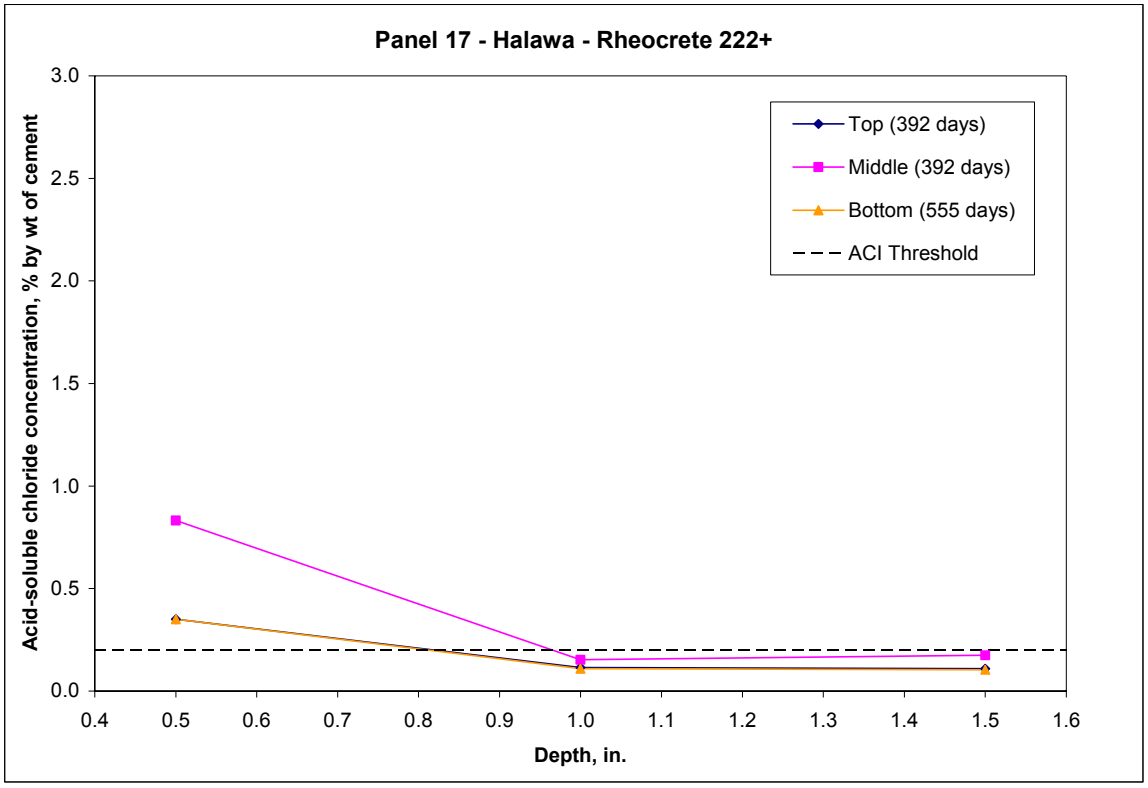

Figure 4.15. Acid-soluble chloride concentration vs. depth for panel 17.

Chloride concentrations for panel 17A are slightly higher than panel 17. The chloride concentrations for all three tests holes are higher near the surface of the concrete and decrease near the reinforcing steel. The bottom test hole has the highest concentrations at a depth of 0.5 in. (13 mm), followed by the top and middle hole. Concentrations at depths of 1.0 in. (25 mm) and 1.5 in. (38 mm) for the top and middle test holes are below the 0.20% ACI threshold, while the concentrations for the bottom hole are at or above the ACI threshold at the same depths.

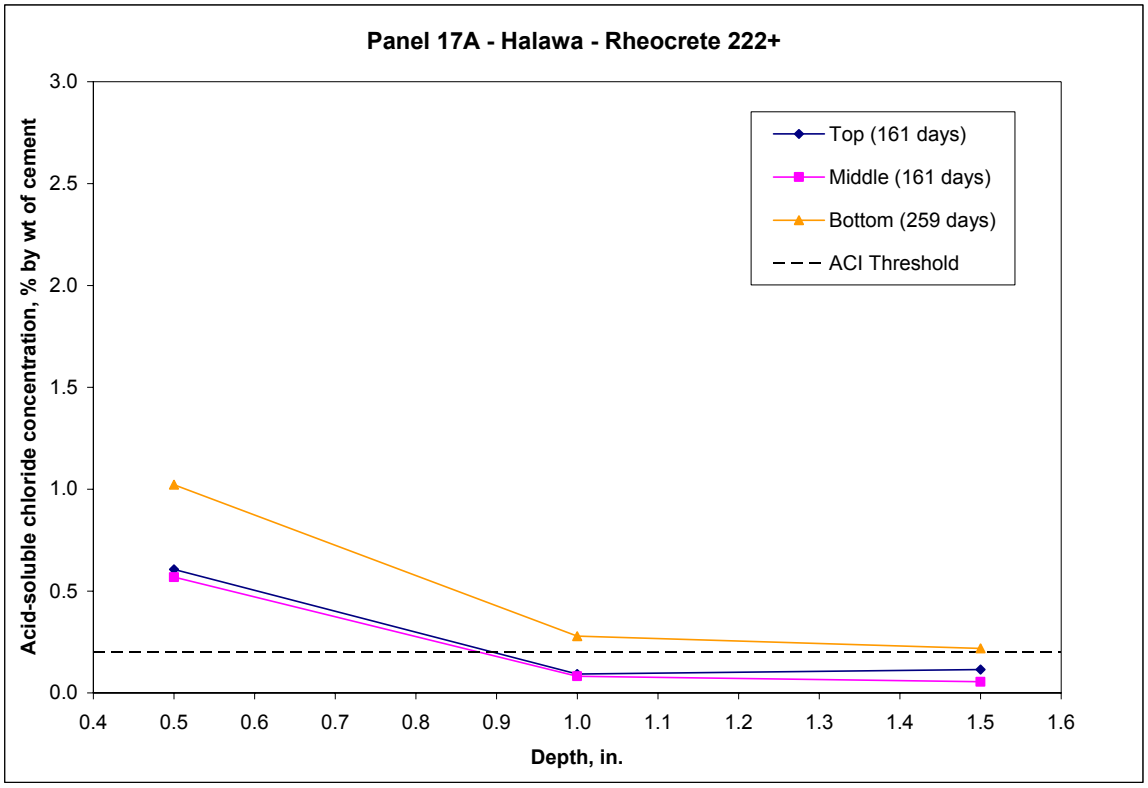

Figure 4.16. Acid-soluble chloride concentration vs. depth for panel 17A.

4.4.5 FerroGard 901 mixtures

The results of the chloride concentration tests for the FerroGard 901 panels are provided in Figure 4.17, Figure 4.18, and Figure 4.19. Chloride concentrations decrease at increasing depths for the three test holes of panel 18 except for the middle test hole. The middle test hole has concentrations that are significantly higher than the top and bottom holes. The concentration increases from the 0.5 (13 mm) depth to the 1.0 in. (25 mm) depth, and then decreases to the 1.5 in. (38 mm) depth. This unusual result may indicate an error in the 1.0 in depth reading. Concentrations at a depth of 1.5 in. (38 mm) are near or below the 0.20% ACI threshold for all three test holes, which indicates that corrosion probably is not taking place at the level of the steel.

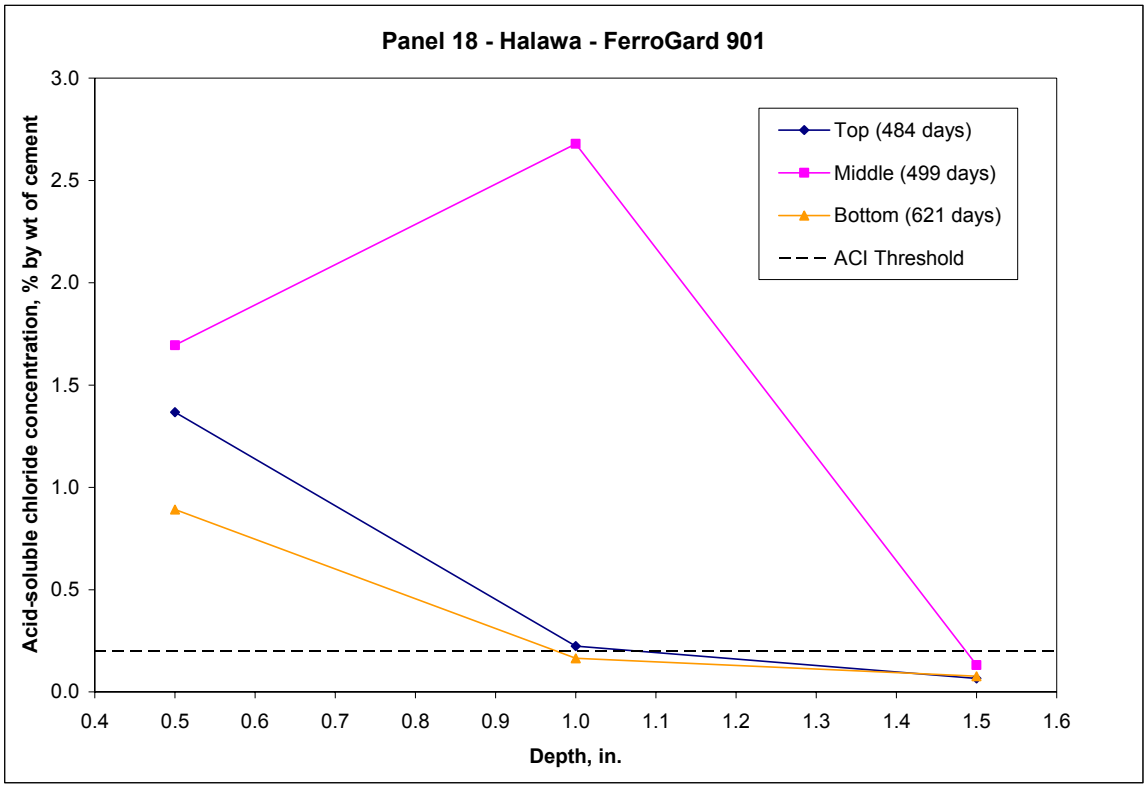

Figure 4.17. Acid-soluble chloride concentration vs. depth for panel 18.

Chloride concentrations for panel 19 are collectively lower than panel 18. The chloride concentrations for all three tests holes are higher near the surface of the concrete and decrease near the reinforcing steel. The bottom test hole has the highest concentrations at each depth, followed by the middle hole and the top hole. Concentrations at depths of 1.0 in. (25 mm) and 1.5 in. (38 mm) for all the test holes are below the 0.20% ACI threshold, which suggests that corrosion probably is not occurring at the depth of the steel for panel 18.

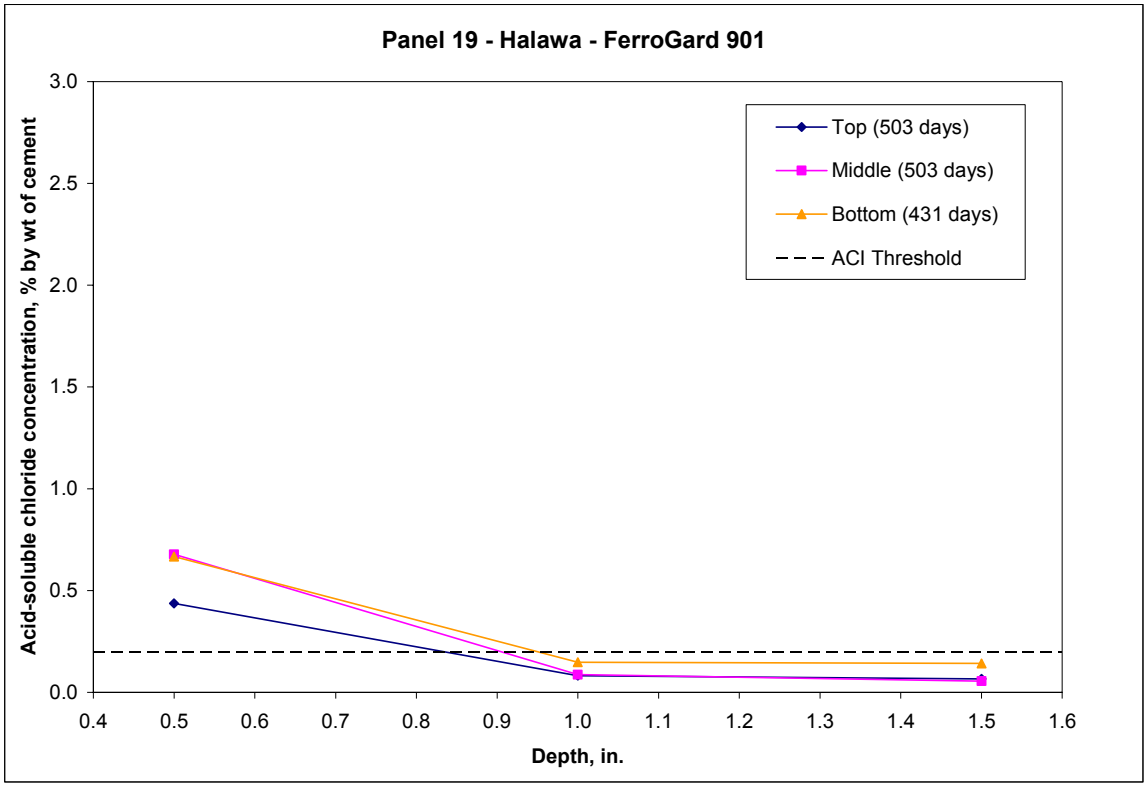

Figure 4.18. Acid-soluble chloride concentration vs. depth for panel 19.

Chloride concentrations for panel 20 are also generally lower than panel 18. Overall, the chloride concentrations are higher near the surface of the concrete and decrease near the reinforcing steel. The middle test hole had the highest chloride concentrations at all depths, followed by the top and bottom holes with the exception of the result from the top hole at the 1.0 in. (25 mm) depth. Concentrations at depths of 1.0 in. (25 mm) and 1.5 in. (38 mm) for all three test holes are below the 0.20% ACI threshold, with the exception of the result from the top hole at the 1.0 in. (25 mm) depth.

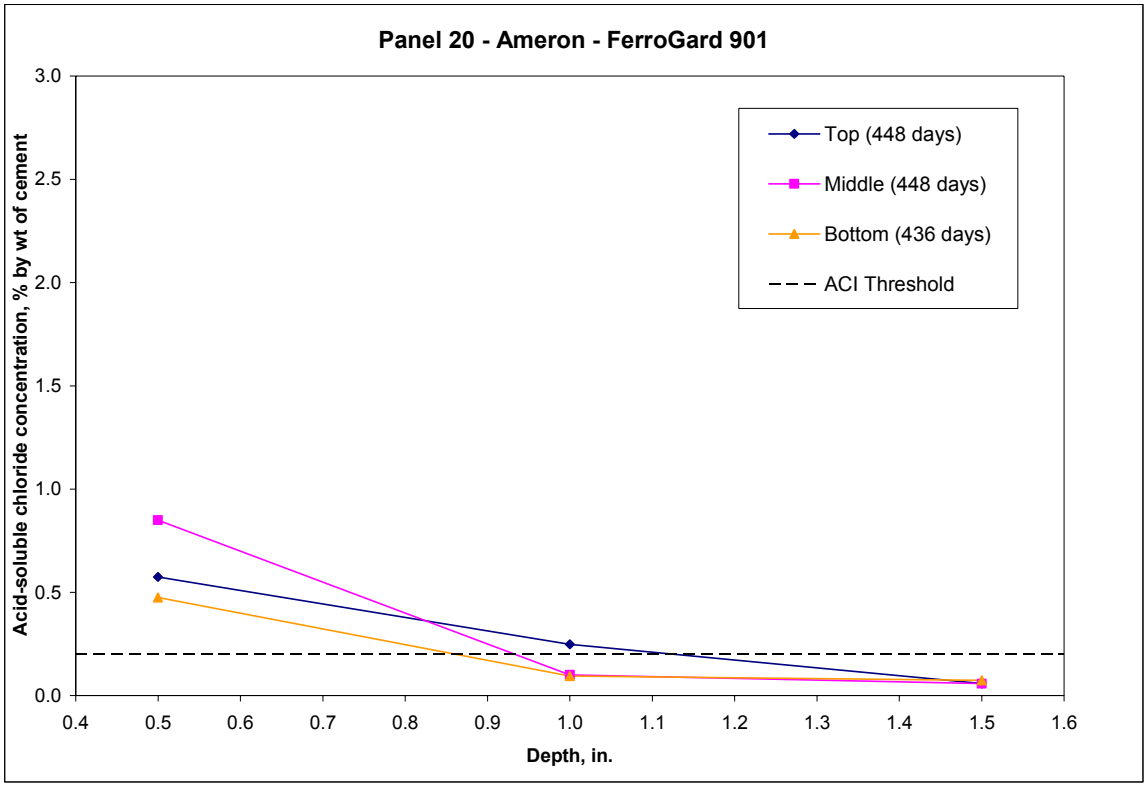

Figure 4.19. Acid-soluble chloride concentration vs. depth for panel 20.

4.4.6 Xypex Admix C-2000 mixture

The results of the chloride concentration tests for the Xypex Admix C-2000 panel are provided in Figure 4.20. Chloride concentrations decrease at increasing depths for all test holes. The middle test hole has the highest chloride concentrations at each depth, followed by the bottom and top. However, the top hole has the highest concentration at a depth 1.0 in. (25 mm). Concentrations at a depth of 1.5 in. (38 mm) are near or below the 0.20% ACI threshold for all three test holes, which indicates that corrosion probably is not occurring at the level of the steel.

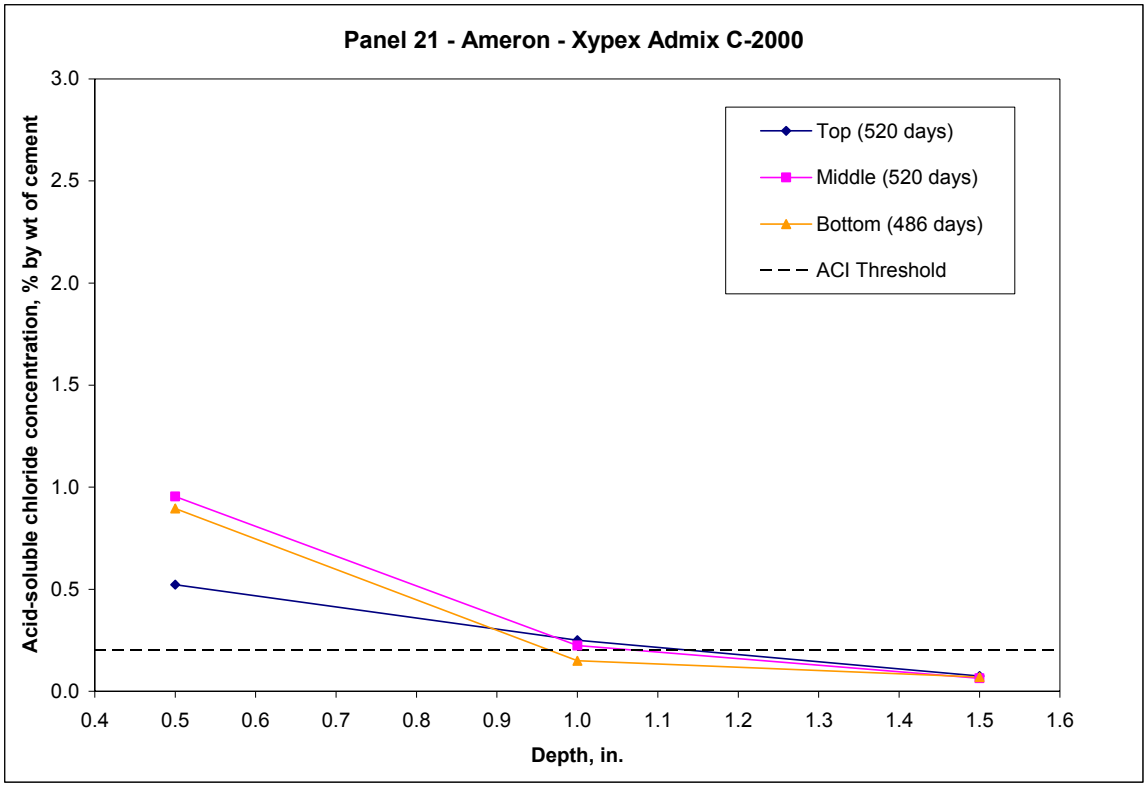

Figure 4.20. Acid-soluble chloride concentration vs. depth for panel 21.

4.4.7 Latex-modified mixture

The results of the chloride concentration tests for the latex-modified panel are provided in Figure 4.21. Chloride concentrations decrease at increasing depths for the three test holes. The bottom test hole has the highest chloride concentration followed by the top and middle holes. Concentrations at a depth of 1.0 in. (25 mm) and 1.5 in. (38 mm) are below the 0.20% ACI threshold for all three test holes, which indicates that corrosion probably is not taking place at the depth of the steel.

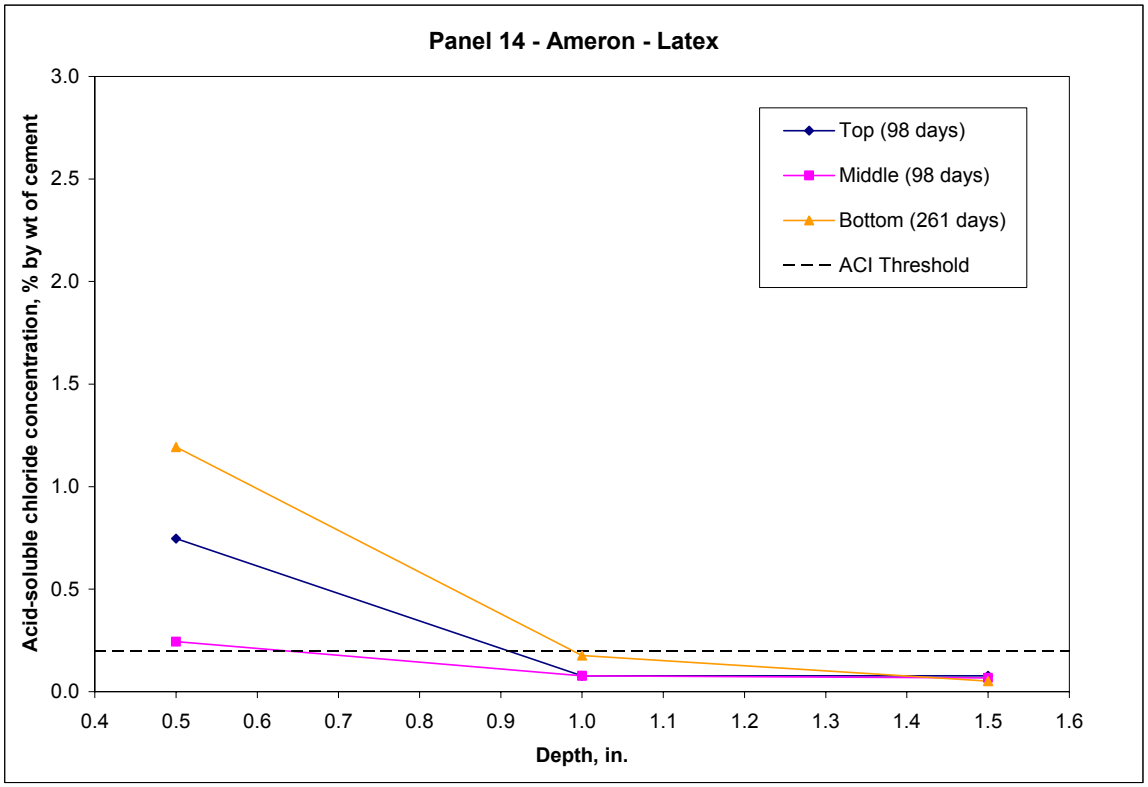

Figure 4.21. Acid-soluble chloride concentration vs. depth for panel 14.

4.4.8 Fly ash mixtures

The results of the chloride concentration tests for the fly ash panels are provided in Figure 4.22, Figure 4.23, and Figure 4.24. The bottom test hole has concentrations that are significantly higher than the middle and top holes. Chloride concentrations decrease at increasing depths for the three test holes of panel 11 except for the top test hole. The concentration for the top hole increases from the 0.5 (13 mm) depth to the 1.0 in. (25 mm) depth, and then decreases to the 1.5 in. (38 mm) depth. Concentrations at a depth of 1.5 in. (38 mm) are near or below the 0.20% ACI threshold for all three test holes, which indicates that corrosion probably is not occurring at the level of the steel for panel 11.

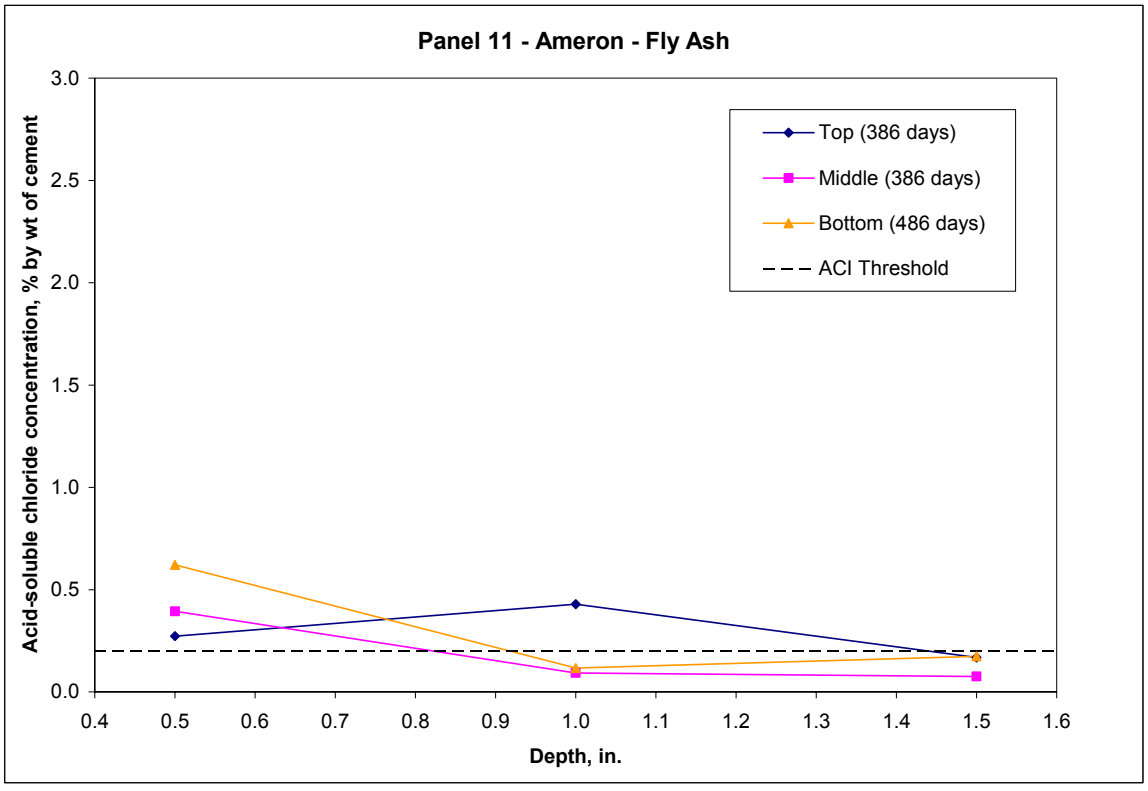

Figure 4.22. Acid-soluble chloride concentration vs. depth for panel 11.

Chloride concentrations for panel 12 are similar to panel 11. The chloride concentrations for all three tests holes are higher near the surface of the concrete and generally decrease near the reinforcing steel. The bottom test hole has the highest concentrations at each depth, followed by the top and middle hole. Concentrations at depths of 1.0 in. (25 mm) and 1.5 in. (38 mm) for all the test holes are below the 0.20% ACI threshold, which suggests that corrosion probably is not taking place at the level of the steel.

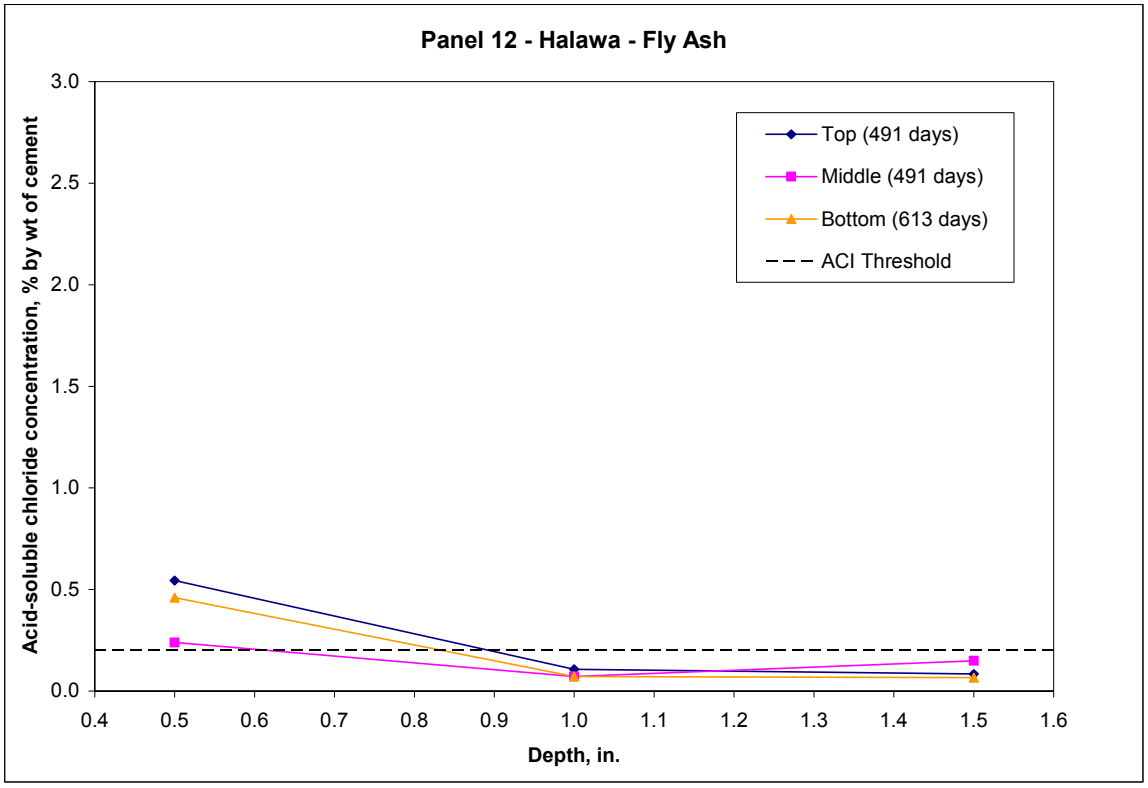

Figure 4.23. Acid-soluble chloride concentration vs. depth for panel 12.

Chloride concentrations for panel 13 are similar to panel 12. Overall, the chloride concentrations are higher near the surface of the concrete and decrease near the reinforcing steel. The top test hole had the highest chloride concentrations at all depths, followed by the middle and bottom holes. Concentrations at depths of 1.0 in. (25 mm) and 1.5 in. (38 mm) for all three test holes are below the 0.20% ACI threshold, which shows that corrosion probably is not occurring at the level of the steel.

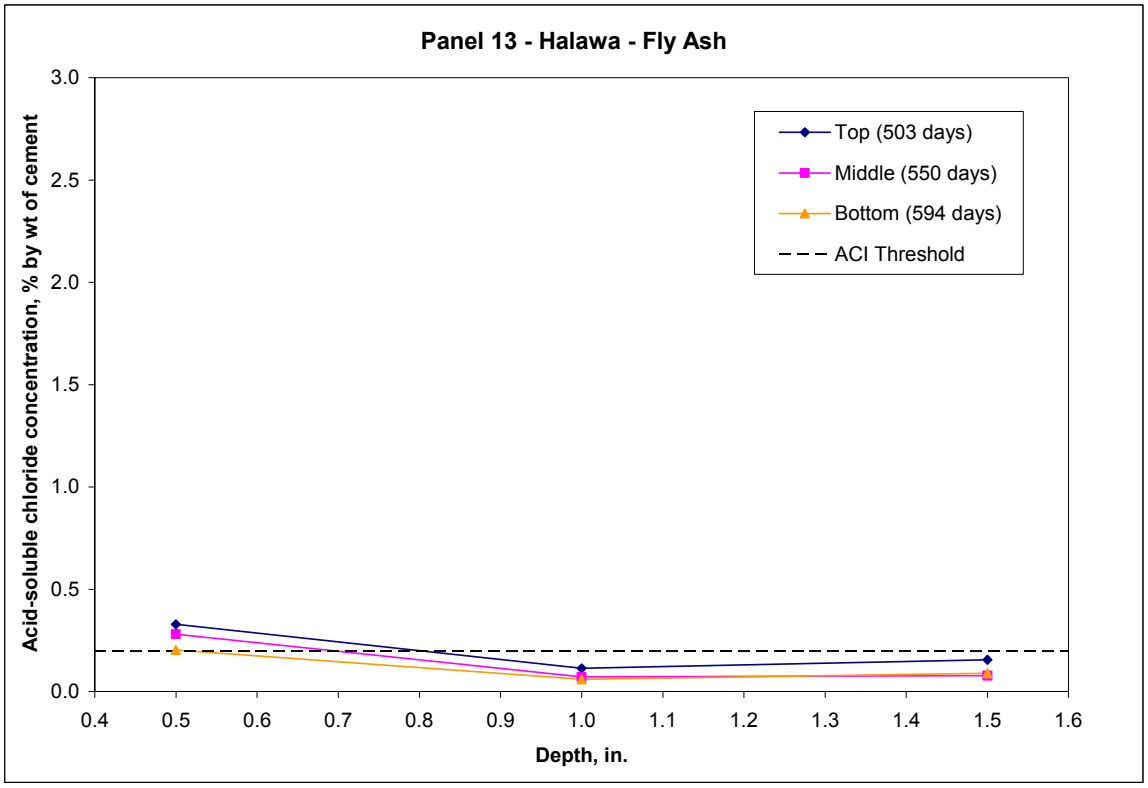

Figure 4.24. Acid-soluble chloride concentration vs. depth for panel 13.

4.4.9 Silica fume mixtures

The results of the chloride concentration tests for the panels proportioned with silica fume are provided in Figure 4.25, Figure 4.26, and Figure 4.27. Chloride concentrations decrease at increasing depths for the top and bottom test holes of panel 5. The concentrations increase with increasing depth for the middle test hole. Concentrations at a depth of 1.0 (25 mm) and 1.5 in. (38 mm) are below the 0.20% ACI threshold for the top and bottom test holes, which indicates that corrosion probably has not reached the level of the steel. The concentrations at the same depths for the middle test hole are above the 0.20% ACI threshold.

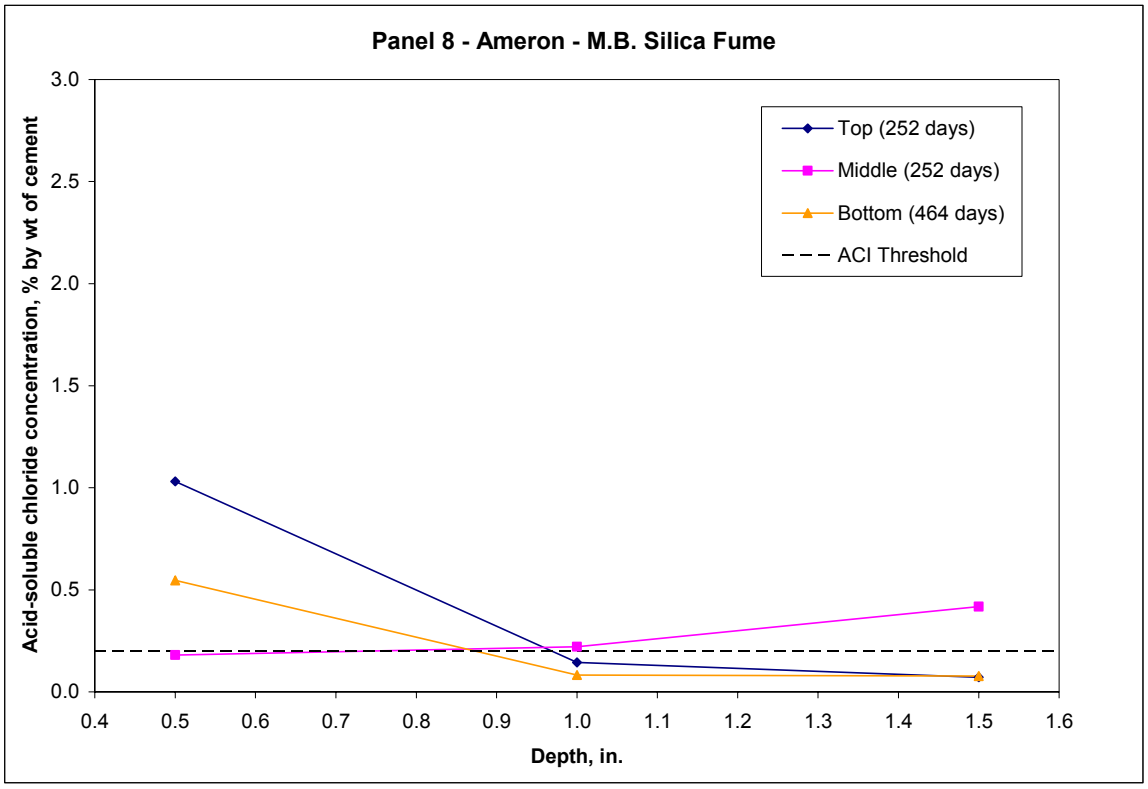

Figure 4.25. Acid-soluble chloride concentration vs. depth for panel 8.

Chloride concentrations for panel 9 are collectively lower than those of panel 8. Overall, the chloride concentrations are higher near the surface of the concrete, decrease at a depth of 1.0 in. (25 mm), and increase near the reinforcing steel. The middle test hole has the highest concentrations at each depth, followed by the bottom and top hole. Chloride concentrations at all depths for all three test holes are near or below the 0.20% ACI threshold, which suggests that corrosion probably is not taking place at the level of the steel.

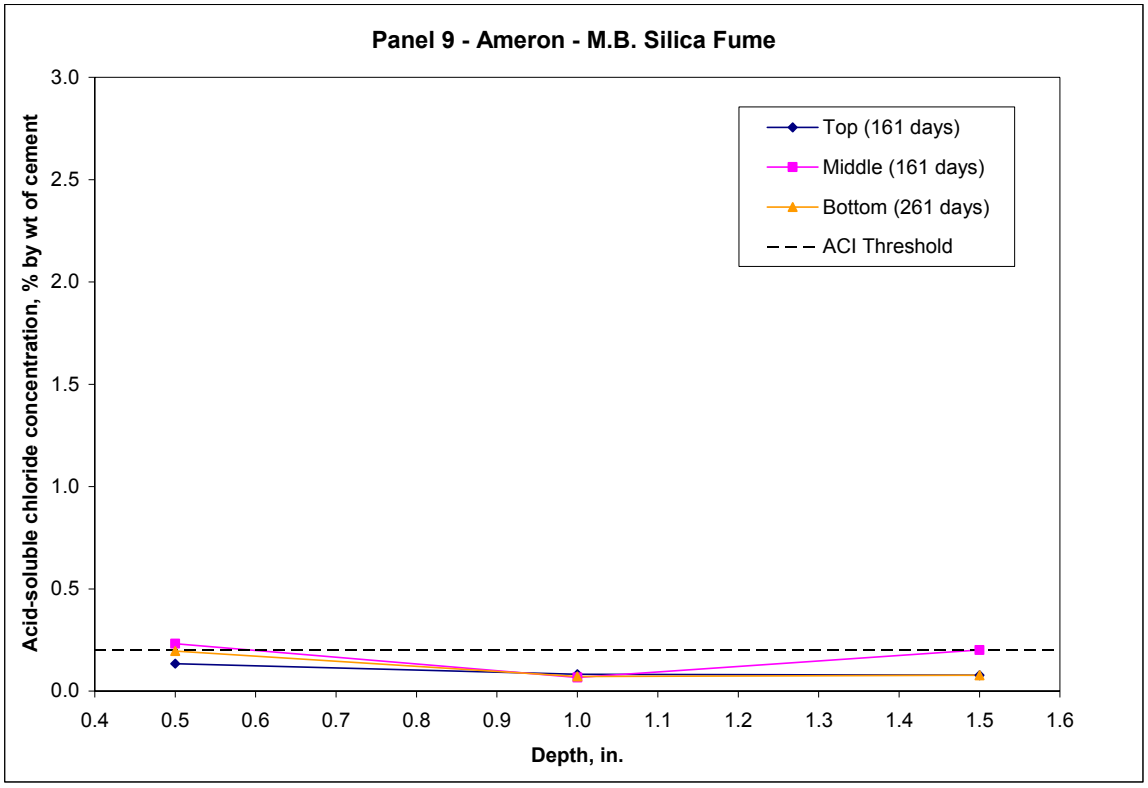

Figure 4.26. Acid-soluble chloride concentration vs. depth for panel 9.

Chloride concentrations for panel 10 are also generally lower than panel 8, except for the value at near the surface of the concrete at the bottom hole. Overall, the chloride concentrations are higher near the surface of the concrete and decrease near the reinforcing steel. The bottom test hole has the highest concentrations at each depth, followed by the top and middle hole. Concentrations for all test holes at all depths except for the bottom hole at a depth of 0.5 in. (13 mm) are below the 0.20% ACI threshold, which indicates that corrosion probably is not occurring at the level of the steel.

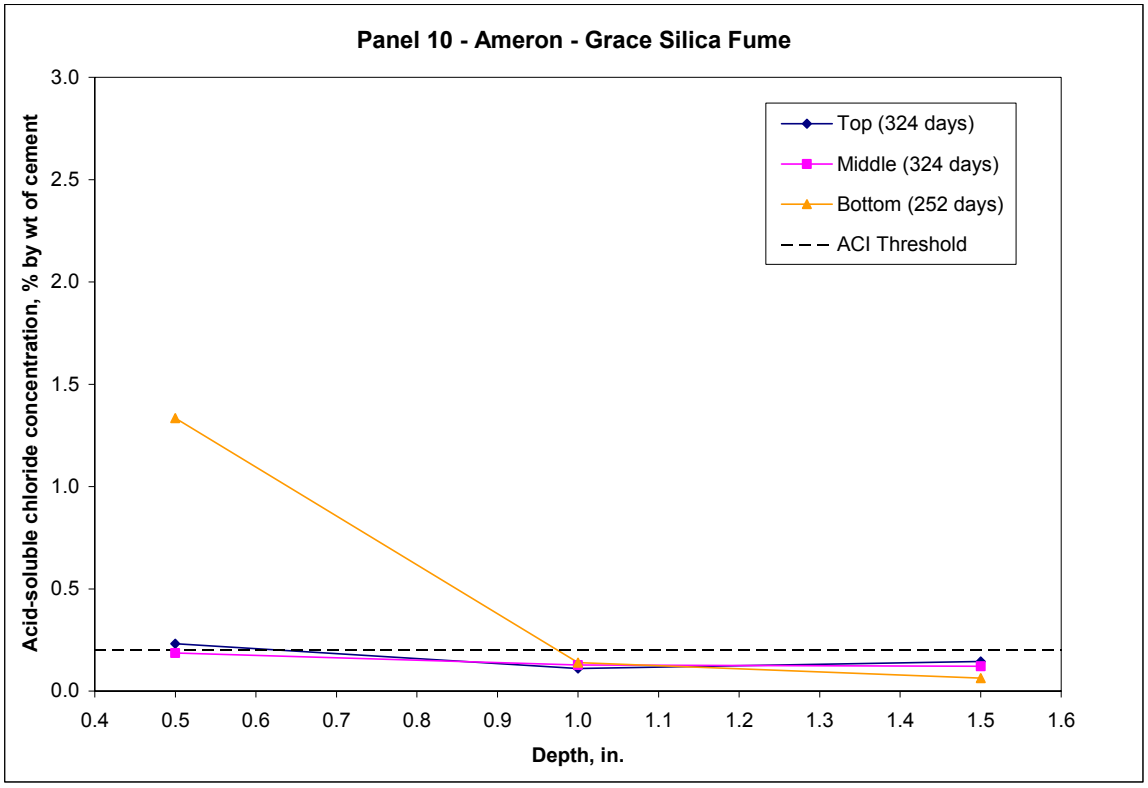

Figure 4.27. Acid-soluble chloride concentration vs. depth for panel 10.

4.4.10 Kryton KIM mixture

The results of the chloride concentration tests for the Kryton KIM panel are provided in Figure 4.28. The chloride concentrations decrease at increasing depths for panel 22. Concentrations at a depth of 1.0 in. (25 mm) and 1.5 in. (38 mm) for the top and middle tests holes are near or below the 0.20% ACI threshold, which indicates that corrosion probably has not reached the level of the steel for panel 22. The chloride concentrations for all the depths of the bottom test hole are above the ACI threshold, which suggests that corrosion probably is not taking place at the depth of the steel.

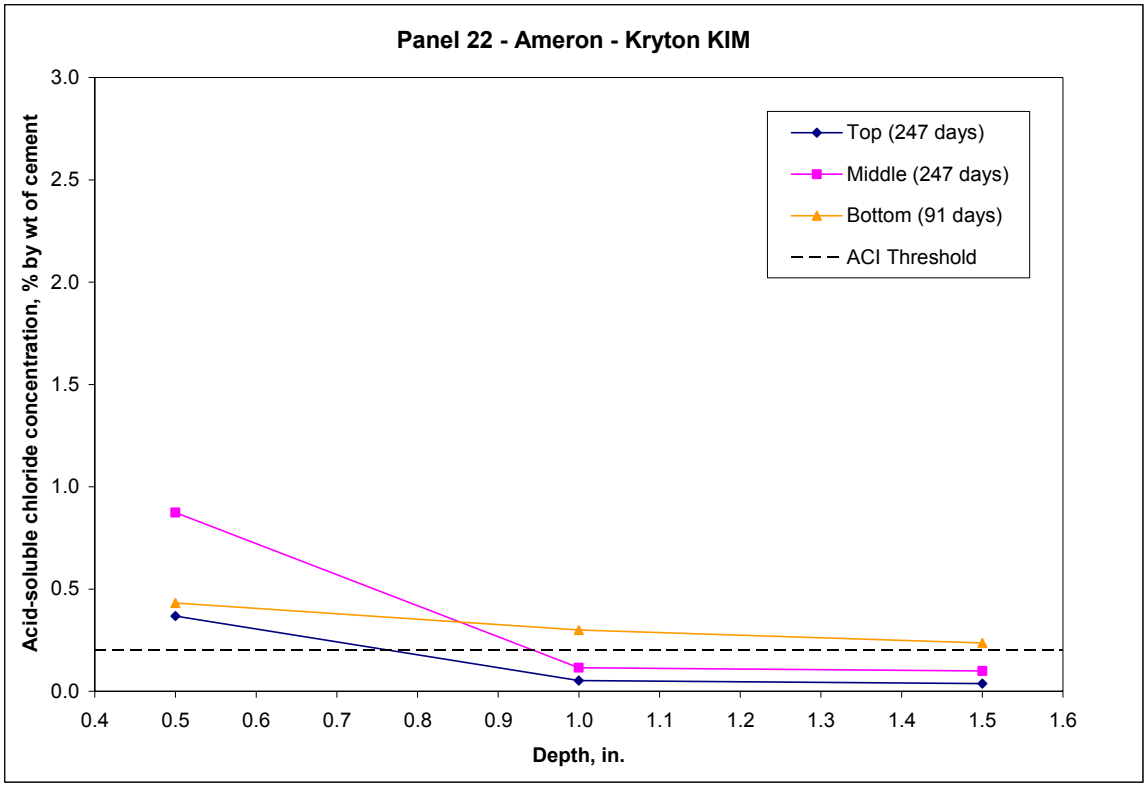

Figure 4.28. Acid-soluble chloride concentration vs. depth for panel 22.

4.5 pH

pH test results for all twenty-five panels at depths of 1.5 in. (38 mm) are provided in Table 4.14. In general, the values for pH are the same for all three locations on each panel. All of the mixtures had a pH greater than 12, which indicates that the concrete still maintains its natural alkalinity (Hope and Ip 1987). For some mixtures, a samples size less than 0.11 oz (3 grams) was available for testing. The actual amount tested is reported in Appendix C. Each sample, regardless of amount, was tested using a one-to-one ratio of milliliters of water to grams of concrete powder.

Table 4.14. pH test results.

Specimen	Top pH	Middle pH	Bottom pH
Control panel 1	12.55	12.05	12.55
Control panel 2	12.50	12.52	12.60
Control panel 7	12.47	12.43	12.43
DCI panel 3	12.53	12.54	12.64
DCI panel 3A	N/A	12.51	12.64
DCI panel 4	12.52	12.52	12.50
Rheocrete CNI panel 5	12.53	12.50	12.51
Rheocrete CNI panel 5A	12.52	12.36	12.46
Rheocrete CNI panel 6	12.42	12.43	12.42
Rheocrete 222+ panel 15	12.34	12.26	12.26
Rheocrete 222+ panel 16	12.21	12.23	12.24
Rheocrete 222+ panel 17	12.57	12.40	12.37
Rheocrete 222+ panel 17A	12.30	12.29	12.28
FerroGard 901 panel 18	12.30	12.29	12.28
FerroGard 901 panel 19	N/A	12.14	12.51
FerroGard 901 panel 20	12.40	12.39	12.40
Xypex Admix C-2000 panel 21	12.39	12.39	12.35
Latex panel 14	12.16	12.40	12.42
Fly ash panel 11	12.22	12.20	12.22
Fly ash panel 12	12.02	12.03	12.18
Fly ash panel 13	12.12	12.18	12.21
M.B. silica fume panel 8	12.61	12.50	12.56
M.B. silica fume panel 9	12.42	12.27	12.27
Grace silica fume panel 10	12.33	12.23	12.52
Kryton KIM panel 22	12.40	12.32	12.30

4.6 Air permeability

The air permeability test is used to rate the protective quality of each panel. The criteria for the protective quality of each concrete panel was taken from the instruction manual for the Poroscope Plus (James Instruments, Inc. 1998), as shown in Table 4.15. Protective quality of the concrete ranged from the lowest value of 0, which indicates high permeability or poor quality, to the highest value of 4, which denotes low permeability or excellent quality. The results for the air permeability tests are presented in Table 4.16.

Table 4.15. Quality values for air permeability (James Instruments, Inc. 1998).

Concrete Category	Air Permeability Time, (sec)	Protective Quality
0	<30	Poor
1	30-100	Not Very Good
2	100-300	Fair
3	300-1000	Good
4	>1000	Excellent

The test results indicate that all twenty-five panels have a protective quality less than "excellent." Three panels, 2, 17, and 17A, had "poor" ratings. Panel 2 is a control mixture and panels 17 and 17A are designed with Rheocrete 222+, and each is mixed using the coarse aggregate from the Halawa quarry.

Ten panels 1, 4, 6, 7, 12, 14, 16, 18, 19, and 21 have a protective quality of "not very good." Panels 1 and 7 are control mixtures using Ameron aggregates. Panel 4 is a DCI mixture using Halawa aggregates. Panel 6 is a Rheocrete CNI mixture using Ameron aggregates. Panel 12 is designed using fly ash and Halawa aggregates. Panel 14 is a latex-modified mixture using Ameron aggregates. Panel 16 is a Rheocrete 222+ mixture using Ameron aggregates. Panels 18 and 19 are FerroGard 901 mixtures using

Halawa aggregates. Panel 21 is a Xypex Admix C-2000 mixture using Ameron aggregates.

Eleven panels, 3, 3A, 5, 5A, 8, 9, 11, 13, 15, 20, and 22, have a protective quality of "fair." Panels 3 and 3A are DCI mixtures using Ameron aggregates. Panels 5 and 5A are Rheocrete CNI mixtures using Ameron aggregates. Panels 8 and 9 are made using silica fume from Master Builders, Inc. and Ameron aggregates. Panels 11 and 13 are fly ash mixtures using Ameron and Halawa aggregates respectively. Panel 15 is a Rheocrete 222+ mixture using Ameron aggregates. Panel 20 is a FerroGard 901 mixture using Ameron aggregates. Panel 22 is a Kryton KIM mixture using Ameron aggregates.

Only one panel had a protective quality of "good." Panel 10 is a mixture designed using silica fume from W.R. Grace and Ameron aggregates.

Table 4.16. Air permeability test results.

Specimen	Age (days)	Time (sec)	Protective Quality
Control panel 1	694	83	Not Very Good
Control panel 2	714	22	Poor
Control panel 7	694	89	Not Very Good
DCI panel 3	694	154	Fair
DCI panel 3A	366	142	Fair
DCI panel 4	714	66	Not Very Good
Rheocrete CNI panel 5	667	102	Fair
Rheocrete CNI panel 5A	366	131	Fair
Rheocrete CNI panel 6	597	66	Not Very Good
Rheocrete 222+ panel 15	667	111	Fair
Rheocrete 222+ panel 16	666	33	Not Very Good
Rheocrete 222+ panel 17	666	25	Poor
Rheocrete 222+ panel 17A	372	11	Poor
FerroGard 901 panel 18	714	70	Not Very Good
FerroGard 901 panel 19	697	84	Not Very Good
FerroGard 901 panel 20	526	125	Fair
Xypex Admix C-2000 panel 21	597	52	Not Very Good
Latex panel 14	372	61	Not Very Good
Fly ash panel 11	597	173	Fair
Fly ash panel 12	706	83	Not Very Good
Fly ash panel 13	697	108	Fair
M.B. Silica fume panel 8	518	205	Fair
M.B. Silica fume panel 9	372	151	Fair
Grace Silica fume panel 10	518	311	Good
Kryton KIM panel 22	366	128	Fair

4.7 Half-cell potential

The half-cell potential test determines the probability of corrosion occurring in the field panels. The ranges for the probabilities of corrosion using a copper sulfate electrode (CSE) are presented in Table 4.17. The results for the tests are obtained using a saturated calomel electrode (SCE) and therefore have to be converted to results using a copper sulfate electrode (CSE) by subtracting 77 mV (Corrosion Doctors 2004).

Table 4.17. Corrosion ranges for half-cell potential test results.

Measured Potential (mV)	Statistical risk of corrosion occurring
< -350	90%
Between -350 and -200	50%
> -200	10%

4.7.1 Control mixtures

Half-cell potential measurements for the control panels are presented in Table 4.18. Panel 1 has a low risk of corrosion occurring at all ten locations at an age of 2 years. At 2.1 years, panel 2 has a 50% or unknown risk of corrosion for the first two locations and a low risk for locations 3 to 10. There is a 50% chance of corrosion taking place for all ten locations on panel 7 at 2 years.

Table 4.18. Half-cell potential test results for control panels.

		Corrosion Potential (mV)									
Specimen	Age (yrs)	1	2	3	4	5	6	7	8	9	10
Panel 1	2.0	-152	-155	-140	-143	-153	-144	-162	-162	-102	-111
Panel 2	2.1	-231	-219	-189	-188	-183	-177	-15	-161	-177	-189
Panel 7	2.0	-268	-250	-260	-245	-268	-257	-281	-233	-274	-274

4.7.2 DCI mixtures

The measurements for half-cell potential for the DCI panels are provided in Table 4.19. At 2.0 years, panel 3 has a low risk of corrosion at all ten locations. Panel 3A has a low chance of corrosion occurring at locations 1, 2, and 9, and a 50% probability of corrosion at the remaining locations at 1.1 years. Panel 4 has a low risk of corrosion taking place at all ten locations at 2.1 years.

Table 4.19. Half-cell potential test results for DCI panels.

		Corrosion Potential (mV)									
Specimen	Age (yrs)	1	2	3	4	5	6	7	8	9	10
Panel 3	2.0	-196	-136	-159	-175	-178	-132	-138	-152	-174	-130
Panel 3A	1.1	-121	-139	-242	-212	-205	-215	-207	-207	-180	-217
Panel 4	2.1	-126	-125	-112	-112	-97	-108	-108	-101	-108	-108

4.7.3 Rheocrete CNI mixtures

Half-cell potential measurements for the Rheocrete CNI panels are presented in Table 4.20. At 1.9 years, panel 5 has a 50% or unknown risk of corrosion occurring at locations 2 and 5, and a high risk of corrosion at the remaining locations. Panel 5A has a low probability of corrosion taking place at locations 1, 2, 9, and 10, and a 50% chance of corrosion at the remaining locations at 1.1 years. Panel 6 has a 50% chance of corrosion occurring at all ten locations at 1.7 years.

Table 4.20. Half-cell potential test results for Rheocrete CNI panels.

		Corrosion Potential (mV)									
Specimen	Age (yrs)	1	2	3	4	5	6	7	8	9	10
Panel 5	1.9	-389	-345	-375	-361	-337	-369	-411	-419	-376	-399
Panel 5A	1.1	-113	-156	-195	-213	-201	-206	-207	-207	-129	-133
Panel 6	1.7	-237	-221	-221	-253	-252	-238	-247	-242	-243	-238

4.7.4 Rheocrete 222+ mixtures

The measurements for half-cell potential for the Rheocrete 222+ panels are provided in Table 4.21. At 1.9 years, panel 15 has a low chance of corrosion taking place at all ten locations. At 1.9 years, panel 16 has a low risk of corrosion occurring at location 1, a 50% probability of corrosion taking place at locations 2, 5, 6, 9, and 10, and a high chance of corrosion occurring at locations 3, 4, 7, and 8. Panel 17 has low risk of corrosion at location 4 and 5, and a 50% probability of corrosion taking place at the locations at 1.9 years. Panel 17A has a 50% chance of corrosion occurring at location 1 and 3, and a low risk of corrosion taking place at the remaining locations at 1.1 years.

Table 4.21. Half-cell potential test results for Rheocrete 222+ panels.

		Corrosion Potential (mV)									
Specimen	Age (yrs)	1	2	3	4	5	6	7	8	9	10
Panel 15	1.9	-112	-109	-145	-152	-180	-177	-192	-187	-144	-164
Panel 16	1.9	-186	-329	-353	-351	-280	-284	-364	-358	-337	-319
Panel 17	1.9	-306	-205	-217	-177	-146	-269	-251	-291	-317	-319
Panel 17A	1.1	-211	-199	-206	-196	-176	-186	-184	-179	-178	-164

4.7.5 FerroGard 901 mixtures

Half-cell potential measurements for the FerroGard 901 panels are presented in Table 4.22. At 2.1 years, panel 18 has a low risk of corrosion taking place at all ten locations. Panel 19 has a 50% probability of corrosion occurring at locations 1 and 2, and a low chance of corrosion at the remaining locations at 2.0 years. The readings for Panel 20 were not reported due to errors that occurred during field testing.

Table 4.22. Half-cell potential test results for FerroGard 901 panels.

		Corrosion Potential (mV)									
Specimen	Age (yrs)	1	2	3	4	5	6	7	8	9	10
Panel 18	2.1	-189	-164	-139	-131	-116	-106	-74	-82	-102	-113
Panel 19	2.0	-207	-203	-137	-146	-152	-162	-144	-140	-157	-168

4.7.6 Xypex Admix C-2000 mixture

The measurements for half-cell potential for the Xypex Admix C-2000 panel are provided in Table 4.23. At 1.7 years, there is a low chance of corrosion at location 6. There is a 50% risk of corrosion taking place at the remaining locations.

Table 4.23. Half-cell potential test results for Xypex Admix C-2000 panel.

		Corrosion Potential (mV)									
Specimen	Age (yrs)	1	2	3	4	5	6	7	8	9	10
Panel 21	1.7	-229	-241	-210	-207	-222	-199	-262	-222	-311	-296

4.7.7 Latex-modified mixture

Half-cell potential measurements for the latex-modified panel are presented in Table 4.24. At 1.1 years, there is a very low risk of corrosion occurring at all ten locations on panel 14.

Table 4.24. Half-cell potential test results for latex panel.

		Corrosion Potential (mV)									
Specimen	Age (yrs)	1	2	3	4	5	6	7	8	9	10
Panel 14	1.1	-60	-27	-57	-76	-33	-51	-49	-40	-36	-33

4.7.8 Fly ash mixtures

The measurements for half-cell potential for the fly ash panels are provided in Table 4.25. Panel 11 has a 50% probability of corrosion taking place at all ten locations at 1.7 years. At 2.0 years, there is a low chance of corrosion at all ten locations on panel 12. At 2.0 years, there is also a low risk of corrosion occurring at all ten locations of panel 13.

Table 4.25. Half-cell potential test results for fly ash panels.

		Corrosion Potential (mV)									
Specimen	Age (yrs)	1	2	3	4	5	6	7	8	9	10
Panel 11	1.7	-308	-291	-316	-330	-284	-275	-270	-263	-319	-323
Panel 12	2.0	-160	-136	-159	-175	-178	-132	-138	-152	-174	-130
Panel 13	2.0	-121	-135	-86	-89	-127	-95	-95	-105	-104	-114

4.7.9 Silica fume mixtures

Half-cell potential measurements for the silica fume panels are presented in Table 4.26. At 1.5 years, there is a high probability of corrosion taking place at location 9, and a 50% or unknown chance of corrosion at the remaining locations. Panel 9 has a high risk of corrosion occurring at locations 2, 3, 4, and 10, and a 50% probability of corrosion occurring at the remaining locations at 1.1 years. Panel 10 has a low chance of corrosion taking place at all ten locations at 1.5 years.

Table 4.26. Half-cell potential test results for silica fume panels.

		Corrosion Potential (mV)									
Specimen	Age (yrs)	1	2	3	4	5	6	7	8	9	10
Panel 8	1.5	-287	-295	-319	-311	-311	-308	-296	-289	-352	-328
Panel 9	1.1	-262	-363	-354	-352	-314	-339	-320	-316	-341	-360
Panel 10	1.5	-93	-111	-172	-178	-172	-162	-184	-186	-164	-167

4.7.10 Kryton KIM mixture

The measurements for half-cell potential for the Kryton KIM panel are provided in Table 4.27. At 1.1 years, there is a 50% or unknown risk of corrosion occurring at all ten locations.

Table 4.27. Half-cell potential test results for Kryton KIM panel.

		Corrosion Potential (mV)									
Specimen	Age (yrs)	1	2	3	4	5	6	7	8	9	10
Panel 22	1.1	-271	-287	-282	-294	-305	-302	-295	-290	-282	-288

4.8 Life-365

The computer program Life-365 was used to predict chloride concentrations of the control, DCI, Rheocrete CNI, Rheocrete 222+, fly ash, and silica fume panels. The predictions were plotted alongside the actual measured chloride concentrations for comparison. A maximum surface concentration of 0.80% by weight of concrete was assumed for the chloride concentrations measured in the field for comparison with Life-365 predictions. All data produced by Life-365 for chloride concentration is presented as a percentage by weight of the concrete. The accuracy of the Life-365 predictions was determined by dividing the predicted value by the measured value. A complete listing of the values produced from Life-365 can be found in Appendix E.

4.8.1 Control mixtures

The chloride concentrations for the control panels predicted by the computer program Life-365 are presented in Figure 4.29, Figure 4.30, and Figure 4.31. Overall, the predictions calculated using Life-365 for control panel 1 averaged 5.1 times the measured chloride concentrations. Estimated chloride concentration values for the top test hole averaged 2.9 times the amount measured, an average of 8.5 times the measured values of the middle hole, and an average of 3.9 times the concentration of the bottom hole.

In general, the predictions calculated using Life-365 for control panel 2 averaged 9.0 times the observed chloride concentrations. Estimated chloride concentration values for the top test hole averaged 6.9 times the amount measured, an average of 9.0 times the measured values of the middle hole, and an average of 11.2 times the chloride concentration of the bottom hole.

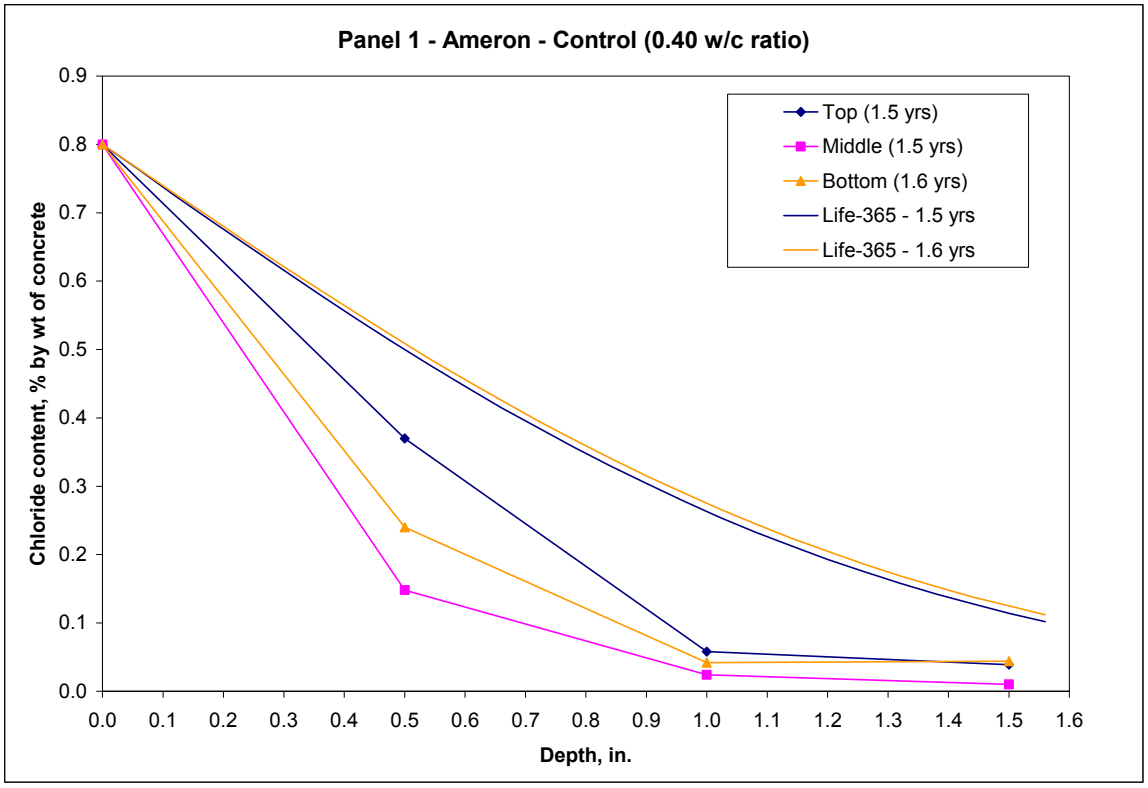

Figure 4.29. Life-365 predictions for panel 1.

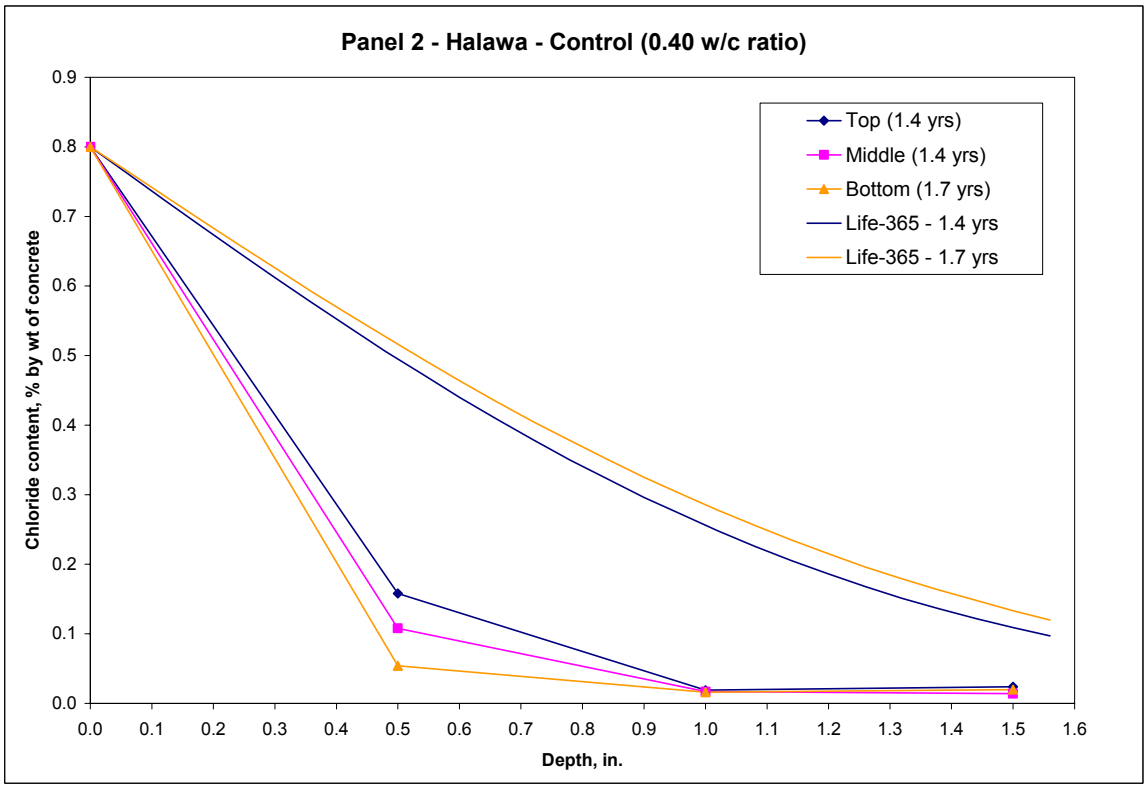

Figure 4.30. Life-365 predictions for panel 2.

The overall predictions calculated using Life-365 for control panel 7 averaged 6.6 times the measured chloride concentrations. Estimated chloride concentration values for the top test hole averaged 9.7 times the amount measured, an average of 6.6 times the measured values of the middle hole, and an average of 3.5 times the chloride concentration of the bottom hole.

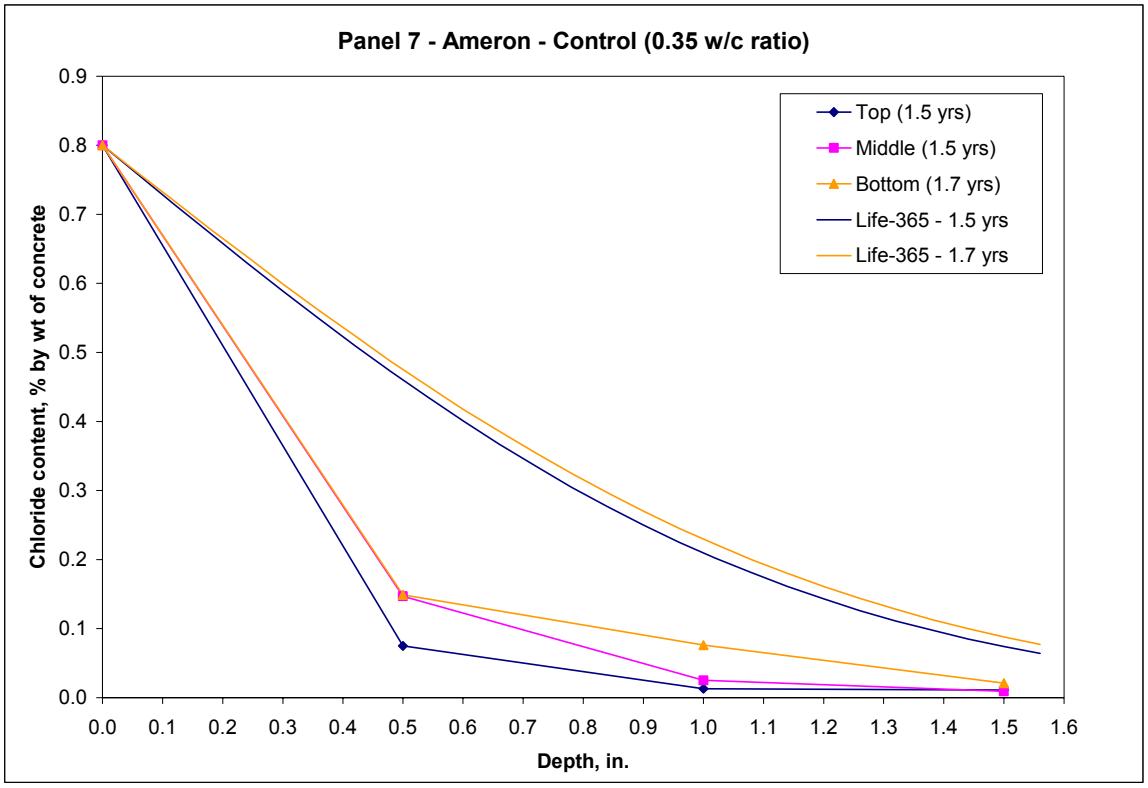

Figure 4.31. Life-365 predictions for panel 7.

4.8.2 DCI mixtures

The chloride concentrations for the DCI panels predicted by the computer program Life-365 are presented in Figure 4.32, Figure 4.33, and Figure 4.34. Overall, the predictions calculated using Life-365 for control panel 3 averaged 5.1 times the measured chloride concentrations. Estimated chloride concentration values for the top test hole averaged 4.9 times the amount measured, an average of 6.8 times the measured values of the middle hole, and an average of 3.5 times the chloride concentration of the bottom hole.

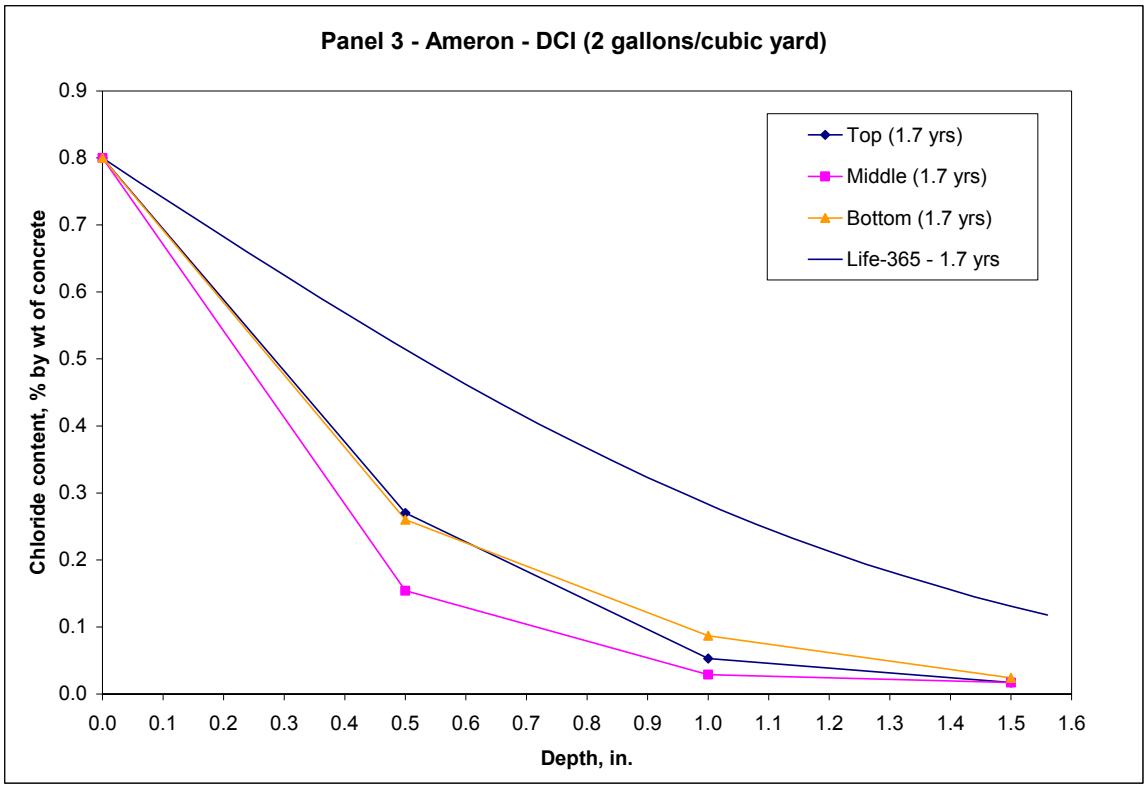

Figure 4.32. Life-365 predictions for panel 3.

In general, the predictions calculated using Life-365 for control panel 3A averaged 5.4 times the observed chloride concentrations. Estimated chloride concentration values for the top test hole averaged 11.1 times the amount measured, an average of 1.8 times the measured values of the middle hole, and an average of 3.3 times the chloride concentration of the bottom hole.

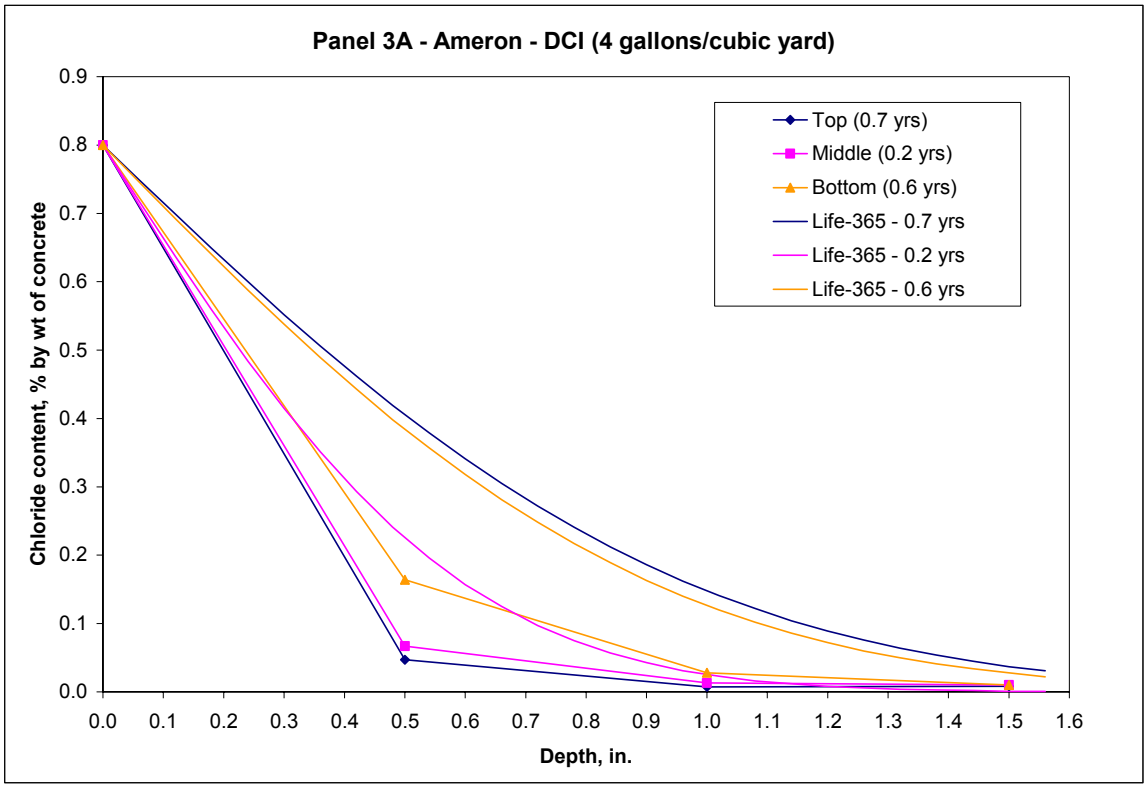

Figure 4.33. Life-365 predictions for panel 3A.

The overall predictions calculated using Life-365 for control panel 4 averaged 8.2 times the measured chloride concentrations. Estimated chloride concentration values for the top test hole averaged 2.2 times the amount measured, an average of 11.1 times the measured values of the middle hole, and an average of 11.2 times the chloride concentration of the bottom hole.

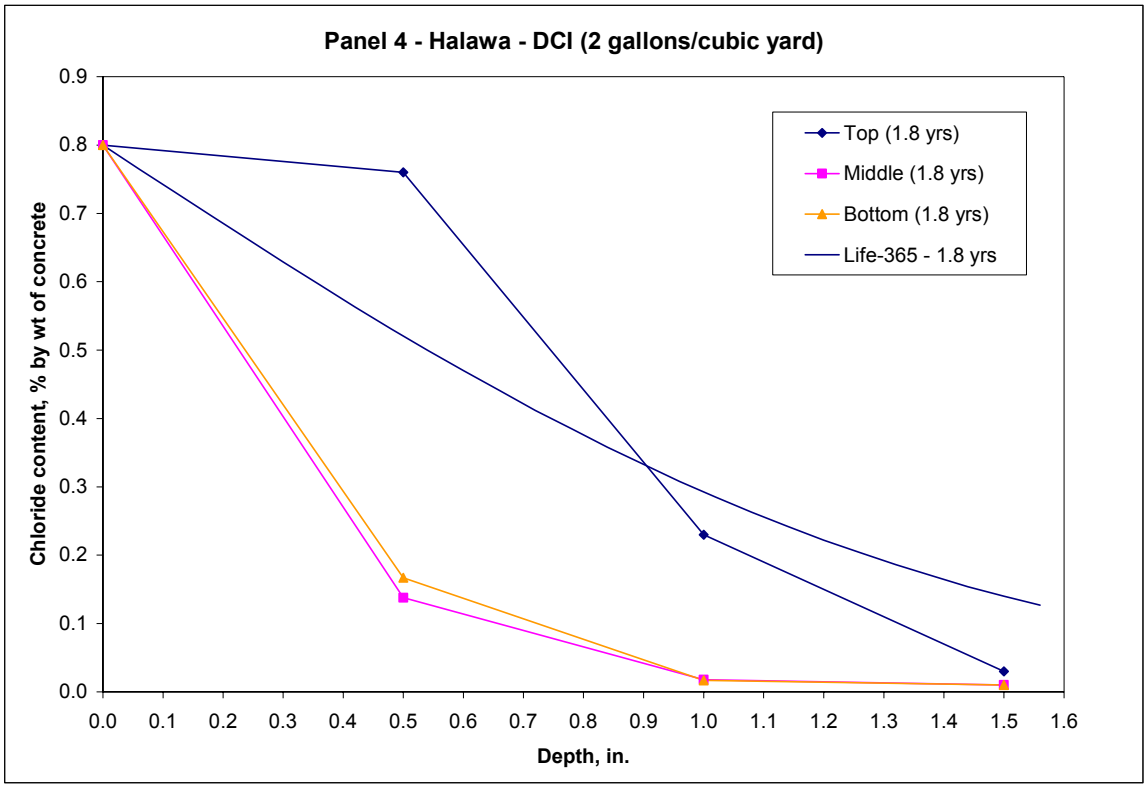

Figure 4.34. Life-365 predictions for panel 4.

4.8.3 Rheocrete CNI mixtures

The chloride concentrations for the control panels predicted by the computer program Life-365 are presented in Figure 4.35, Figure 4.36, and Figure 4.37. Overall, the predictions calculated using Life-365 for control panel 5 averaged 3.7 times the measured chloride concentrations. Estimated chloride concentration values for the top test hole averaged 5.7 times the amounts measured, an average of 4.3 times the measured values of the middle hole, and an average of 1.2 times the chloride concentrations of the bottom hole.

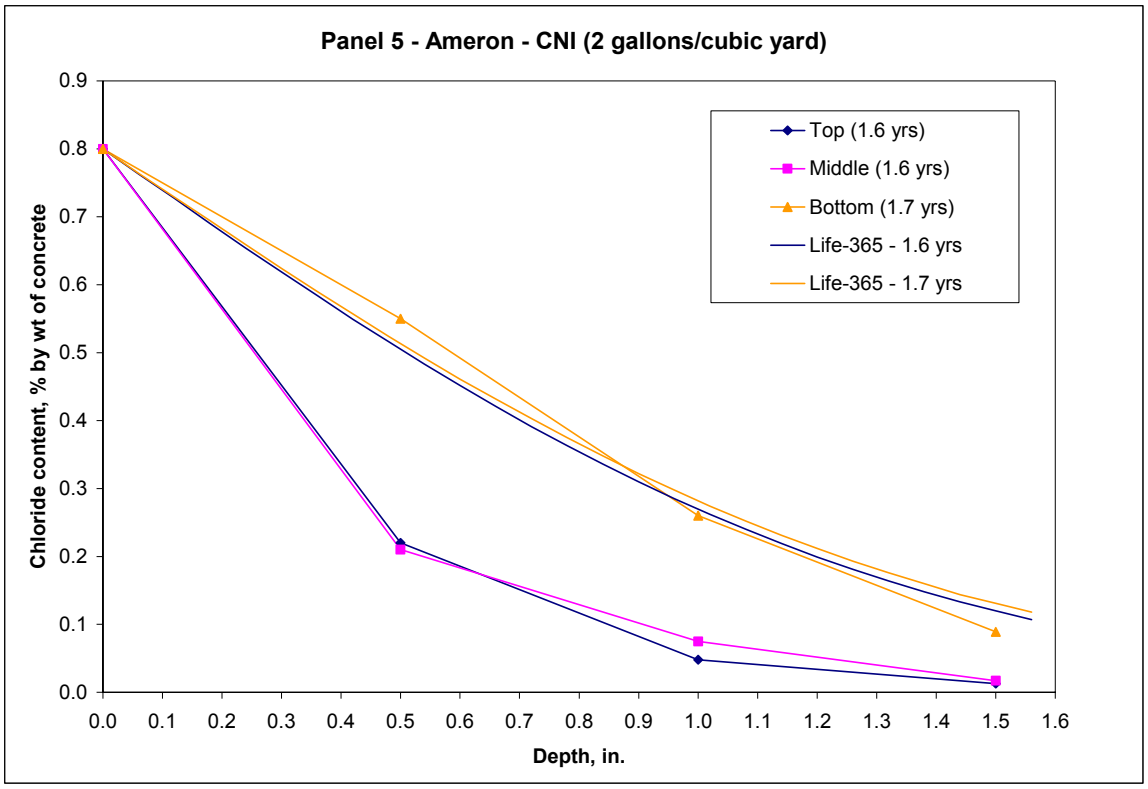

Figure 4.35. Life-365 predictions for panel 5.

In general, the predictions calculated using Life-365 for control panel 5A averaged 2.3 times the observed chloride concentrations. Estimated chloride concentration values for the top test hole averaged 2.1 times the amount measured, an average of 1.7 times the measured values of the middle hole, and an average of 3.2 times the chloride concentrations of the bottom hole.

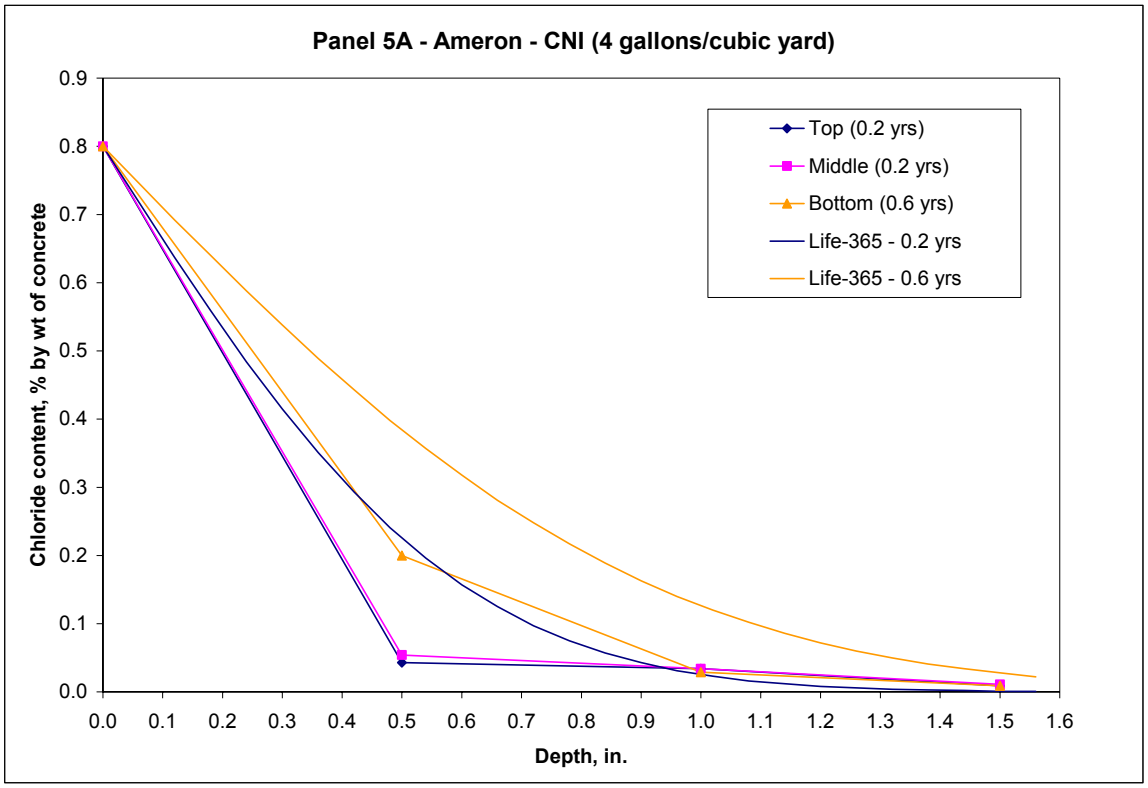

Figure 4.36. Life-365 predictions for panel 5A.

The overall predictions calculated using Life-365 for control panel 6 averaged 6.3 times the measured chloride concentrations. Estimated chloride concentration values for the top test hole averaged 6.3 times the amounts measured, an average of 4.6 times the measured values of the middle hole, and an average of 8.0 times the chloride concentrations of the bottom hole.

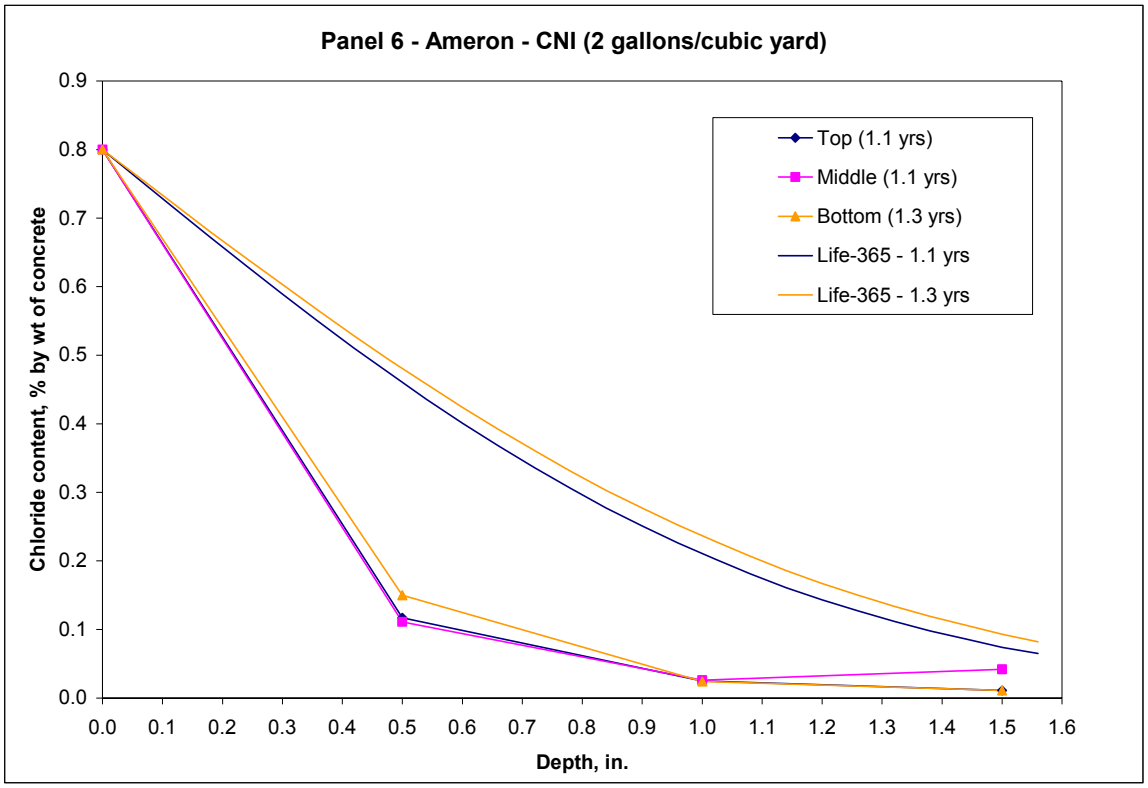

Figure 4.37. Life-365 predictions for panel 6.

4.8.4 Rheocrete 222+ mixtures

The chloride concentrations for the control panels predicted by the computer program Life-365 are presented in Figure 4.38, Figure 4.39, Figure 4.40, and Figure 4.41. Overall, the predictions calculated using Life-365 for control panel 15 averaged 8.9 times the measured chloride concentrations. Estimated chloride concentration values for the top test hole averaged 15.1 times the amount measured, an average of 6.2 times the measured values of the middle hole, and an average of 5.3 times the chloride concentrations of the bottom hole.

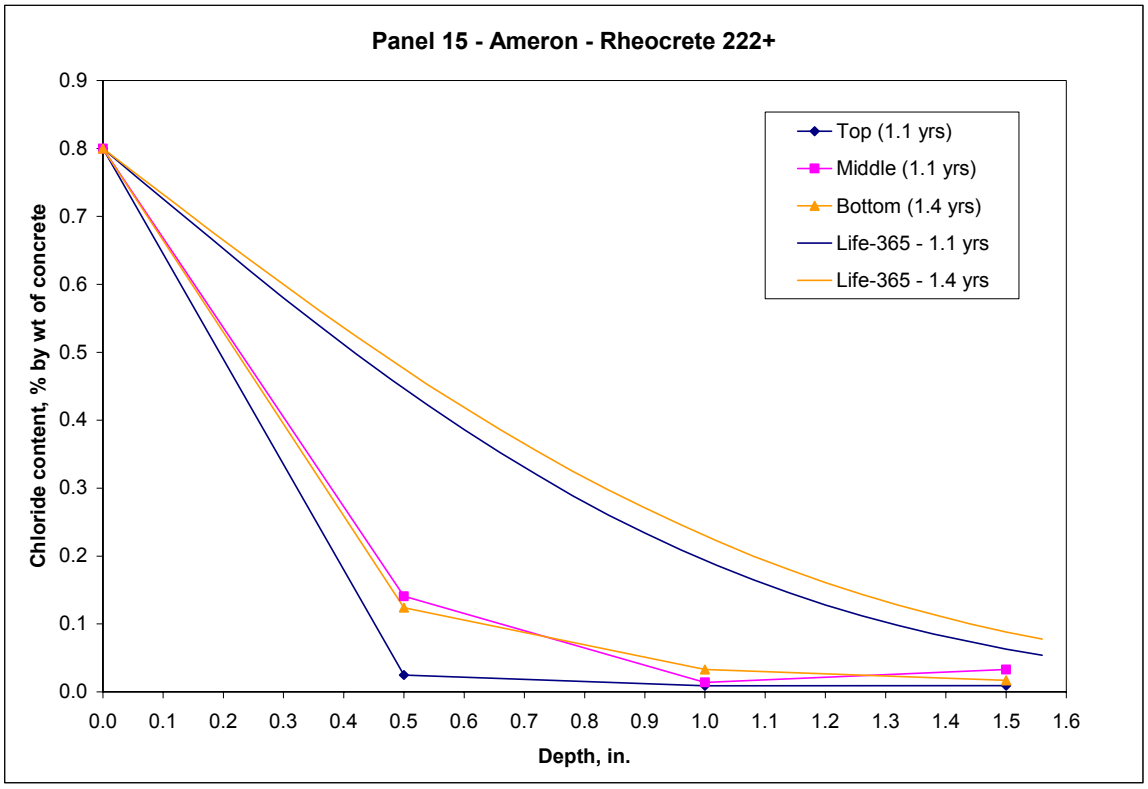

Figure 4.38. Life-365 predictions for panel 15.

In general, the predictions calculated using Life-365 for control panel 16 averaged 2.9 times the observed chloride concentrations. Estimated chloride concentration values for the top test hole averaged 3.8 times the amount measured, an average of 2.9 times the measured values of the middle hole, and an average of 2.1 times the chloride concentrations of the bottom hole.

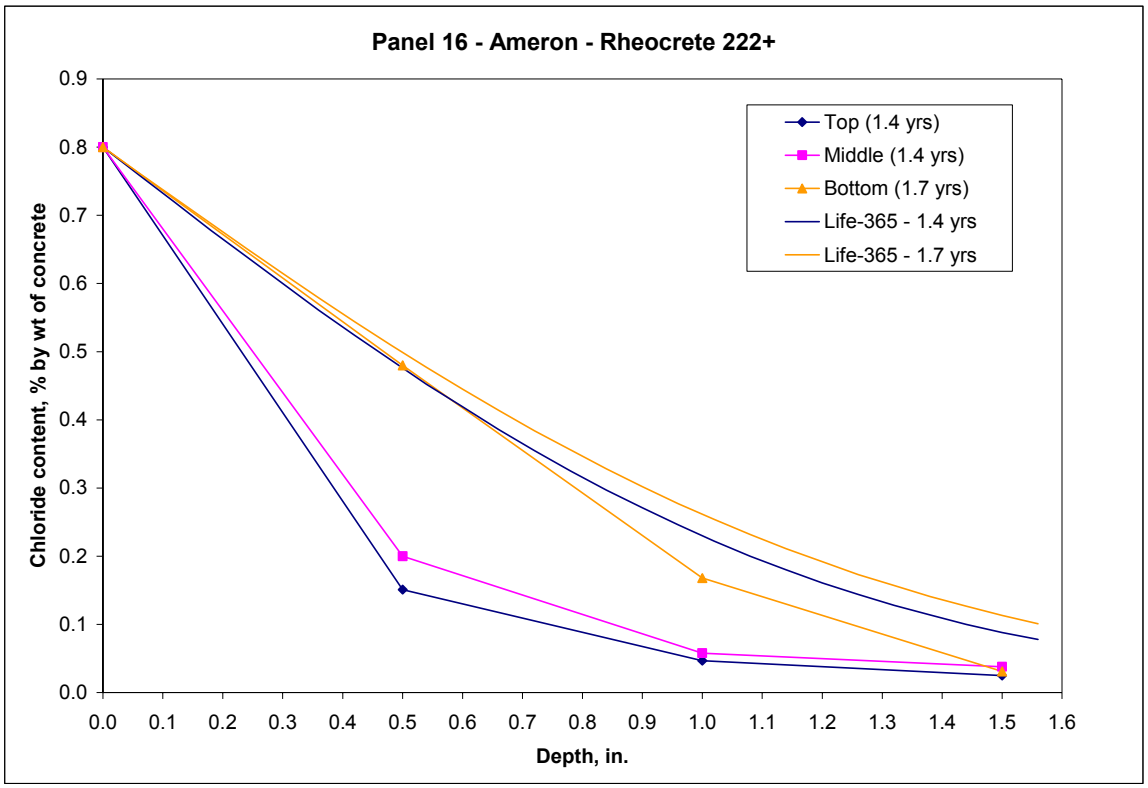

Figure 4.39. Life-365 predictions for panel 16.

The overall predictions calculated using Life-365 for control panel 17 averaged 6.1 times the measured chloride concentrations. Estimated chloride concentration values for the top test hole averaged 6.4 times the amount measured, an average of 3.9 times the measured values of the middle hole, and an average of 8.1 times the chloride concentrations of the bottom hole.

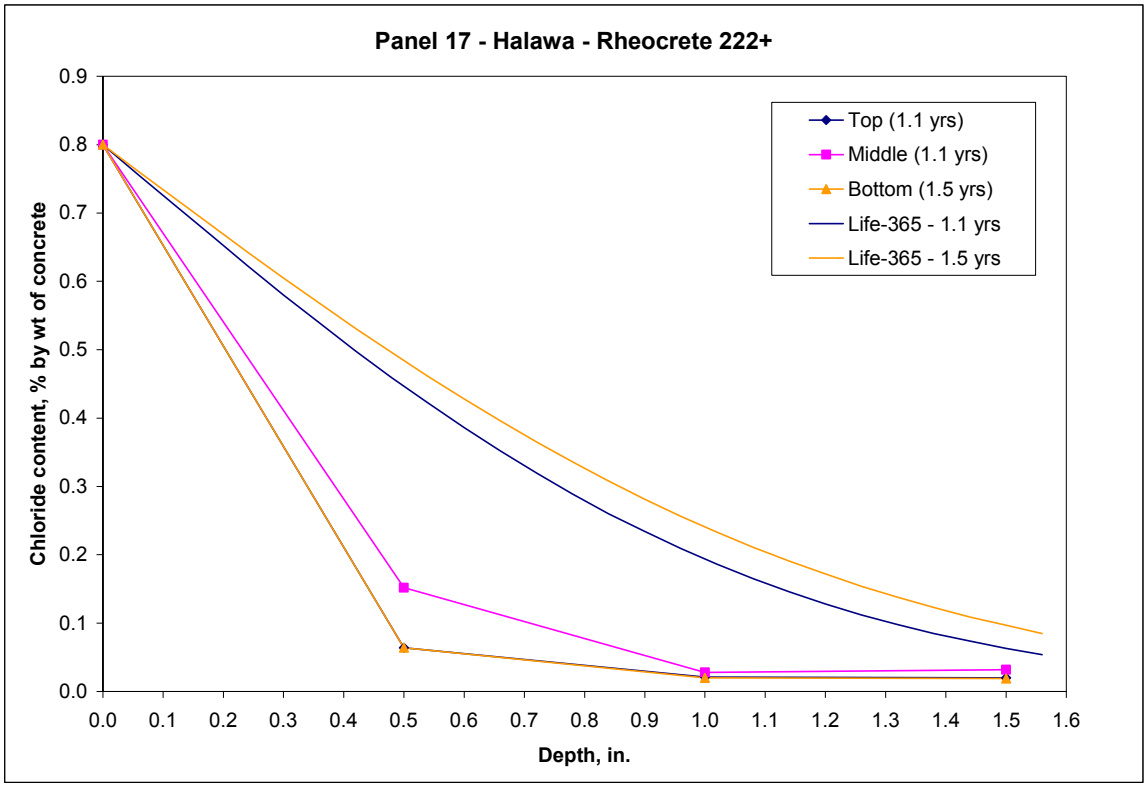

Figure 4.40. Life-365 predictions for panel 17.

The overall predictions calculated using Life-365 for control panel 17A averaged 2.3 times the measured chloride concentrations. Estimated chloride concentration values for the top test hole averaged 2.4 times the amount measured, an average of 2.8 times the measured values of the middle hole, and an average of 1.8 times the chloride concentrations of the bottom hole.

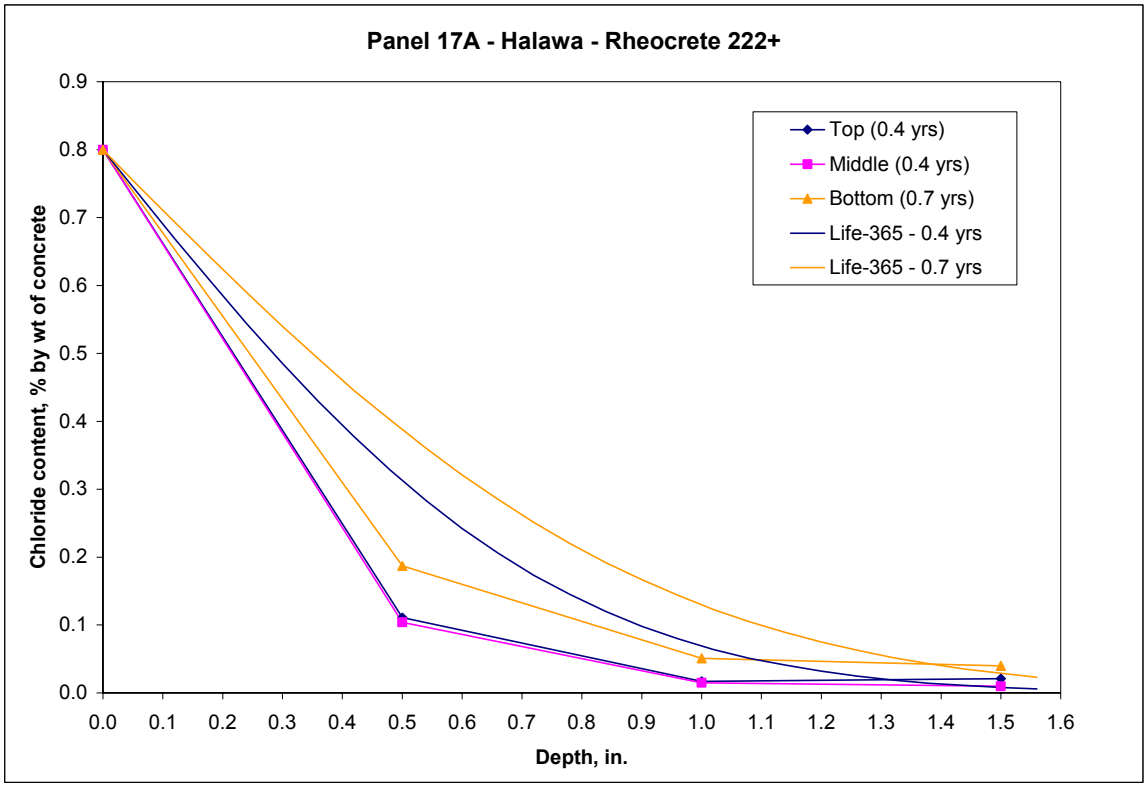

Figure 4.41. Life-365 predictions for panel 17A.

4.8.5 Fly ash mixtures

The chloride concentrations for the control panels predicted by the computer program Life-365 are presented in Figure 4.42, Figure 4.43, and Figure 4.44. Life-365 collectively overestimates the chloride content for control panel 11 by approximately 4.5 times the measured values. The program produces values that are about 3.7 times as large as the measured values for each depth at the top test hole, 5.4 times the measured value for each depth at the middle hole, and 4.2 times the measured value for each depth at the bottom hole.

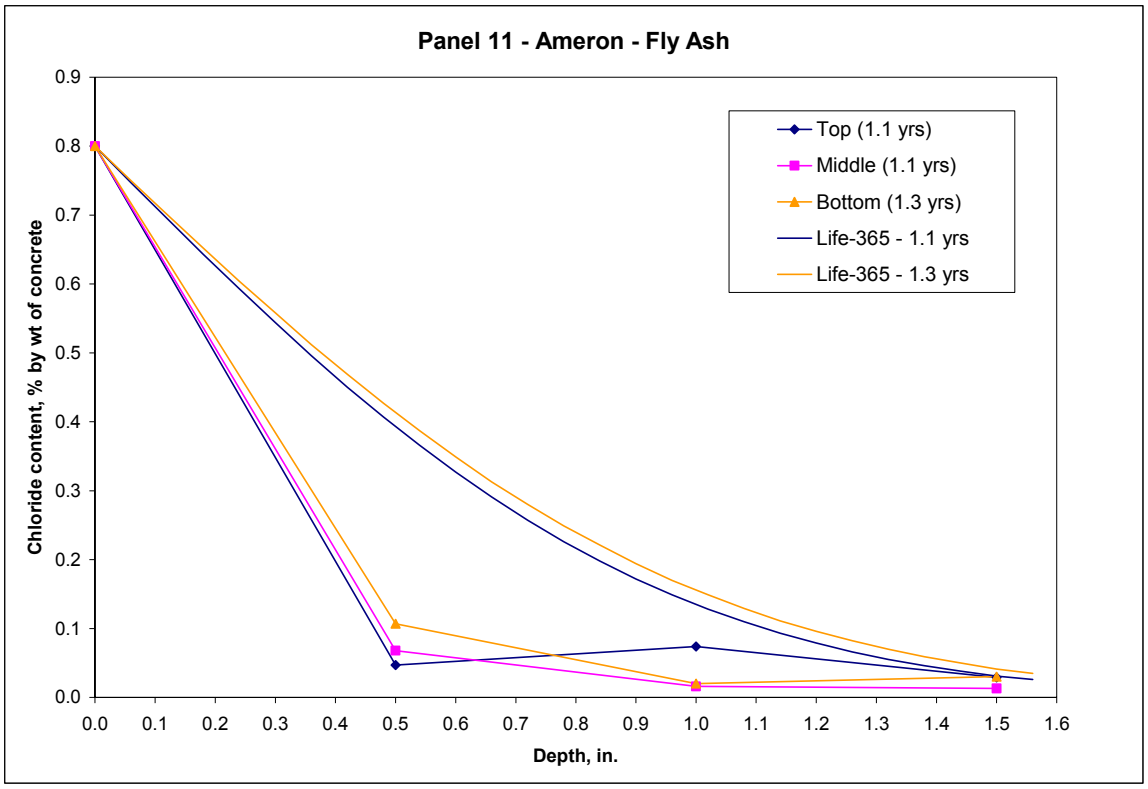

Figure 4.42. Life-365 predictions for panel 11.

In general, the predictions calculated using Life-365 for control panel 12 averaged 7.8 times the observed chloride concentrations. Estimated chloride concentration values for the top test hole averaged 5.6 times the amount measured, an average of 8.5 times the measured values of the middle hole, and an average of 9.2 times the chloride concentrations of the bottom hole.

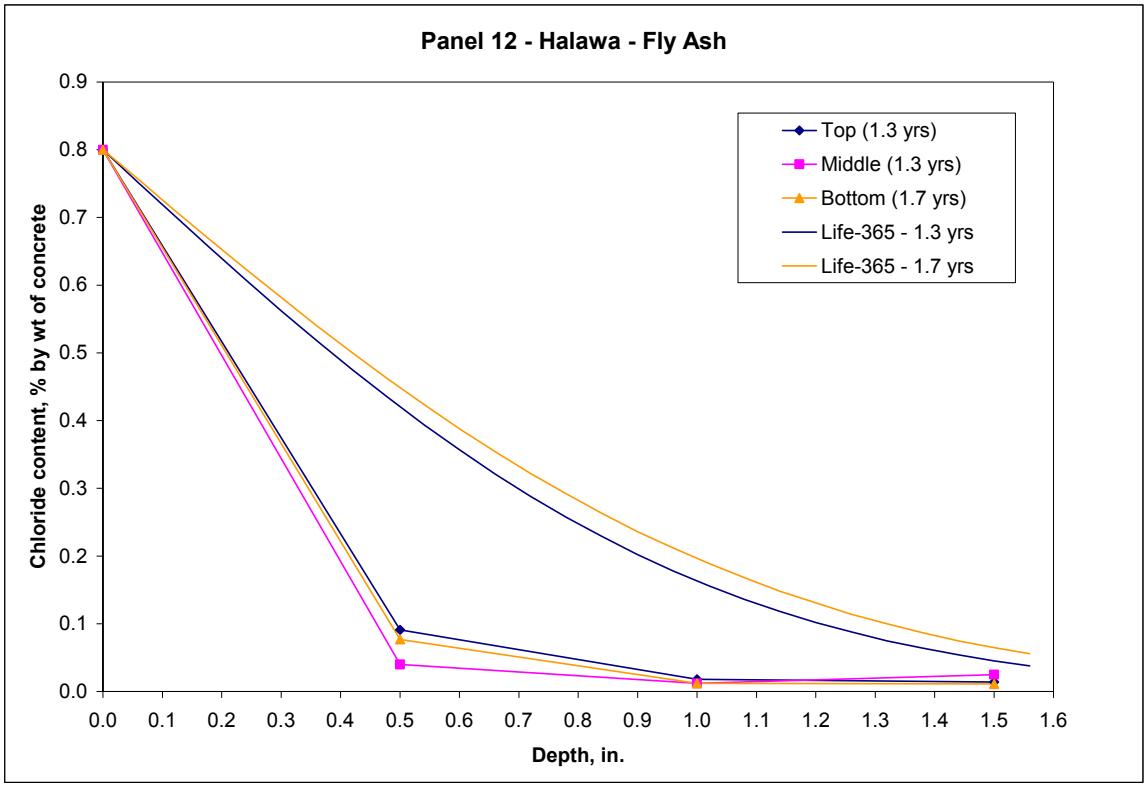

Figure 4.43. Life-365 predictions for panel 12.

The overall predictions calculated using Life-365 for control panel 13 averaged 8.8 times the measured chloride concentrations. Estimated chloride concentration values for the top test hole averaged 6.2 times the amount measured, an average of 9.5 times the measured values of the middle hole, and an average of 10.7 times the chloride concentrations of the bottom hole.

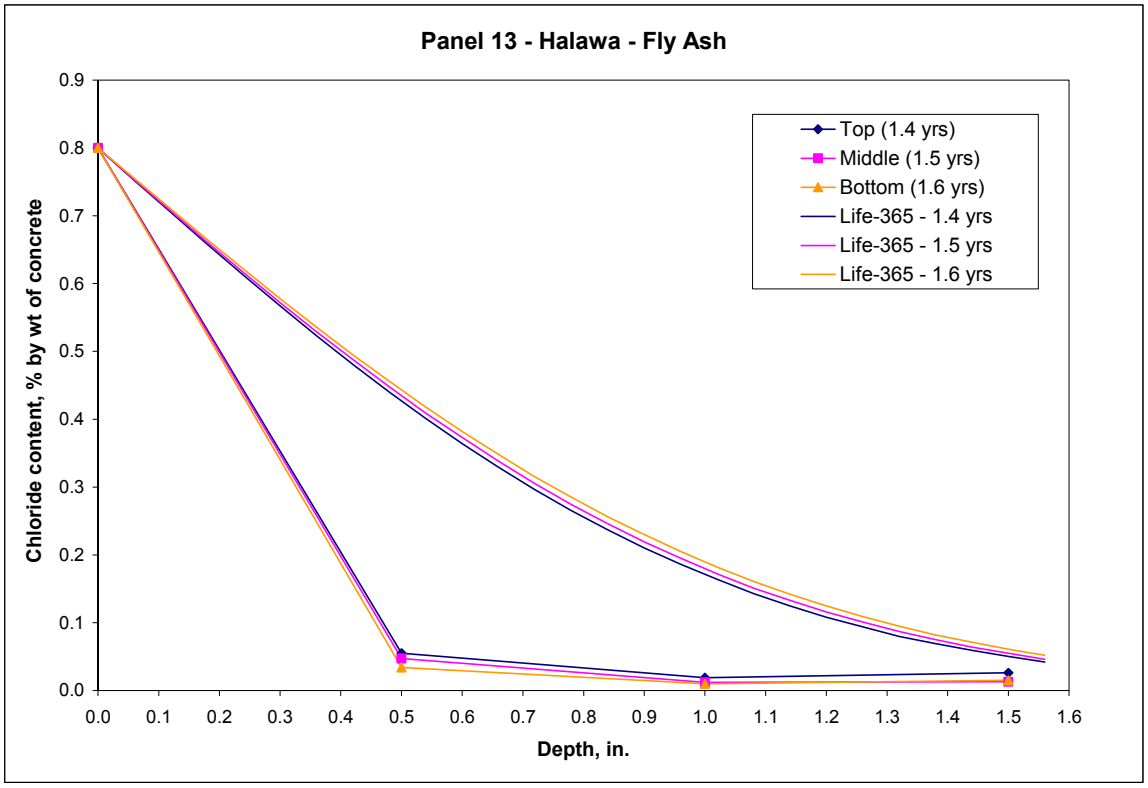

Figure 4.44. Life-365 predictions for panel 13.

4.8.6 Silica fume mixtures

The chloride concentrations for the control panels predicted by the computer program Life-365 are presented in Figure 4.45, Figure 4.46, and Figure 4.47. Overall, the predictions calculated using Life-365 for control panel 8 averaged 1.7 times the measured chloride concentrations. Estimated chloride concentration for the top test hole averaged 0.6 times the amount measured, an average of 2.2 times the measured values of the middle hole, and an average of 2.3 times the chloride concentration of the bottom hole.

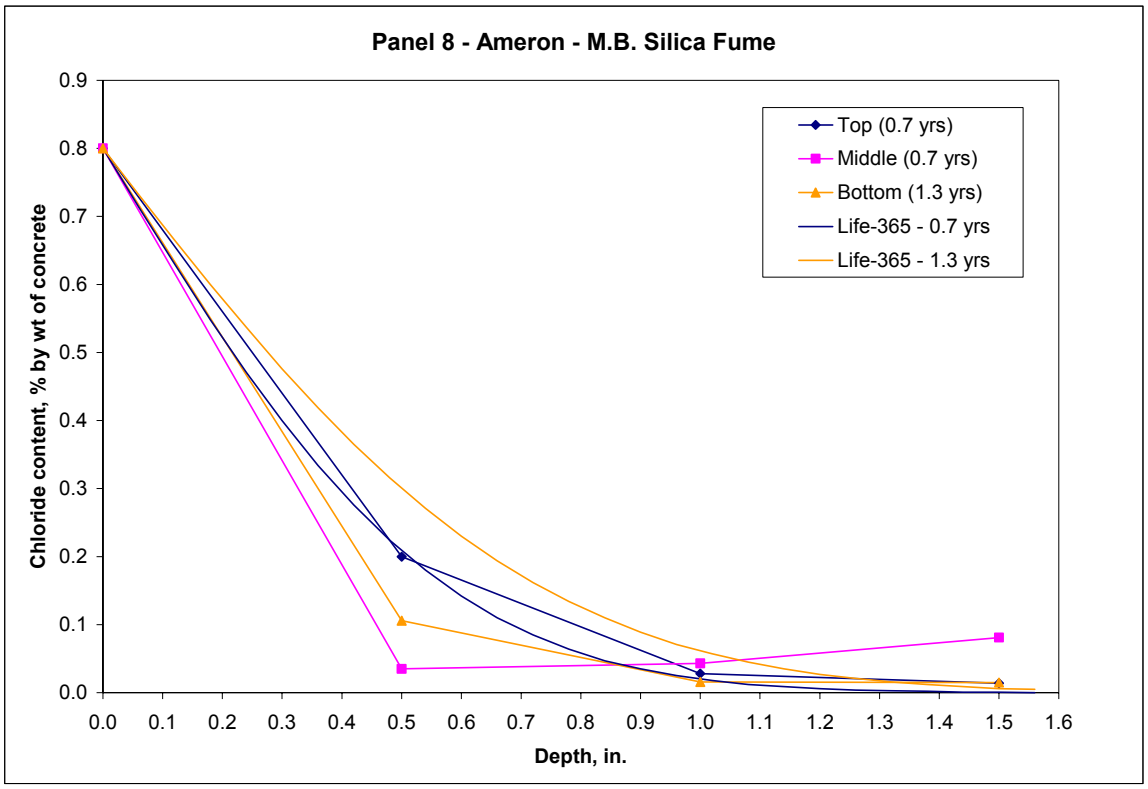

Figure 4.45. Life-365 predictions for panel 8.

In general, the predictions calculated using Life-365 for control panel 9 averaged 1.8 times the observed chloride concentrations. Estimated chloride concentration values for the top test hole averaged 1.9 times the amount measured, an average that was 1.2 times the measured values of the middle hole, and an average of 2.3 times the chloride concentration of the bottom hole.

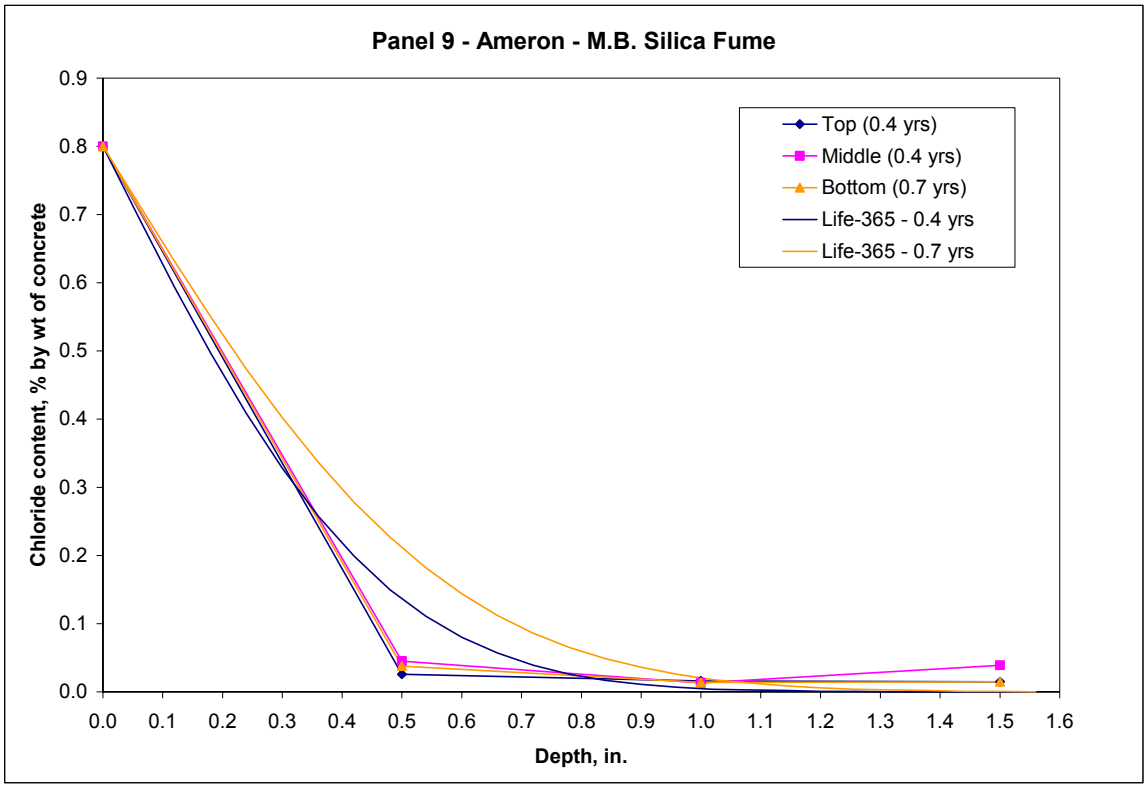

Figure 4.46. Life-365 predictions for panel 9.

The overall predictions calculated using Life-365 for control panel 10 averaged 2.3 times the measured chloride concentrations. Estimated chloride concentration values for the top test hole averaged 2.7 times the amount measured, an average of 3.1 times the measured values of the middle hole, and an average that was 1.2 times the chloride concentrations of the bottom hole.

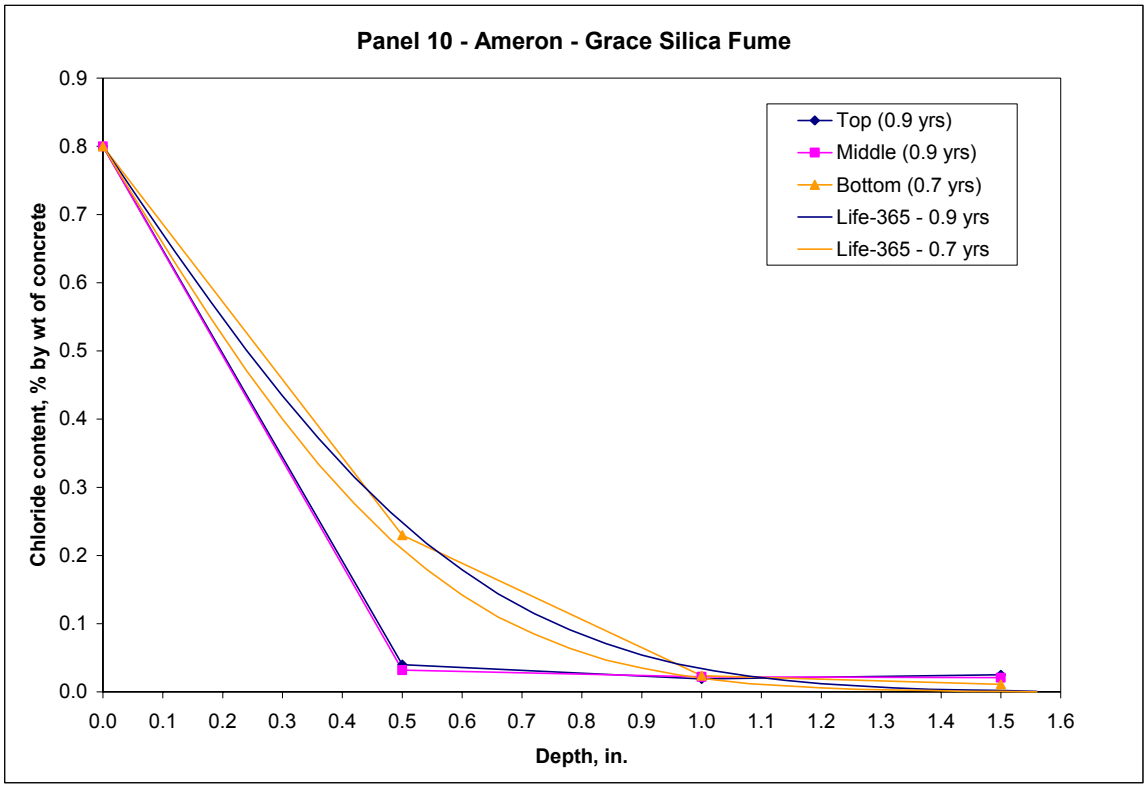

Figure 4.47. Life-365 predictions for panel 10.

4.9 Summary

This chapter presented the measurements for the orientation of all twenty-five reinforced concrete panels, the locations for all test holes, and the location of mean sea level on each panel. Test results for mechanical tests, chemical tests, air permeability, half-cell potential, and Life-365 were also discussed. Some mechanical test results from Phase II of the study were provided as a comparison to the results of this study.

Tests for the mechanical properties of reinforced concrete panels show that mixtures using Ameron aggregates provided higher compressive strengths than mixtures containing Halawa aggregates. Fly ash and silica fume had the highest average compressive strengths. DCI, Rheocrete CNI, and Kryton KIM provided slightly higher average compressive strengths than the control mixtures. FerroGard 901, Xypex Admix C-2000, and latex had little effect on the average compressive strength. The admixture Rheocrete 222+ reduced the compressive strength significantly.

The acid-soluble chloride concentrations for most of the twenty-five panels follow a similar trend of chloride concentration and depth. The chloride concentrations are higher near the surface of the concrete and decrease near the reinforcing steel. Also, the bottom test holes produce the highest chloride concentrations collectively at each depth, followed by the middle and top test holes. Twelve of the twenty-five panels have the highest chloride concentrations from the bottom test holes. Seven of the twenty-five panels have the highest chloride concentration from the middle test holes, and six of the twenty-five panels have the highest chloride concentrations from the top test holes.

All twenty-five reinforced concrete panels had a pH between 12 and 13, which indicates the concrete is still maintaining an alkaline environment around the steel and

thus inhibiting corrosion. None of the panels had a permeability quality level of "excellent". The control and Rheocrete 222+ panels made using Halawa aggregate had a quality rating of "poor." The control, latex, and Xypex Admix C-2000 panels using Ameron aggregates and DCI, Rheocrete CNI, and FerroGard 901 panels using Halawa aggregates had a quality rating of "not very good." The DCI, Rheocrete CNI, M.B. silica fume, fly ash, FerroGard 901, and Kryton KIM panels using Ameron aggregates produced a quality rating of "fair." Two panels of Rheocrete 222+ using Ameron aggregates had quality ratings of "not very good" and "fair." Also, two panels of fly ash using Halawa aggregates produced a "not very good" quality rating and a "fair" quality rating. The panel made of Grace silica fume was the only panel to produce a quality rating of "good."

The half-cell potential test determined the probability of corrosion occurring in the reinforcing steel. Panels 1, 3, 4, 10, 12, 13, 14, 15, and 18 had a risk of less than 10% for all ten locations. Panels 6, 7, 11, 21, and 22 had a 50% or unknown risk of corrosion taking place at all ten locations. The remaining panels had various risks of corrosion occurring at all ten locations. The readings for panel 20 were not reported due to errors that occurred during the field testing.

The computer program Life-365 was used to predict the chloride content (as a % by weight of concrete) at a given depth and time. The program overestimated the chloride contents for all the control panels, all the DCI panels and one of the two Rheocrete CNI panel with a dosage of 2.0 gallons per cubic yard (9.9 $1/m^3$), and all the panels proportioned with fly ash. It slightly overestimates the chloride contents for the DCI and CNI panels with dosages of 4.0 gallons per cubic yard (19.8 $1/m^3$). The

program closely predicted the chloride contents for all the panels proportioned with silica fume. Life-365 closely predicted the chloride contents of the bottom test hole of the other Rheocrete CNI panel and overestimated the top and middle test holes. It overestimated the chloride contents for two of the Rheocrete 222+ panels, and slightly overestimated the remaining two panels.

CHAPTER 5
COMPARISON OF CHLORIDE CONCENTRATIONS

5.1 Introduction

This chapter presents the results of the chloride concentration tests from the Phase II laboratory study and compares them with the results from the Phase III field study. An attempt is made to develop a correlation between the number of cycles for the laboratory specimens and the time of exposure for the field panels. The chloride concentrations at the level of the reinforcement, 1.0 in. (25 cm) below the top surface, in the laboratory specimens were plotted against the number of ponding cycles. Linear regression was used to determine a correlation between chloride concentration and number of cycles for the laboratory specimens. The chloride concentration data from the Phase III study field panels was then used with this laboratory correlation to estimate the number of laboratory cycles which are equivalent to one year of exposure in the field. Chloride concentration test results for the laboratory specimens of Phase II are provided in Appendix F.

5.2 Chloride comparisons

Comparisons between laboratory and field data were only performed on the control, DCI, Rheocrete 222+, FerroGard 901, latex, and silica fume mixtures using the aggregates from the Ameron Kapaa quarry. A limited amount of laboratory specimens were fabricated for the mixtures proportioned using the Halawa quarry aggregates and chloride data was not collected at early cycles.

In the laboratory specimens of the Phase II study, a concrete dust sample was collected for the chloride concentration tests using a ¾ in. (19 mm) diameter drill bit between a depth of 1.0 in. (25 mm) and 1.5 in. (38 mm) below the top surface, and designated as a sample at a 1.0 in. (25 mm) depth. These results were compared with the chloride concentration samples collected at depths of 1.0 in. (25 mm) for each test hole of the field panels of the Phase III study. All chloride concentrations in the following sections are reported as percentage by weight of cement.

5.2.1 Control mixtures

Chloride concentrations for mixture C2 of the Phase II study were plotted against the number of cycles to determine the cycles that were equivalent to one year field exposure for control panel 1 as shown in Figure 5.1. The approximate correlations are 1.72 cycles per year for the top test hole, 0.71 cycles per year for the middle hole, and 1.18 cycles per year for the bottom hole. The average of the values at all three test holes is 1.21 cycles per year for panel 1 (Table 5.1). This represents a ratio of 10 months field exposure per laboratory ponding cycle.

Table 5.1. Ponding cycle correlation for control panel 1.

Location	Cl conc.	Age (yrs)	Cycles	Cycles per year	Months per cycle
T - 1.0	0.306	1.5	2.58	1.72	7
M - 1.0	0.127	1.5	1.07	0.71	17
B - 1.0	0.222	1.6	1.87	1.18	10
Average	0.218	1.5	1.84	1.21	10

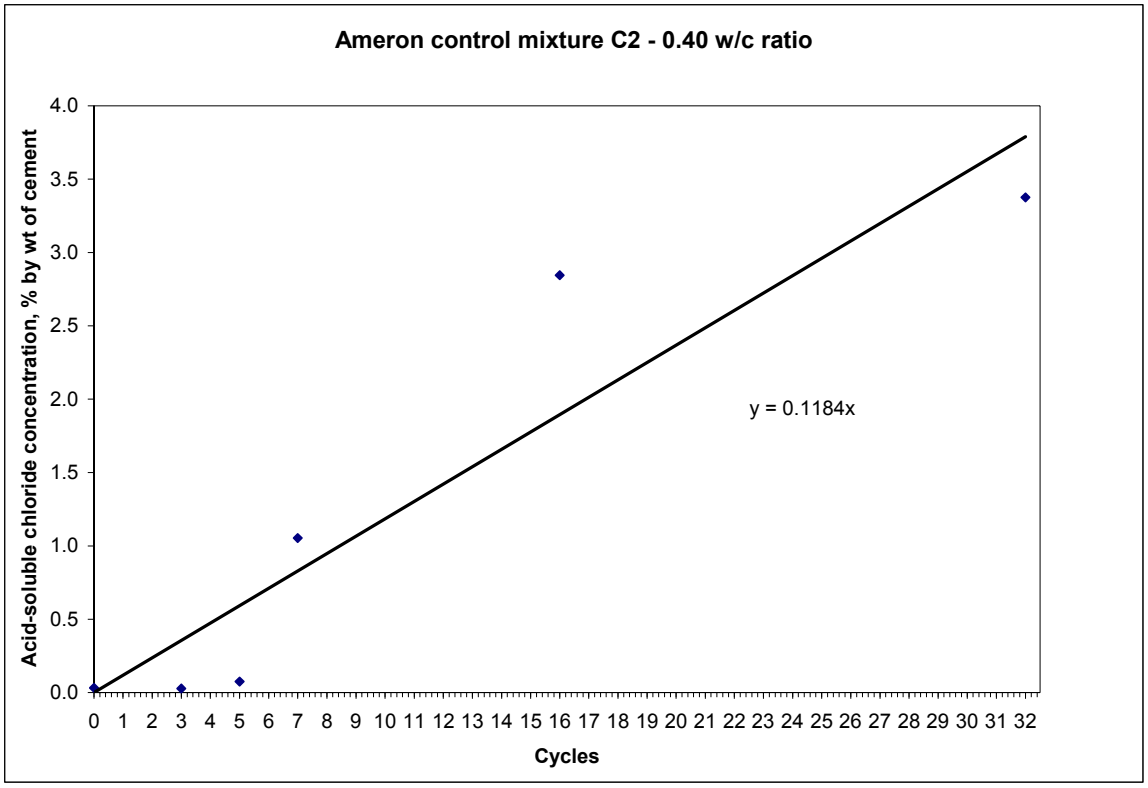

Figure 5.1. Chloride concentration vs. cycles for mixture C2.

Results from mixture C1 of the Phase II study for chloride concentrations were plotted against the number of cycles to determine cycles that were equivalent to one year of field exposure for control panel 7. Panel 7 had a lower water-cement ratio of 0.35 compared to 0.40 for panel 1. Approximately 0.41 cycles per year correlate to the top test hole result, 0.80 cycles per year for the middle hole, and 2.27 cycles per year for the bottom hole. The average of the three values at all three test holes is 1.16 cycles per year for panel 7 (Table 5.2). This represents a ratio of 10 months field exposure per laboratory ponding cycle.

Table 5.2. Ponding cycle correlation for control panel 7.

Location	Cl conc.	Age (yrs)	Cycles	Cycles per year	Months per cycle
T - 1.0	0.065	1.5	0.62	0.41	29
M - 1.0	0.125	1.5	1.19	0.80	15
B - 1.0	0.378	1.6	3.63	2.27	5
Average	0.189	1.5	1.81	1.16	10

5.2.2 DCI mixtures

Chloride concentrations for mixture D4 of the Phase II study were plotted against the number of cycles to determine the cycles that were equivalent to one year field exposure for DCI panel 3. Approximately 1.01 cycles per year correlate to the top test hole, 0.55 cycles per year for the middle hole, and 1.65 cycles per year for the bottom hole. The average of the three values at all three test holes indicated is 1.07 cycles per year for panel 3 (Table 5.3). This represents a ratio of 11 months field exposure per laboratory ponding cycle.

Table 5.3. Ponding cycle correlation for DCI panel 3.

Location	Cl conc.	Age (yrs)	Cycles	Cycles per year	Months per cycle
T - 1.0	0.279	1.7	1.71	1.01	12
M - 1.0	0.153	1.7	0.94	0.55	22
B - 1.0	0.458	1.7	2.81	1.65	7
Average	0.297	1.7	1.82	1.07	11

Results from mixture D5 of the Phase II study for chloride concentrations were plotted against the number of cycles to determine the cycles that were equivalent to one year field exposure for DCI panel 3A. Approximately 0.33 cycles per year correlate to the top test hole, 1.35 cycles per year for the middle hole, and 1.45 cycles per year for the bottom hole. The average of the three values at all three test holes is 1.05 cycles per year

for panel 3A (Table 5.4). This represents a ratio of 11 months field exposure per laboratory ponding cycle.

Table 5.4. Ponding cycle correlation for DCI panel 3A.

Location	Cl conc.	Age (yrs)	Cycles	Cycles per year	Months per cycle
T - 1.0	0.039	0.7	0.23	0.33	36
M - 1.0	0.068	0.3	0.41	1.35	9
B - 1.0	0.148	0.6	0.87	1.45	8
Average	0.085	0.5	0.50	1.05	11

5.2.3 Rheocrete 222+ mixtures

Chloride concentrations for mixture RHE2 of the Phase II study were plotted against the number of cycles to determine the cycles that were equivalent to one year field exposure for Rheocrete 222+ panel 15. Approximately 0.31 cycles per year correlate to the top test hole, 0.47 cycles per year for the middle hole, and 0.87 cycles per year for the bottom hole. The average of the three values at all three test holes indicated is 0.55 cycles per year for panel 15 (Table 5.5). This represents a ratio of 22 months field exposure per laboratory ponding cycle.

Table 5.5. Ponding cycle correlation for Rheocrete 222+ panel 15.

Location	Cl conc.	Age (yrs)	Cycles	Cycles per year	Months per cycle
T - 1.0	0.048	1.1	0.34	0.31	39
M - 1.0	0.074	1.1	0.52	0.47	26
B - 1.0	0.174	1.4	1.22	0.87	14
Average	0.099	1.2	0.69	0.55	22

Results from mixture RHE2 of the Phase II study for chloride concentrations were plotted against the number of cycles to determine the cycles that were equivalent to one year field exposure for Rheocrete 222+ panel 16. Approximately 1.24 cycles per year

correlate to the top test hole, 1.53 cycles per year for the middle hole, and 3.65 cycles per year for the bottom hole. The average of the three values at all three test holes is 2.14 cycles per year for panel 16 (Table 5.6). This represents a ratio of 6 months field exposure per laboratory ponding cycle.

Table 5.6. Ponding cycle correlation for Rheocrete 222+ panel 16.

Location	Cl conc.	Age (yrs)	Cycles	Cycles per year	Months per cycle
T - 1.0	0.248	1.4	1.74	1.24	10
M - 1.0	0.306	1.4	2.14	1.53	8
B - 1.0	0.887	1.7	6.20	3.65	3
Average	0.480	1.5	3.36	2.24	6

5.2.4 FerroGard 901 mixtures

Chloride concentrations for mixture FER2 of the Phase II study were plotted against the number of cycles to determine the cycles that were equivalent to one year field exposure for FerroGard panel 20. Approximately 1.73 cycles per year correlate to the top test hole, 0.70 cycles per year for the middle hole, and 0.66 cycles per year for the bottom hole. The average of the three values at all three test holes indicated is 1.03 cycles per year for panel 20 (Table 5.7). This represents a ratio of 12 months field exposure per laboratory ponding cycle.

Table 5.7. Ponding cycle correlation for FerroGard 901 panel 20.

Location	Cl conc.	Age (yrs)	Cycles	Cycles per year	Months per cycle
T - 1.0	0.248	1.2	2.08	1.73	7
M - 1.0	0.100	1.2	0.84	0.70	17
B - 1.0	0.095	1.2	0.80	0.66	18
Average	0.148	1.2	1.24	1.03	12

5.2.5 Latex-modified mixtures

Results from mixture L5 of the Phase II study for chloride concentrations were plotted against the number of cycles to determine the cycles that were equivalent to one year field exposure for latex panel 14. Approximately 1.48 cycles per year correlate to the top test hole, 1.48 cycles per year for the middle hole, and 1.44 cycles per year for the bottom hole. The average of the three values at all three test holes is 1.47 cycles per year for panel 14 (Table 5.8). This represents a ratio of 8 months field exposure per laboratory ponding cycle.

Table 5.8. Ponding cycle correlation for latex panel 14.

Location	Cl conc.	Age (yrs)	Cycles	Cycles per year	Months per cycle
T - 1.0	0.078	0.3	0.45	1.48	8
M - 1.0	0.078	0.3	0.45	1.48	8
B - 1.0	0.176	0.7	1.01	1.44	8
Average	0.111	0.4	0.63	1.47	8

5.2.6 Silica fume mixtures

Chloride concentrations for mixture SF2 of the Phase II study were plotted against the number of cycles to determine the cycles that were equivalent to one year field exposure for silica fume panel 8. Approximately 2.88 cycles per year correlate to the top test hole, 4.42 cycles per year for the middle hole, and 0.88 cycles per year for the bottom hole. The average of the three values at all three test holes indicated is 2.73 cycles per year for panel 8 (Table 5.9). This represents a ratio of 4 months field exposure per laboratory ponding cycle.

Table 5.9. Ponding cycle correlation for silica fume panel 8.

Location	Cl conc.	Age (yrs)	Cycles	Cycles per year	Months per cycle
T - 1.0	0.144	0.7	2.01	2.88	4
M - 1.0	0.222	0.7	3.09	4.42	3
B - 1.0	0.082	1.3	1.15	0.88	14
Average	0.149	0.9	2.08	2.73	4

Results from mixture SF2 of the Phase II study for chloride concentrations were plotted against the number of cycles to determine the cycles that were equivalent to one year field exposure for silica fume panel 9. Approximately 2.87 cycles per year correlate to the top test hole, 2.33 cycles per year for the middle hole, and 1.44 cycles per year for the bottom hole. The average of the three values at all three test holes is 2.21 cycles per year for panel 9 (Table 5.10). This represents a ratio of 5 months field exposure per laboratory ponding cycle.

Table 5.10. Ponding cycle correlation for silica fume panel 9.

Location	Cl conc.	Age (yrs)	Cycles	Cycles per year	Months per cycle
T - 1.0	0.082	0.4	1.15	2.87	4
M - 1.0	0.067	0.4	0.93	2.33	5
B - 1.0	0.072	0.7	1.01	1.44	8
Average	0.074	0.5	1.03	2.06	5

Chloride concentrations for mixture SF2 of the Phase II study were plotted against the number of cycles to determine the cycles that were equivalent to one year field exposure for silica fume panel 10. Approximately 1.71 cycles per year correlate to the top test hole, 1.98 cycles per year for the middle hole, and 2.77 cycles per year for the bottom hole. The average of the three values at all three test holes indicated is 2.15 cycles per year for panel 10 (Table 5.11). This represents a ratio of 6 months field exposure per laboratory ponding cycle.

Table 5.11. Ponding cycle correlation for silica fume panel 10.

Location	Cl conc.	Age (yrs)	Cycles	Cycles per year	Months per cycle
T - 1.0	0.110	0.9	1.54	1.71	7
M - 1.0	0.128	0.9	1.78	1.98	6
B - 1.0	0.139	0.7	1.94	2.77	4
Average	0.126	0.8	1.75	2.15	6

5.3 Chloride comparison overview

An overview of the correlation of chloride concentration data from the previous sections is provided in Figure 5.2. The figure shows a comparison of the correlation of laboratory ponding cycles per year of field exposure for each panel.

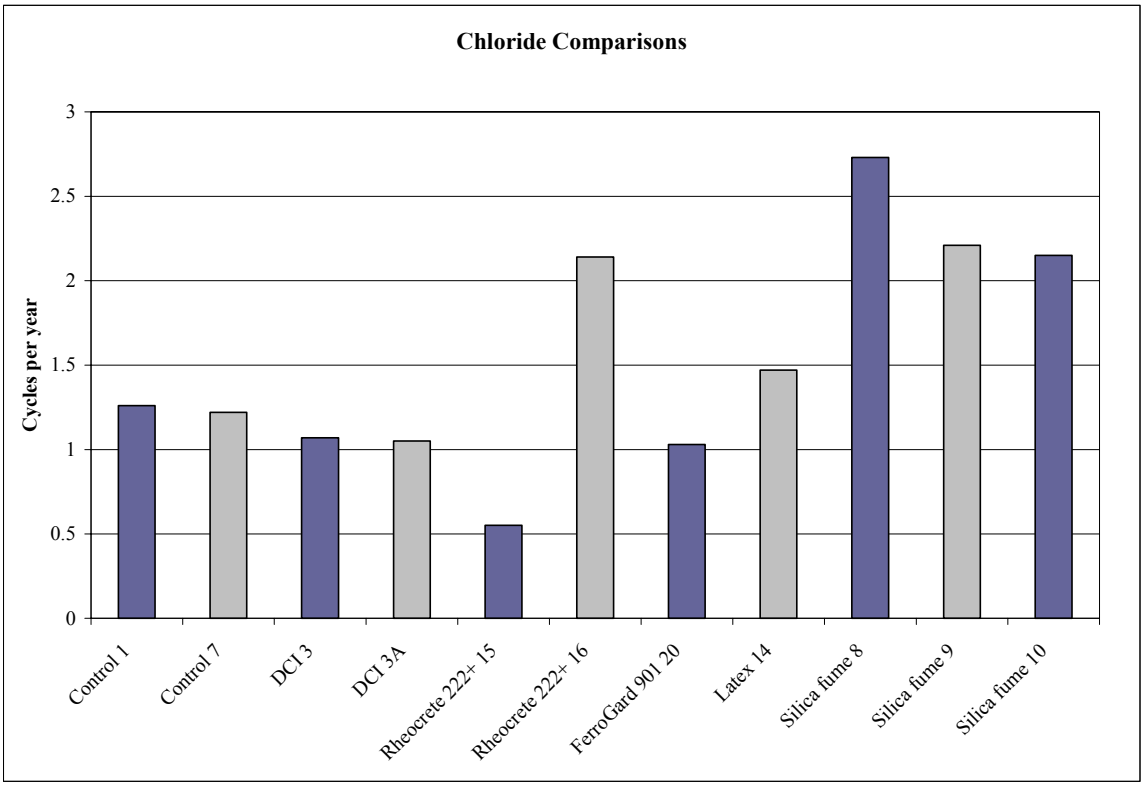

Figure 5.2. Comparison of the correlation of laboratory and field data.

It should be noted that these results do not indicate whether a particular panel has higher or lower chloride permeability than any other panel since the comparison is made between nominally identical mixtures in the field panels and the laboratory specimens. The correlation indicates whether it is possible to establish a common ratio between laboratory ponding cycles and exposure time in the field for any concrete mixture.

Both panels 1 and 7 displayed similar results despite the difference in water cement ratios for the two mixtures. DCI panels 3 and 3A also showed similar results despite the different admixture dosages (note that this admixture is not intended to reduce permeability). Rheocrete 222+ panels, using the same mixture proportions, produced results that were very inconsistent. The FerroGard 901 panel provided results that were similar to the control mixtures. The latex panel required slightly more ponding cycles than the control mixtures to simulate field conditions. Silica fume required the most laboratory ponding cycles per year of field exposure. For all panels, excluding the Rheocrete 222+ and silica fume panels, the average correlation between field and laboratory exposure is that 1.2 laboratory cycles simulate one year field exposure, or one laboratory cycle is equivalent to 10.3 months field exposure. For the silica fume specimens, the correlation is that 2.4 laboratory cycles simulate one year field exposure, or one laboratory cycle is equivalent to 5.1 months field exposure.

5.4 Summary

This chapter presented a comparison of chloride concentration data from the Phase II and III studies to determine a correlation between laboratory ponding cycles and years of exposure in a marine environment. For the control, DCI, Ferrogard 901 and

Latex mixtures, 1.2 laboratory cycles simulate one year field exposure, while for the silica fume mixtures, 2.4 laboratory cycles simulate one year field exposure.

CHAPTER 6
LIFE-365 RECOMMENDATIONS

6.1 Introduction

This chapter presents a comparison between the chloride concentrations measured at various depths in the cover concrete of the field panels compared with predictions made using the computer program Life-365. The default input parameters used by Life-365 produced results that were overly conservative for all of the panel mixtures except the silica fume mixtures. Modified input parameters are proposed for the user defined corrosion protection scenarios in Life-365 based on measured results of chloride concentration collected in this study. Recommendations presented in the following sections are for the control, DCI, Rheocrete CNI, Rheocrete 222+, and fly ash panels. The other admixtures used in this study were not included in the Life-365 database.

6.2 Life-365 recommendations

The figures in this section present the chloride concentration profiles at each of the three holes drilled on each field panel, along with the Life-365 prediction using default input parameters for the worst field profile. Input parameters in Life-365 include the diffusion coefficient, an m variable, corrosion threshold and propagation time. Since the corrosion threshold and propagation time do not influence the chloride infusion rate, they were not adjusted. The diffusion coefficient and m variable were adjusted to improve the Life-365 predictions based on the field measurements. The input values were adjusted for the control mixtures with 0.40 water-cement ratio, and these same values were used for the DCI, Rheocrete CNI, and Rheocrete 222+ since they had the same 0.40

water-cement ratio, and these admixtures are not expected to affect the chloride infusion rate. Separate adjusted values were determined for the control mixture with a 0.35 water-cement ratio and fly ash mixtures, based on the worst chloride concentration values for each type of mixture.

Adjusted predictions were only performed for the test hole with the highest overall chloride concentrations for each panel or the next highest chloride concentrations with the most consistent results. The values for the diffusion coefficient and the m variable were adjusted to fit the Life-365 prediction curve to the measured values with a priority on the measured values at a depth of 0.5 in. (13 mm). This was because these values best represent the intrusive chloride concentration and not the existing chloride concentration introduced by the concrete constituents. The accuracy of the Life-365 predictions was determined by dividing the predicted value by the measured value.

6.2.1 Control mixtures

The Life-365 predictions for control panel 1 using both the default and adjusted variables are presented in Figure 6.1. Using the default values, Life-365 overestimated the average chloride concentration of the top test hole by approximately 2.9 times the measured values. By decreasing the diffusion coefficient and increasing the m variable, Life-365 overestimated the average chloride concentration of the top hole by about 1.2 times the measured valued.

Table 6.1. Default and adjusted input values for Ameron control panel 1.

	Default values	Adjusted values
Diffusion coefficient	7.94E-12	5.50E-12
m	0.20	0.38
Corrosion threshold	0.05	0.05

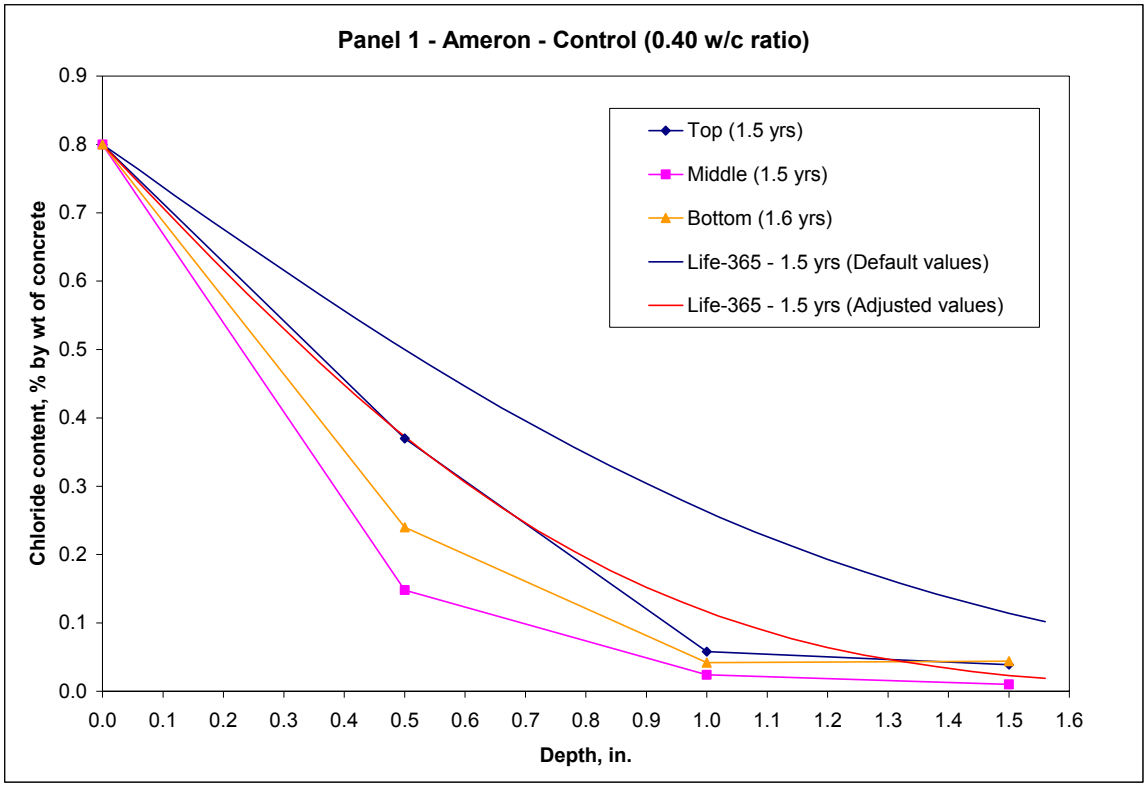

Figure 6.1. Life-365 predictions using default and adjusted values for panel 1.

Predictions calculated with the default and adjusted variables for control panel 2 are shown in Figure 6.2. Life-365 overestimated the average chloride concentration of the top test hole of panel 2 by approximately 6.9 times the measured values using the default input values. By decreasing the adjusted diffusion coefficient and m variable in, Life-365 underestimated the average chloride concentration of the top hole by about 0.5 times the measured value.

Table 6.2. Default and adjusted values for Halawa panel 2.

	Default values	Adjusted values
Diffusion coefficient	7.94E-12	1.67E-12
m	0.20	0.38
Corrosion threshold	0.05	0.05

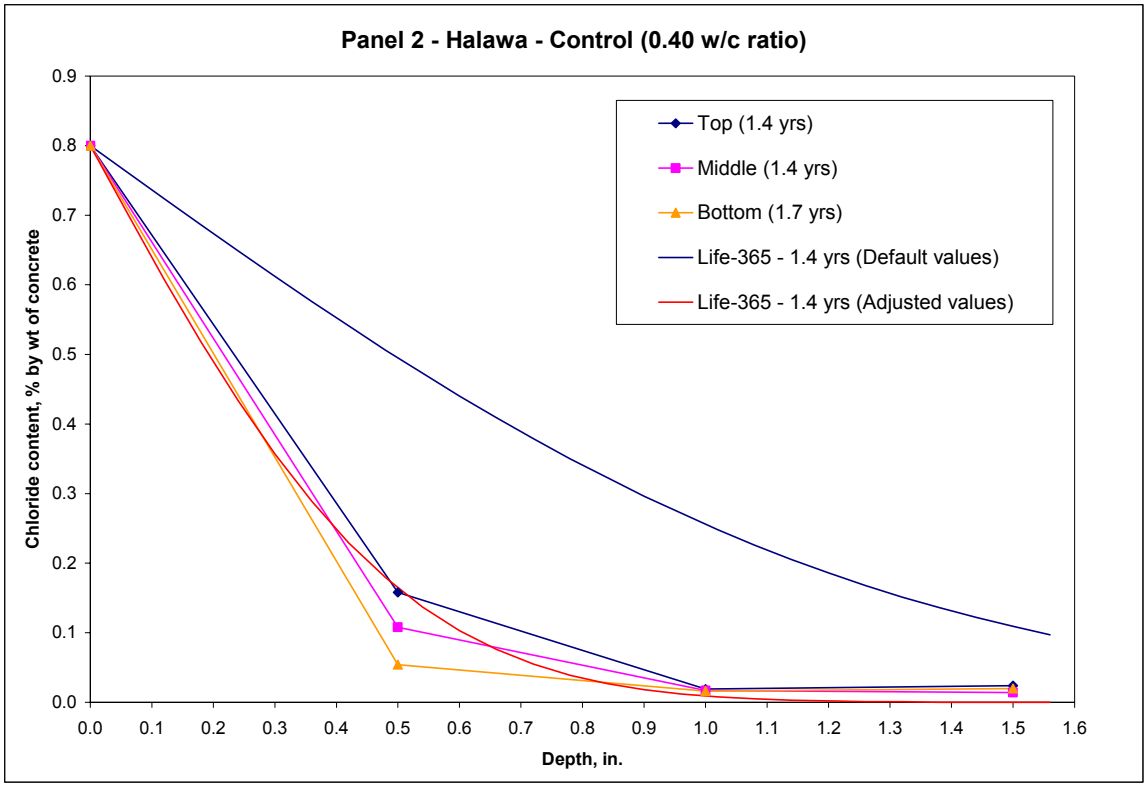

Figure 6.2. Life-365 predictions using default and adjusted values for panel 2.

Estimated chloride concentrations using both the default and adjusted variables for control panel 7 are presented in Figure 6.3. Predictions using the default values overestimated the average chloride concentration of the bottom test hole by about 3.5 times the measured values. By decreasing the diffusion coefficient and increasing the m variable, Life-365 improved its predictions by underestimating the average chloride concentration of the bottom hole by approximately 0.4 times the measured value.

Table 6.3. Default and adjusted values for Ameron control panel 7.

	Default values	Adjusted values
Diffusion coefficient	6.03E-12	1.53E-12
m	0.20	0.41
Corrosion threshold	0.05	0.05

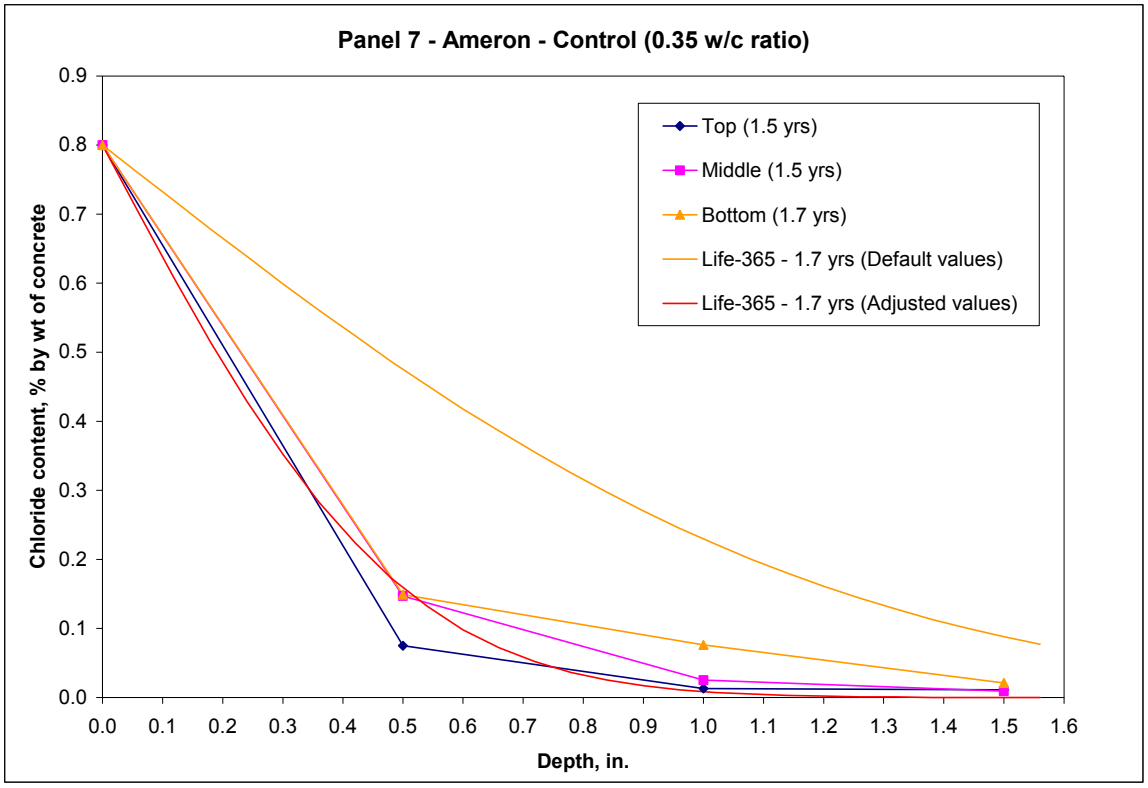

Figure 6.3. Life-365 predictions using default and adjusted values for panel 7.

6.2.2 DCI mixtures

The predictions for DCI panel 3 using both the default and adjusted variables are presented in Figure 6.4. Using the default values, Life-365 overestimated the average chloride concentration of the bottom test hole by approximately 3.5 times the measured values. Life-365 overestimated the average chloride concentration of the bottom hole by

about 1.6 times the measured valued using the same diffusion coefficient and m variable as control panel 1.

Table 6.4. Default and adjusted values for Ameron DCI panels 3.

	Default values	Adjusted values
Diffusion coefficient	7.94E-12	5.50E-12
m	0.20	0.38
Corrosion threshold	0.15	0.15

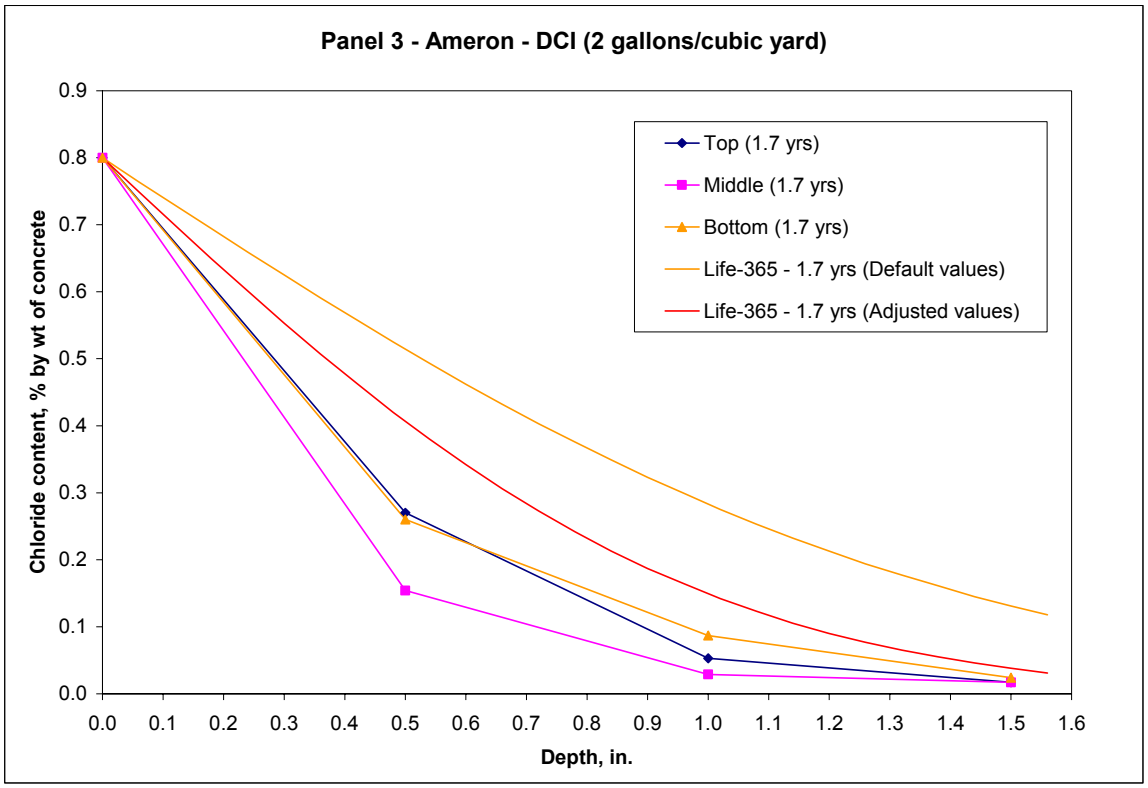

Figure 6.4. Life-365 predictions using default and adjusted values for panel 3.

Predictions calculated with the default and adjusted variables for DCI panel 3A are shown in Figure 6.5. Life-365 overestimated the average chloride concentration of the bottom test hole of panel 3A by approximately 3.3 times the measured values using the default input values. Using the same adjusted diffusion coefficient and m variable as

DCI panel 3 and the default corrosion threshold value recommended for the admixture dosage amount, Life-365 overestimated the average chloride concentration of the bottom hole by about 1.3 times the measured value.

Table 6.5. Default and adjusted values for Ameron DCI panel 3A.

	Default values	Adjusted values
Diffusion coefficient	7.94E-12	5.50E-12
m	0.20	0.38
Corrosion threshold	0.32	0.32

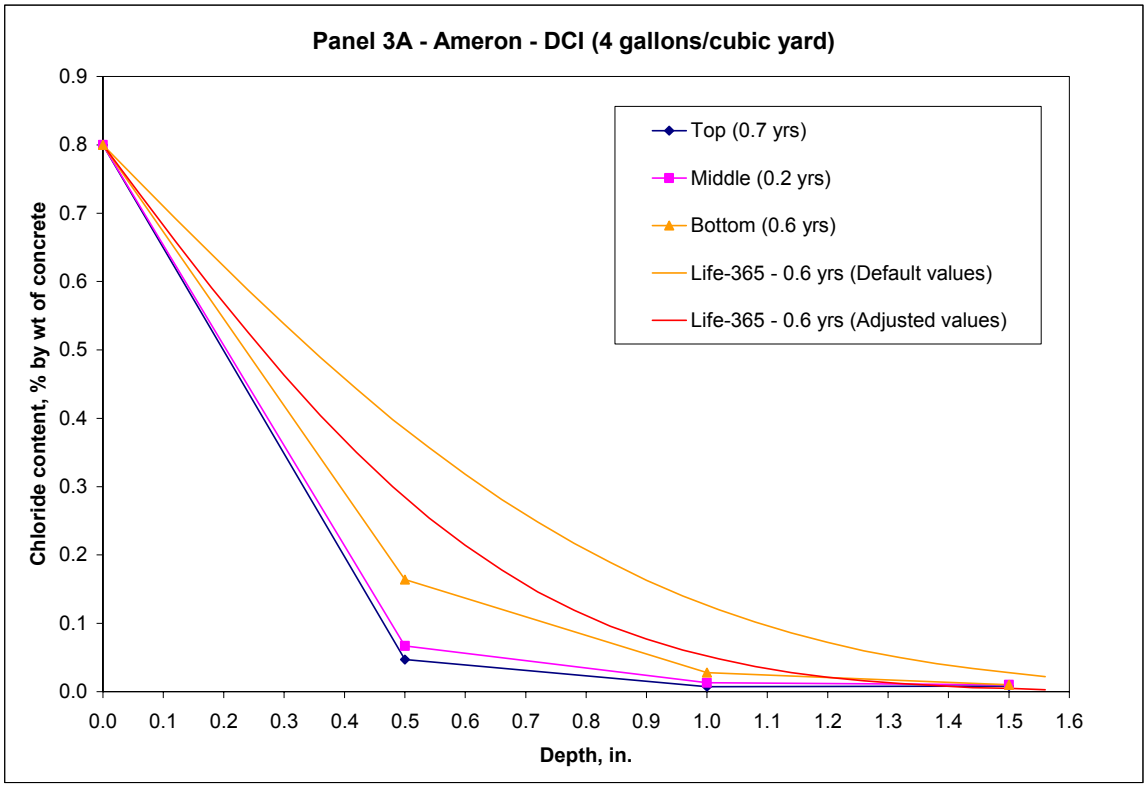

Figure 6.5. Life-365 predictions using default and adjusted values for panel 3A.

Estimated chloride concentrations using both the default and adjusted variables for DCI panel 4 are presented in Figure 6.6. Predictions using the default values overestimated the average chloride concentration of the bottom test hole by about 11.2

times the measured values. Because panel 4 was proportioned using Halawa aggregates, the same diffusion coefficient and m variable as control panel 2 was used. Life-365 improved its predictions by underestimating the average chloride concentration of the bottom hole by approximately 0.7 times the measured value.

Table 6.6. Default and adjusted values for Halawa DCI panels 4.

	Default values	Adjusted values
Diffusion coefficient	7.94E-12	1.67E-12
m	0.20	0.38
Corrosion threshold	0.15	0.15

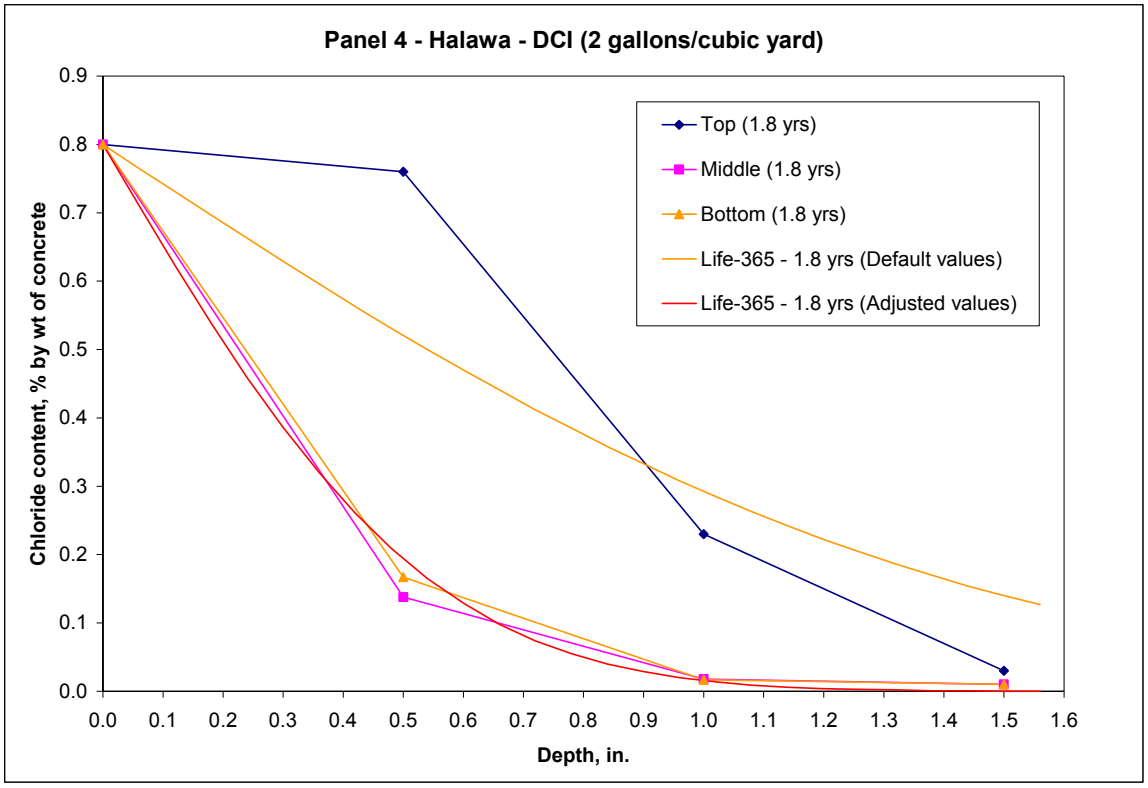

Figure 6.6. Life-365 predictions using default and adjusted values for panel 4.

6.2.3 Rheocrete CNI mixtures

The predictions for Rheocrete CNI panel 5 using both the default and adjusted variables are presented in Figure 6.7. Using the default values, Life-365 overestimated the average chloride concentration of the middle test hole by approximately 4.6 times the measured values. By using the same diffusion coefficient and the m variable as control panel 1, Life-365 overestimated the average chloride concentration of the middle hole by about 1.9 times the measured valued.

Table 6.7. Default and adjusted values for Ameron Rheocrete CNI panels 5 and 6.

	Default values	Adjusted values
Diffusion coefficient	7.94E-12	5.50E-12
m	0.20	0.38
Corrosion threshold	0.15	0.15

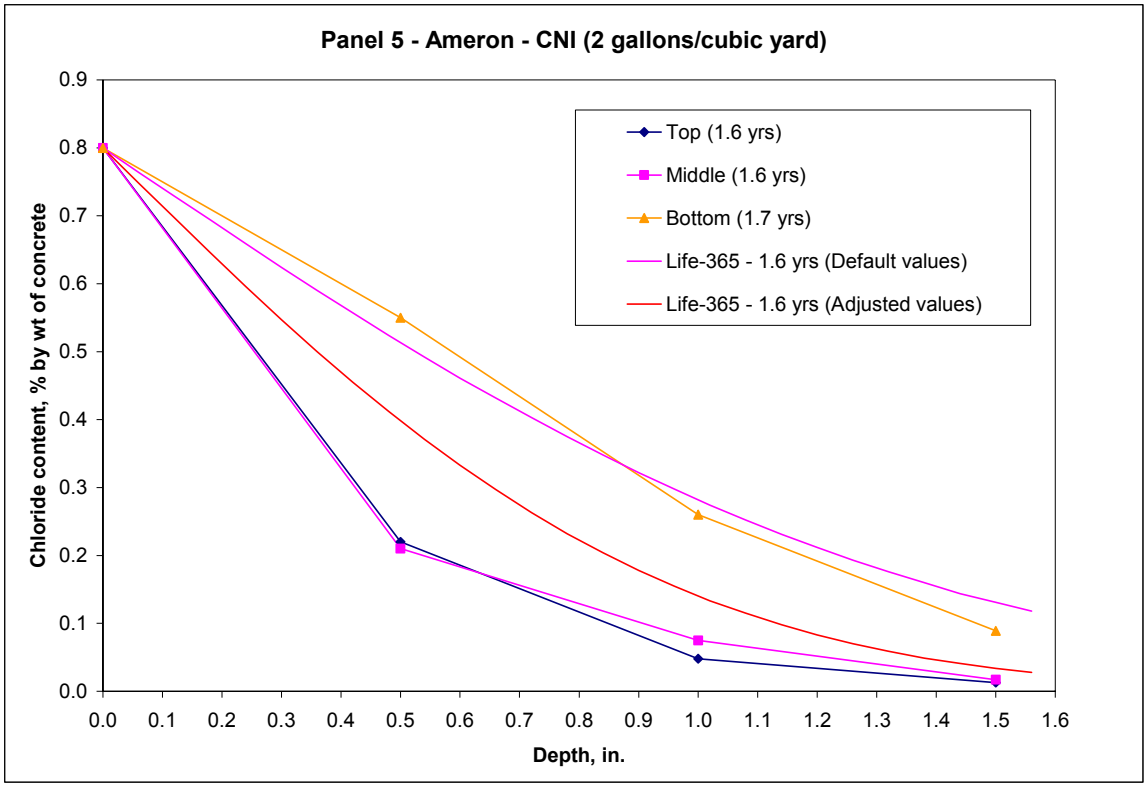

Figure 6.7. Life-365 predictions using default and adjusted values for panel 5.

Predictions calculated with the default and adjusted variables for Rheocrete CNI panel 5A are shown in Figure 6.8. Life-365 overestimated the average chloride concentration of the bottom test hole of panel 5A by approximately 3.2 times the measured values using the default input values. Using the same adjusted diffusion coefficient and m variable as Rheocrete CNI panel 5 and the default corrosion threshold value recommended for the admixture dosage amount, Life-365 overestimated the average chloride concentration of the bottom hole by about 1.2 times the measured value.

Table 6.8. Default and adjusted values for Rheocrete CNI panel 5A.

	Default values	Adjusted values
Diffusion coefficient	7.94E-12	5.50E-12
m	0.20	0.38
Corrosion threshold	0.32	0.32

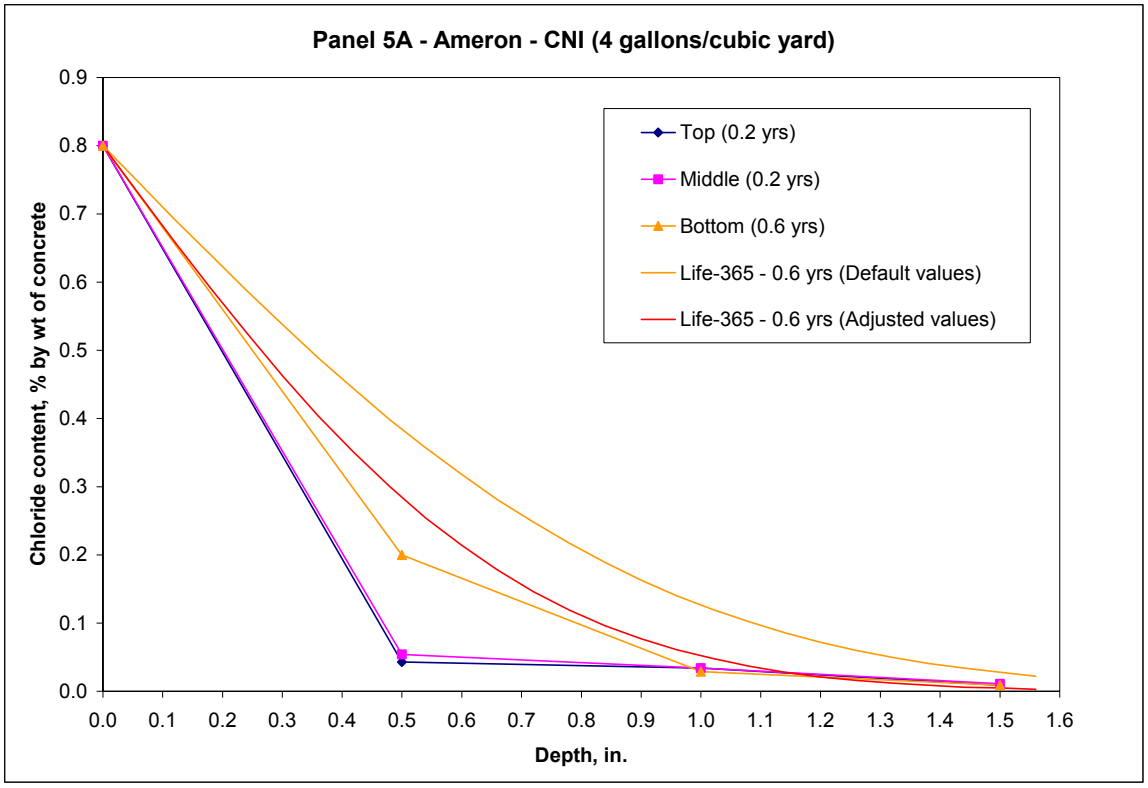

Figure 6.8. Life-365 predictions using default and adjusted values for panel 5A.

Estimated chloride concentrations using both the default and adjusted variables for Rheocrete CNI panel 6 are presented in Figure 6.9. Predictions using the default values overestimated the average chloride concentration of the bottom test hole by about 7.2 times the measured values. By using the same diffusion coefficient and m variable as Rheocrete CNI panel 5, Life-365 improved its predictions by overestimating the average chloride concentration of the bottom hole by approximately 3.0 times the measured value.

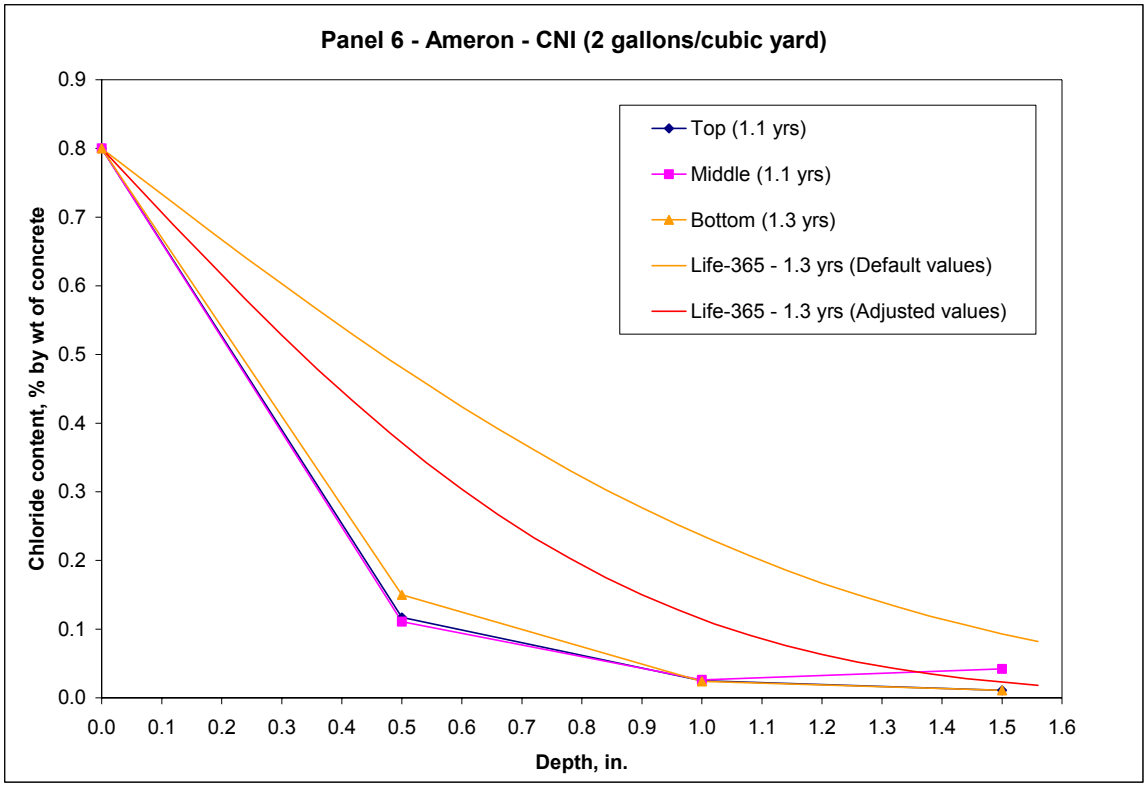

Figure 6.9. Life-365 predictions using default and adjusted values for panel 6.

6.2.4 Rheocrete 222+ mixtures

The predictions for Rheocrete 222+ panel 15 using both the default and adjusted variables are presented in Figure 6.10. Using the default values, Life-365 overestimated the average chloride concentration of the bottom test hole by approximately 6.2 times the measured values. Life-365 overestimated the average chloride concentration of the bottom hole by about 3.4 times the measured valued using the same diffusion coefficient and m variable as control panel 1.

Table 6.9. Default and adjusted values for Rheocrete 222+ panels 15 and 16.

	Default values	Adjusted values
Diffusion coefficient	7.94E-12	5.50E-12
m	0.20	0.38
Corrosion threshold	0.12	0.12

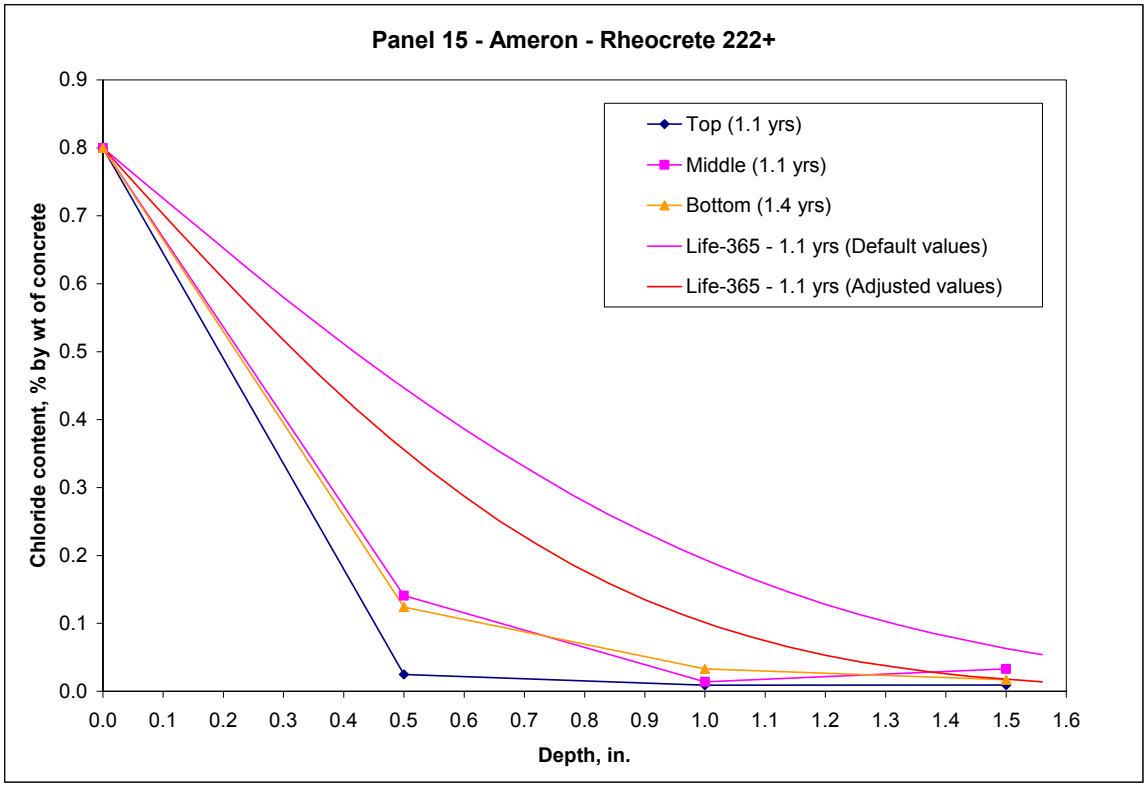

Figure 6.10. Life-365 predictions using default and adjusted values for panel 15.

Predictions calculated with the default and adjusted variables for Rheocrete 222+ panel 16 are shown in Figure 6.11. Life-365 overestimated the average chloride concentration of the bottom test hole of this panel by approximately 2.1 times the measured values using the default input values. Using the same adjusted diffusion coefficient and m variable as Rheocrete 222+ panel 15, Life-365 estimated the chloride concentration of the bottom hole by an average of about 1.0 times the measured value.

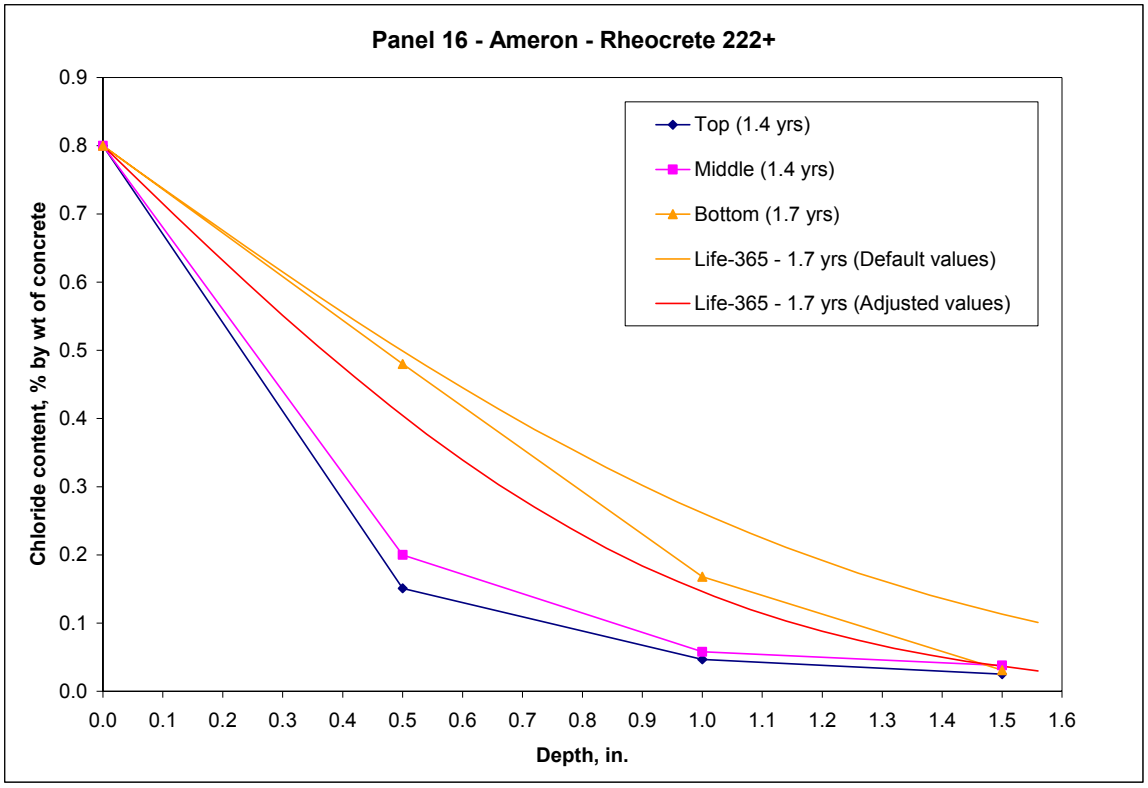

Figure 6.11. Life-365 prediction using default and adjusted values for panel 16.

Estimated chloride concentrations using both the default and adjusted variables for Rheocrete 222+ panel 17 are presented in Figure 6.12. Predictions using the default values overestimated the average chloride concentration of the middle test hole by about 3.9 times the measured values. By using the same diffusion coefficient and m variable as Rheocrete 222+ panel 15, Life-365 underestimated the average chloride concentration of the middle hole by approximately 0.3 times the measured value.

Table 6.10. Default and adjusted values for Rheocrete 222+ panels 17 and 17A.

	Default values	Adjusted values
Diffusion coefficient	7.94E-12	1.67E-12
m	0.20	0.38
Corrosion threshold	0.12	0.12

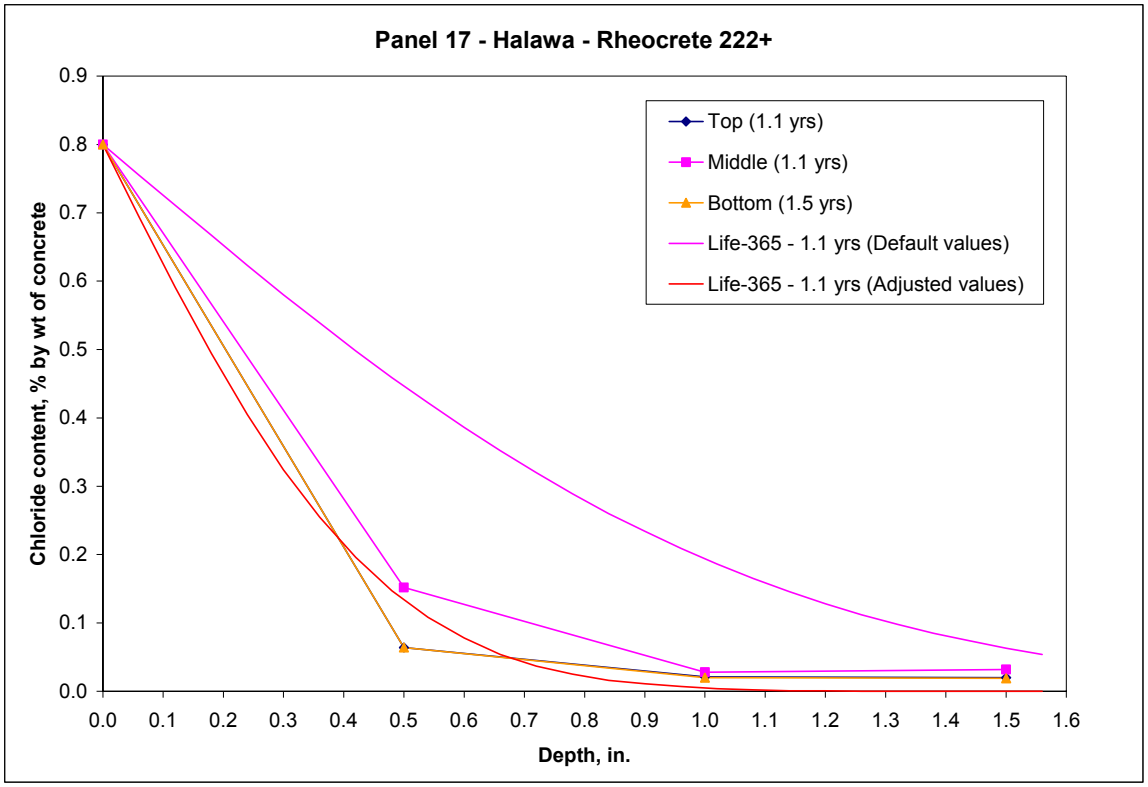

Figure 6.12. Life-365 predictions using default and adjusted values for panel 17.

Predictions calculated with the default and adjusted variables for Rheocrete 222+ panel 17A are shown in Figure 6.13. Life-365 overestimated the average chloride concentration of the bottom test hole of this panel by approximately 1.8 times the measured values using the default input values. Using the same adjusted diffusion coefficient and m variable as Rheocrete 222+ panel 15, Life-365 underestimated the average chloride concentration of the bottom hole by about 0.2 times the measured value.

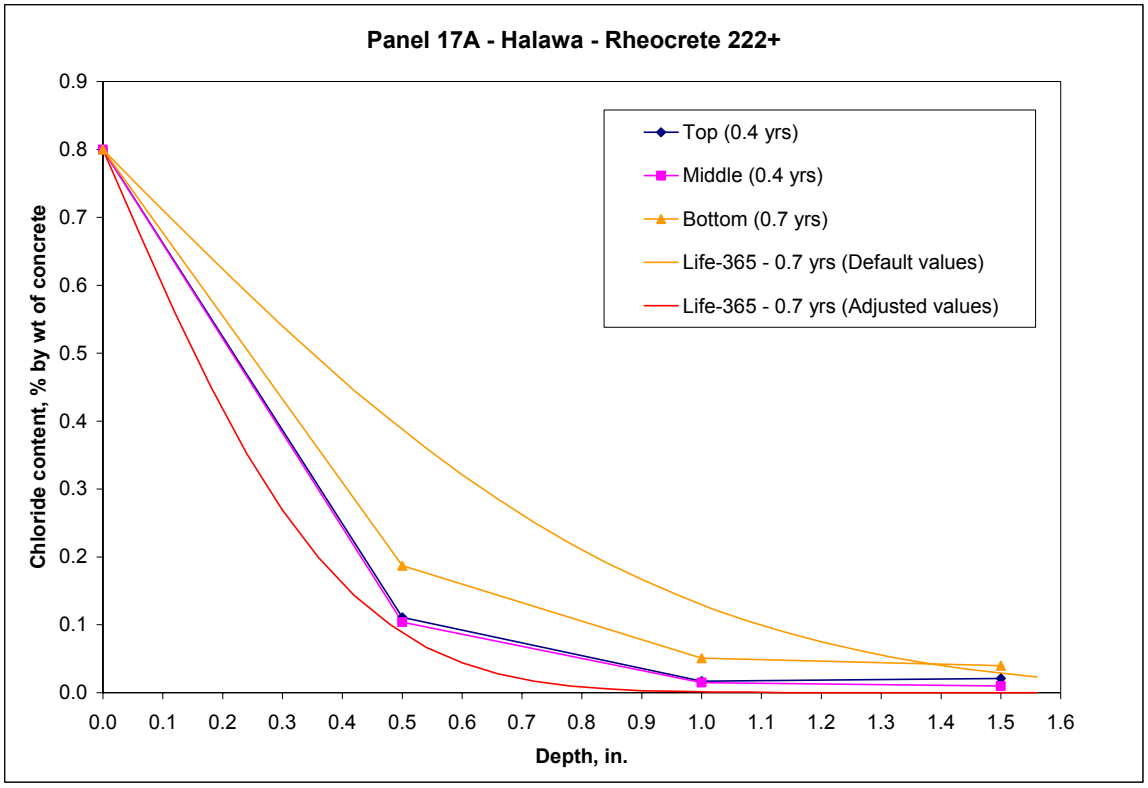

Figure 6.13. Life-365 predictions using default and adjusted values for panel 17A.

6.2.5 Fly ash mixtures

The predictions for fly ash panel 11 using both the default and adjusted variables are presented in Figure 6.13. Using the default values, Life-365 overestimated the average chloride concentration of the bottom test hole by approximately 4.2 times the measured values. By decreasing the diffusion coefficient and increasing the m variable, Life-365 improved its predictions by underestimating the average chloride concentration of the bottom hole by about 0.4 times the measured valued.

Table 6.11. Default and adjusted values for fly ash panels 11, 12, and 13.

	Default values	Adjusted values
Diffusion coefficient	6.37E-12	1.50E-12
M	0.32	0.45
Corrosion threshold	0.05	0.05

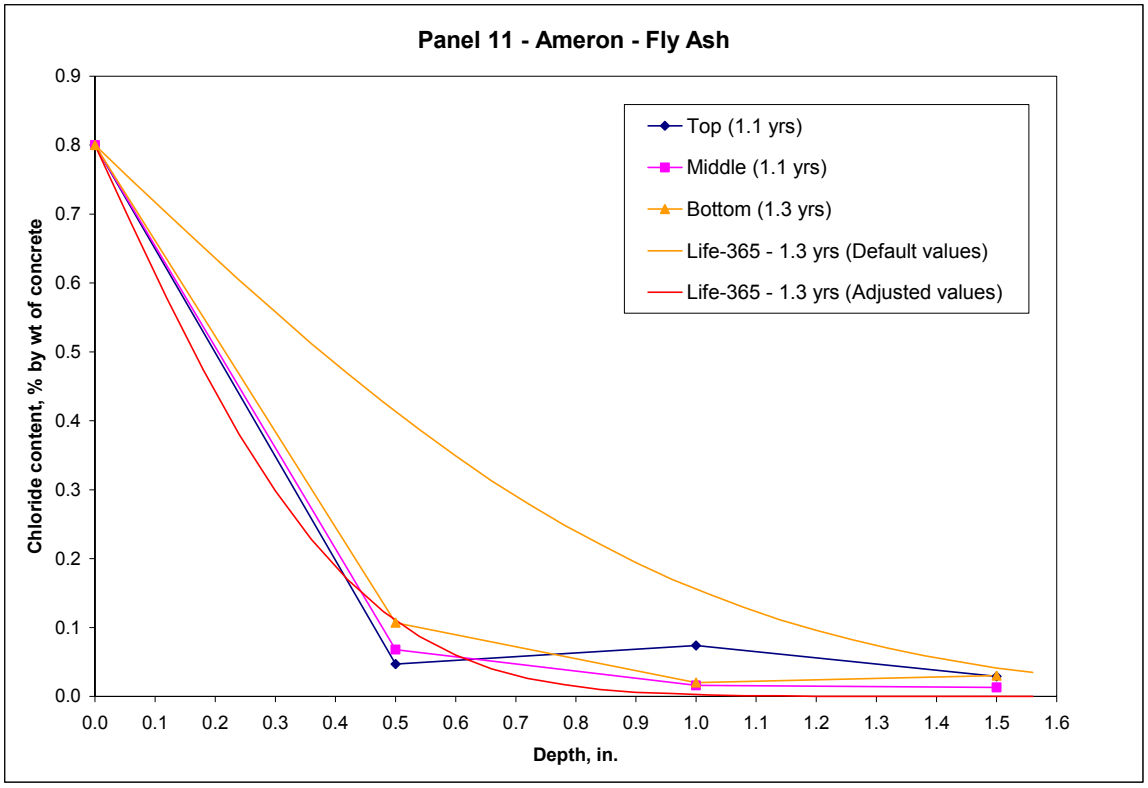

Figure 6.14. Life-365 predictions using default and adjusted values for panel 11.

Predictions calculated with the default and adjusted variables for fly ash panel 12 are shown in Figure 6.15. Life-365 overestimated the average chloride concentration of the top test hole of panel 12 by approximately 5.3 times the measured values using the default input values. Using the same adjusted diffusion coefficient and m variable as fly ash panel 11, Life-365 underestimated the average chloride concentration of the top hole by about 0.5 times the measured value.

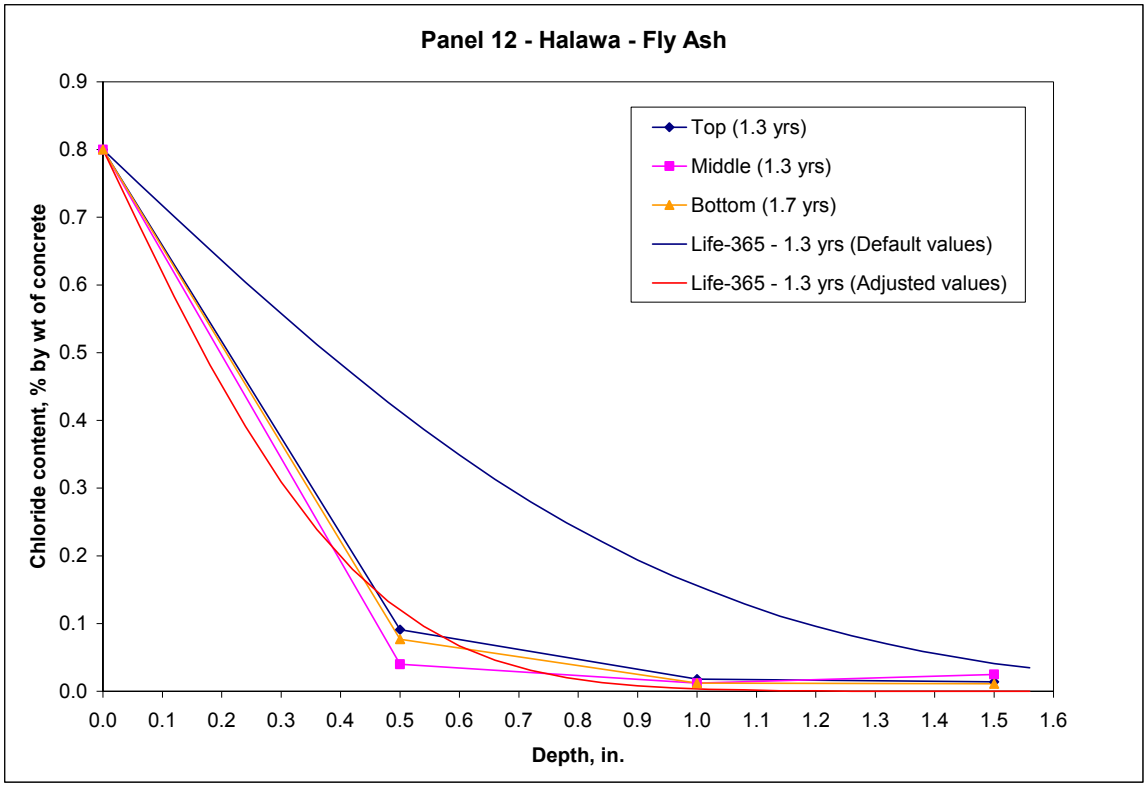

Figure 6.15. Life-365 predictions using default and adjusted values for panel 12.

Estimated chloride concentrations using both the default and adjusted variables for fly ash panel 13 are presented in Figure 6.16. Predictions using the default values overestimated the average chloride concentration of the top test hole by about 6.2 times the measured values. By using the same diffusion coefficient and m variable as fly ash panel 11, Life-365 improved its predictions by underestimating the average chloride concentration of the top hole by approximately 0.9 times the measured value.

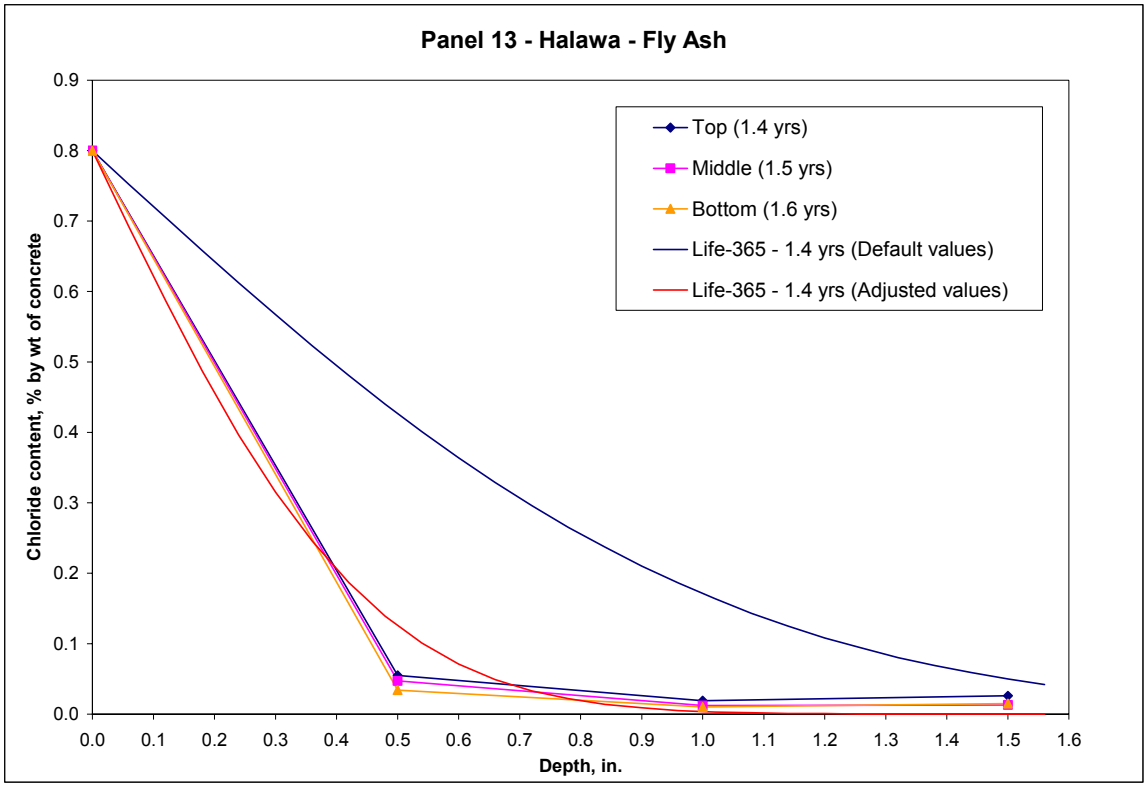

Figure 6.16. Life-365 predictions using default and adjusted values for panel 13.

6.3 Summary

This chapter presented chloride concentration predictions from Life-365 using default and adjusted variables for the diffusion coefficient and m variable. By reducing the diffusion coefficient and increasing the m variable, improved predictions were produced. Future chloride concentration measurements from these field panels will help to confirm or improve these adjusted variables. Further studies of concrete produced with local aggregates exposed to local field conditions should be conducted to improve these diffusion coefficients and m variables.

CHAPTER 7
SUMMARY AND CONCLUSIONS

7.1 Introduction

The purpose of this research was to investigate the effects of chloride concentrations in reinforced concrete exposed to marine conditions and compare them to reinforced concrete specimens exposed to simulated laboratory conditions in order to determine a correlation between field exposure time and laboratory ponding cycles. Nine corrosion-inhibiting admixtures including, DCI, Rheocrete CNI, Rheocrete 222+, FerroGard 901, Xypex Admix C-2000, latex, fly ash, silica fume, and Kryton KIM were proportioned with the concrete mixtures to examine their effects on reinforced concrete. This chapter summarizes the results from the tests performed to evaluate the properties of concrete, the comparison between the laboratory specimens and field panels, and the results from the computer program Life-365.

7.2 Summary

Each reinforced concrete panel was tested for compressive strength, elastic modulus, Poisson's ratio, air content, chloride concentration, pH, air permeability and half-cell potential. Overall, the panels proportioned with fly ash and silica fume had the highest average compressive strength. Fly ash and silica fume were expected to provide higher compressive strengths because both are known to increase density and bond strength in concrete.

DCI, Rheocrete CNI, and Kryton KIM had average compressive strengths that were slightly higher than the control mixtures. DCI and Rheocrete CNI are both non-

chloride accelerators that can produce higher strengths at early ages. Kryton KIM prolongs the hydration of the cementitous materials which can lead to higher strengths.

FerroGard 901, Xypex Admix C-2000, and latex had average compressive strengths that were similar to the control mixtures. All three were not expected to provide increased compressive strengths according to manufacturer specifications and previous research.

Rheocrete 222+ significantly reduced the compressive strength in all the mixtures. The admixture is supposed to provide only marginal effects on compressive strength, according to Nmai et al. (1992). The same mixtures of the Phase II study produced compressive strengths that were higher than the results of this phase of the study. The high air content of the mixtures in this phase of the study could account for the irregular results.

The elastic modulus for all of the panels ranged from 2154 ksi (14.9 GPa) to 4700 ksi (32.4 GPa). Measurements of air content for all the panels ranged from 1% to 11%.

Acid-soluble chloride concentration tests were performed to examine the chloride diffusion rate for each mixture by determining the amount of chlorides at various depths through the concrete cover. All of the panels had a chloride concentration at the level of the reinforcement that was below the 0.20% (by weight of cement) chloride threshold stated by the ACI Building Code (ACI Committee 318). Most of the panels followed similar trends of chloride concentration and depth. The chloride concentrations are higher near the surface of the concrete and decrease near the reinforcing steel. Also, the bottom test holes produce the highest chloride concentrations collectively at each depth, followed by the middle and top test holes.

Tests for pH in the panels at the level of the reinforcing revealed that all twenty-five reinforced concrete panels had a pH between 12 and 13. Values in this range indicated the concrete is still maintaining an alkaline environment around the steel and thus inhibiting corrosion.

The test for air permeability indicated that three panels had a "poor" quality level, ten panels had a "not very good" quality level, eleven panels had a "fair" quality level, and one panel had a "good" quality level. None of the panels produced a quality level of "excellent." The three panels that had "poor" ratings were the control and Rheocrete 222+ made using Halawa aggregates. Ten panels with the "not very good" ratings were the control, Xypex Admix C-2000, and latex panels proportioned using Ameron aggregates, DCI and FerroGard 901 panels made using Halawa aggregates, one of the Rheocrete CNI panels proportioned with Ameron aggregates, one of the Rheocrete 222+ panels made with Ameron aggregates, and one of the fly ash panels proportioned with Halawa aggregates. The eleven panels that had the "fair" ratings were the DCI, FerroGard 901, fly ash, M.B. silica fume, and Kryton KIM panels using Ameron aggregates, as well as two Rheocrete CNI panels proportioned with Ameron aggregates, one of the Rheocrete 222+ panels made with Ameron aggregates, and one of the fly ash panels proportioned with Halawa aggregates. The only panel to produce a "good" quality rating was the panel made with Grace silica fume.

The half-cell potential test determined the probability of corrosion occurring in the reinforcing steel. The panels that had a risk of corrosion that was less than 10% at all ten testing areas were panels 1, 3, 4, 10, 12, 13, 14, 15, and 18. Panels that had a 50% or unknown chance of corrosion at all ten testing locations were panels 6, 7, 11, 21, and 22.

All the other panels had varied risks of corrosion occurring at all ten testing locations. The readings for panel 20 were not reported due to errors that occurred during the field testing.

The computer program Life-365 was used to predict the chloride content of the panels used in Phase III of this study and compare them to actual measured data. There was no exposure location for Hawaii, so San Juan Puerto Rico was used because it had the most similar climate conditions. After comparing all the default predictions and the measured data, it was concluded that Life-365 was conservative in its predictions. The program overestimated the chloride concentration for the control panels by an average of 6.9 times the measured values. It overestimated the DCI panels by an average of 6.2 times the measured values. The Rheocrete CNI panels were overestimated by an average of 4.1 times the measured values. Rheocrete 222+ panels were overestimated by an average 5.1 times the measured values. The fly ash panels were overestimated by an average of 7.0 times the measured values. Finally, silica fume panels were overestimated by an average 1.9 times the measured values.

The chloride concentration predictions calculated using the computer program Life-365, were improved by adjusting the input values for the diffusion coefficient and the m variable. By decreasing the value for the diffusion coefficient and increasing the m variable, predictions for all the mixtures displayed considerable improvements. Further studies should be conducted to determine more accurate and precise values for these variables.

7.3 Conclusions

Based on the correlations of the chloride concentration test results from Phase II and III of this study, the following conclusions were made:

1. The correlation between chloride concentration at 1.0 in. (25 mm) depth in the laboratory specimens and field panels for the control, DCI, FerroGard 901 and latex-modified mixtures, was an average of 1.2 cycles per year. This rate is also equal to 10.3 months of field exposure per laboratory ponding cycle.
2. The correlation between chloride concentration at 1.0 in. (25 mm) depth in the laboratory specimens and field panels for the silica fume panels was an average of 2.4 cycles per year. The rate is also equivalent to 5.1 months of field exposure per laboratory ponding cycle.
3. Life-365 predictions using default input parameters significantly overestimated the chloride concentrations in the field panels for all mixtures except those with silica fume. Adjusted values for diffusion rate and m variable are suggested based on the field chloride measurements made in this study.

APPENDIX A
COMPRESSIVE STRENGTH FOR ALL TEST CYLINDERS

Table A.1. Compressive strength for all test cylinders.

	Compressive Strength (psi) (MPa)			
Mixtures	Specimen #1	Specimen #2	Specimen #3	Average
1	5713 (39.4)	5801 (40.0)	5837 (40.2)	5784 (39.9)
2	5218 (36.0)	5341 (36.8)	5377 (37.1)	5312 (36.6)
3	8879 (61.2)	8879 (61.2)	8773 (60.5)	8843 (61.0)
3A	8047 (55.5)	8064 (55.6)	8118 (56.0)	8077 (55.7)
4	6703 (46.2)	6845 (47.2)	6880 (47.4)	6809 (46.9)
5	7517 (51.8)	7773 (53.6)	7234 (49.9)	7508 (51.8)
5A	8047 (55.5)	8083 (55.7)	8401 (57.9)	8177 (56.4)
6	7888 (54.4)	8171 (56.3)	7871 (54.3)	7977 (55.0)
7	6739 (46.5)	6756 (46.6)	6686 (46.1)	6727 (46.4)
8	8945 (61.7)	8796 (60.6)	9651 (66.5)	9131 (63.0)
9	9321 (64.3)	9339 (64.4)	9232 (63.7)	9297 (64.1)
10	9305 (64.2)	9560 (65.9)	9366 (64.6)	9410 (64.9)
11	9834 (67.8)	9745 (67.2)	9321 (64.3)	9633 (66.4)
12	8666 (59.7)	8030 (55.4)	8313 (57.3)	8336 (57.5)
13	7641 (52.7)	8136 (56.1)	7782 (53.7)	7853 (54.1)
14	5218 (36.0)	5058 (34.9)	5324 (36.7)	5200 (35.9)
15	4280 (29.5)	4280 (29.5)	4094 (28.2)	4218 (29.1)

Table A.1. Compressive strength for all test cylinders (continued).

	Compressive Strength (psi) (MPa)			
Mixtures	Specimen #1	Specimen #2	Specimen #3	Average
16	3060 (21.1)	3201 (22.1)	3184 (22.0)	3148 (21.7)
17	1609 (11.1)	1574 (10.9)	1583 (10.9)	1576 (10.9)
17A	1910 (13.2)	2122 (14.6)	1999 (13.8)	2010 (13.9)
18	5624 (38.8)	5819 (40.1)	5925 (40.9)	5789 (39.9)
19	6562 (45.2)	6120 (42.2)	6120 (42.2)	6267 (43.2)
20	7544 (52.0)	7746 (53.4)	7351 (50.7)	7547 (52.0)
21	5483 (37.8)	5660 (39.0)	5784 (39.9)	5642 (38.9)
22	8047 (55.5)	7959 (54.9)	8100 (55.8)	8036 (55.4)

APPENDIX B
CHLORIDE CONCENTRATION DATA

Table B.1. Chloride concentration for top holes (% by weight of cement).

Mix	T - 0.5	T - 1.0	T - 1.5
1	0.370	0.058	0.039
2	0.158	0.019	0.024
3	0.270	0.053	0.017
3A	0.047	0.007	0.008
4	0.760	0.230	0.030
5	0.220	0.048	0.013
5A	0.043	0.034	0.009
6	0.117	0.025	0.011
7	0.075	0.013	0.011
8	0.200	0.028	0.014
9	0.026	0.016	0.015
10	0.040	0.019	0.025
11	0.047	0.074	0.029
12	0.091	0.018	0.014
13	0.055	0.019	0.026
14	0.144	0.015	0.015
15	0.025	0.009	0.009
16	0.151	0.047	0.025
17	0.064	0.021	0.020
17A	0.111	0.017	0.021
18	0.250	0.041	0.012
19	0.080	0.015	0.012
20	0.109	0.047	0.011
21	0.098	0.047	0.014
22	0.070	0.010	0.007

Table B.2. Chloride concentration for middle holes (% by weight of cement).

Mix	M - 0.5	M - 1.0	M - 1.5
1	0.148	0.024	0.010
2	0.108	0.017	0.014
3	0.154	0.029	0.017
3A	0.067	0.013	0.010
4	0.138	0.018	0.010
5	0.210	0.075	0.017
5A	0.054	0.034	0.011
6	0.111	0.026	0.042
7	0.147	0.025	0.009
8	0.035	0.043	0.081
9	0.045	0.013	0.039
10	0.032	0.022	0.021
11	0.068	0.016	0.013
12	0.040	0.012	0.025
13	0.047	0.012	0.013
14	0.047	0.015	0.013
15	0.141	0.014	0.033
16	0.200	0.058	0.038
17	0.152	0.028	0.032
17A	0.104	0.015	0.010
18	0.310	0.490	0.024
19	0.124	0.016	0.010
20	0.161	0.019	0.011
21	0.179	0.042	0.012
22	0.166	0.022	0.019

Table B.3. Chloride concentration for bottom holes (% by weight of cement).

Mix	B - 0.5	B - 1.0	B - 1.5
1	0.240	0.042	0.044
2	0.054	0.016	0.020
3	0.260	0.087	0.024
3A	0.164	0.028	0.010
4	0.167	0.017	0.010
5	0.550	0.260	0.089
5A	0.200	0.029	0.009
6	0.150	0.024	0.011
7	0.149	0.076	0.021
8	0.106	0.016	0.015
9	0.038	0.014	0.015
10	0.230	0.024	0.011
11	0.107	0.020	0.030
12	0.077	0.012	0.011
13	0.034	0.010	0.015
14	0.230	0.034	0.010
15	0.124	0.033	0.017
16	0.480	0.168	0.031
17	0.064	0.020	0.019
17A	0.187	0.051	0.040
18	0.163	0.030	0.014
19	0.122	0.027	0.026
20	0.090	0.018	0.014
21	0.168	0.028	0.013
22	0.082	0.057	0.045

APPENDIX C
SAMPLE SIZE FOR PH TESTS

Table C.1. Sample size and pH for each mixture.

Mix	Sample Size	T - 1.5	Sample Size	M - 1.5	Sample Size	B - 1.5
1	1.22	12.55	0.49	12.05	3.00	12.55
2	1.66	12.50	0.40	12.52	3.00	12.60
3	1.52	12.53	3.00	12.54	3.00	12.64
3A	N/A	N/A	3.00	12.51	1.72	12.64
4	2.51	12.52	3.00	12.52	3.00	12.50
5	2.57	12.53	3.00	12.50	0.57	12.51
5A	3.00	12.52	3.00	12.36	2.52	12.46
6	2.42	12.42	2.29	12.43	2.27	12.42
7	1.67	12.47	1.78	12.43	2.75	12.43
8	3.00	12.61	3.00	12.50	3.00	12.56
9	1.65	12.42	0.73	12.27	2.44	12.27
10	2.21	12.33	1.12	12.23	3.00	12.52
11	0.96	12.22	0.78	12.20	1.61	12.22
12	0.49	12.02	0.84	12.03	3.00	12.18
13	1.09	12.12	1.29	12.18	3.00	12.21
14	3.00	12.16	3.00	12.40	2.39	12.42
15	3.00	12.34	2.27	12.26	3.00	12.26
16	1.64	12.21	1.34	12.23	2.24	12.24
17	3.00	12.57	3.00	12.40	2.69	12.37
17A	0.72	12.30	1.09	12.29	1.74	12.28
18	1.60	12.30	1.09	12.29	1.74	12.28
19	N/A	N/A	0.78	12.14	3.00	12.51
20	3.00	12.40	3.00	12.39	3.00	12.40
21	2.87	12.39	2.11	12.39	2.91	12.35
22	2.35	12.40	1.55	12.32	3.00	12.30

APPENDIX D
INPUT VALUES FOR LIFE-365

Table D.1. Month of first exposure for field panels.

Field panel	Month of first exposure (for temp)
8,10,20	1
2,3A,4,5A,9,14,17A,18,22	7
1,3,7,12,13,19	8
5,15,16,17	9
6,11,21	11

Table D.2. Detailed temperatures for Honolulu Harbor.

Month #	Temperature (degrees)
0.5	73.3
1.5	74.3
2.5	74.7
3.5	76.7
4.5	78.0
5.5	80.3
6.5	81.7
7.5	82.7
8.5	81.5
9.5	80.5
10.5	78.0
11.5	75.5

APPENDIX E
OUTPUT VALUES FROM LIFE-365

Table E.1. Life-365 predictions for control panels (% by wt of concrete).

	Panel 1		Panel 2		Panel 7	
Depth	1.5 yrs	1.6yrs	1.4 yrs	1.7 yrs	1.5 yrs	1.7 yrs
0	0.8	0.8	0.8	0.8	0.8	0.8
0.06	0.763	0.764	0.762	0.765	0.757	0.759
0.12	0.725	0.728	0.724	0.73	0.714	0.719
0.18	0.688	0.692	0.686	0.695	0.672	0.678
0.24	0.652	0.656	0.649	0.66	0.63	0.639
0.3	0.616	0.621	0.612	0.626	0.589	0.599
0.36	0.58	0.587	0.576	0.592	0.549	0.561
0.42	0.545	0.553	0.541	0.559	0.51	0.524
0.48	0.511	0.52	0.506	0.527	0.472	0.487
0.54	0.478	0.487	0.473	0.495	0.436	0.452
0.6	0.446	0.456	0.44	0.464	0.401	0.418
0.66	0.415	0.426	0.409	0.434	0.367	0.386
0.72	0.386	0.396	0.379	0.405	0.336	0.355
0.78	0.357	0.368	0.35	0.378	0.305	0.325
0.84	0.33	0.341	0.323	0.351	0.277	0.297
0.9	0.304	0.315	0.296	0.325	0.25	0.27
0.96	0.279	0.291	0.272	0.301	0.225	0.245
1.02	0.255	0.267	0.248	0.278	0.202	0.222
1.08	0.233	0.245	0.226	0.256	0.181	0.2
1.14	0.213	0.224	0.205	0.235	0.161	0.18
1.2	0.193	0.205	0.186	0.215	0.143	0.161
1.26	0.175	0.186	0.168	0.196	0.126	0.144
1.32	0.158	0.169	0.151	0.179	0.111	0.128
1.38	0.142	0.153	0.136	0.163	0.098	0.113
1.44	0.128	0.138	0.122	0.148	0.085	0.1
1.5	0.114	0.125	0.109	0.133	0.074	0.088
1.56	0.102	0.112	0.097	0.12	0.064	0.077

Table E.2. Life-365 predictions for DCI panels (% by wt of concrete).

	Panel 3	Panel 3A			Panel 4
Depth	1.7 yrs	0.7 yrs	0.2 yrs	0.6 yrs	1.8 yrs
0	0.8	0.8	0.8	0.8	0.8
0.06	0.764	0.749	0.718	0.746	0.765
0.12	0.729	0.699	0.637	0.692	0.731
0.18	0.694	0.649	0.559	0.64	0.697
0.24	0.659	0.6	0.484	0.588	0.663
0.3	0.625	0.552	0.415	0.538	0.629
0.36	0.591	0.506	0.351	0.489	0.596
0.42	0.558	0.462	0.293	0.443	0.563
0.48	0.525	0.419	0.241	0.398	0.531
0.54	0.493	0.379	0.196	0.357	0.5
0.6	0.462	0.341	0.157	0.318	0.47
0.66	0.432	0.305	0.125	0.281	0.441
0.72	0.403	0.272	0.097	0.248	0.412
0.78	0.376	0.241	0.075	0.217	0.385
0.84	0.349	0.212	0.057	0.189	0.358
0.9	0.323	0.186	0.043	0.163	0.333
0.96	0.299	0.162	0.031	0.14	0.308
1.02	0.275	0.141	0.023	0.12	0.285
1.08	0.253	0.122	0.016	0.102	0.263
1.14	0.232	0.104	0.012	0.086	0.242
1.2	0.213	0.089	0.008	0.072	0.222
1.26	0.194	0.076	0.006	0.06	0.204
1.32	0.177	0.064	0.004	0.05	0.186
1.38	0.161	0.054	0.003	0.041	0.17
1.44	0.145	0.045	0.002	0.034	0.154
1.5	0.131	0.037	0.001	0.028	0.14
1.56	0.118	0.031	0.001	0.022	0.127

Table E.3. Life-365 predictions for Rheocrete CNI panels (% by wt of concrete).

	Panel 5		Panel 5A		Panel 6	
Depth	1.6 yrs	1.7 yrs	0.2 yrs	0.6 yrs	1.1 yrs	1.3 yrs
0	0.8	0.8	0.8	0.8	0.8	0.8
0.06	0.763	0.764	0.718	0.746	0.757	0.76
0.12	0.727	0.729	0.637	0.692	0.714	0.72
0.18	0.69	0.694	0.559	0.64	0.672	0.68
0.24	0.654	0.659	0.484	0.588	0.63	0.641
0.3	0.619	0.624	0.415	0.538	0.589	0.603
0.36	0.584	0.59	0.351	0.489	0.549	0.565
0.42	0.549	0.557	0.293	0.443	0.51	0.528
0.48	0.516	0.524	0.241	0.398	0.473	0.492
0.54	0.483	0.492	0.196	0.357	0.436	0.458
0.6	0.452	0.461	0.157	0.318	0.401	0.424
0.66	0.421	0.432	0.125	0.281	0.368	0.392
0.72	0.391	0.403	0.097	0.248	0.336	0.361
0.78	0.363	0.375	0.075	0.217	0.306	0.331
0.84	0.336	0.348	0.057	0.189	0.277	0.303
0.9	0.31	0.322	0.043	0.163	0.251	0.277
0.96	0.285	0.298	0.031	0.14	0.226	0.252
1.02	0.262	0.274	0.023	0.12	0.203	0.229
1.08	0.24	0.252	0.016	0.102	0.181	0.207
1.14	0.219	0.231	0.012	0.086	0.161	0.186
1.2	0.199	0.212	0.008	0.072	0.143	0.167
1.26	0.181	0.193	0.006	0.06	0.127	0.15
1.32	0.164	0.176	0.004	0.05	0.112	0.134
1.38	0.148	0.16	0.003	0.041	0.098	0.119
1.44	0.133	0.144	0.002	0.034	0.086	0.106
1.5	0.12	0.131	0.001	0.028	0.074	0.093
1.56	0.107	0.118	0.001	0.022	0.065	0.082

Table E.4. Life-365 predictions for Rheocrete 222+ panels (% by wt of concrete).

	Panel 15		Panel 16		Panel 17		Panel 17A	
Depth	1.1 yrs	1.4 yrs	1.4 yrs	1.7 yrs	1.1 yrs	1.5 yrs	0.4 yrs	0.7 yrs
0	0.8	0.8	0.8	0.8	0.8	0.8	0.8	0.8
0.06	0.755	0.759	0.759	0.762	0.755	0.76	0.734	0.746
0.12	0.711	0.719	0.719	0.725	0.711	0.721	0.669	0.693
0.18	0.667	0.678	0.678	0.688	0.667	0.682	0.606	0.641
0.24	0.623	0.639	0.639	0.651	0.623	0.643	0.544	0.59
0.3	0.58	0.6	0.6	0.615	0.58	0.605	0.485	0.54
0.36	0.539	0.561	0.561	0.579	0.539	0.568	0.429	0.492
0.42	0.498	0.524	0.524	0.544	0.498	0.531	0.377	0.445
0.48	0.459	0.488	0.488	0.51	0.459	0.496	0.328	0.402
0.54	0.422	0.452	0.452	0.477	0.422	0.461	0.283	0.36
0.6	0.386	0.419	0.419	0.445	0.386	0.428	0.242	0.321
0.66	0.352	0.386	0.386	0.414	0.352	0.396	0.206	0.285
0.72	0.32	0.355	0.355	0.384	0.32	0.365	0.173	0.251
0.78	0.289	0.325	0.325	0.356	0.289	0.336	0.145	0.22
0.84	0.26	0.297	0.297	0.328	0.26	0.308	0.12	0.192
0.9	0.234	0.271	0.271	0.302	0.234	0.281	0.098	0.167
0.96	0.209	0.246	0.246	0.277	0.209	0.256	0.08	0.144
1.02	0.186	0.222	0.222	0.254	0.186	0.233	0.064	0.123
1.08	0.165	0.2	0.2	0.232	0.165	0.211	0.051	0.105
1.14	0.146	0.18	0.18	0.211	0.146	0.191	0.041	0.089
1.2	0.128	0.161	0.161	0.192	0.128	0.172	0.032	0.075
1.26	0.112	0.144	0.144	0.173	0.112	0.154	0.025	0.063
1.32	0.098	0.128	0.128	0.157	0.098	0.138	0.019	0.052
1.38	0.085	0.114	0.114	0.141	0.085	0.123	0.014	0.043
1.44	0.074	0.1	0.1	0.127	0.074	0.109	0.011	0.035
1.5	0.063	0.088	0.088	0.113	0.063	0.097	0.008	0.029
1.56	0.054	0.078	0.078	0.101	0.054	0.085	0.006	0.023

Table E.5. Life-365 predictions for fly ash panels (% by wt of concrete).

	Panel 11		Panel 12		Panel 13		
Depth	1.1 yrs	1.3 yrs	1.3 yrs	1.7 yrs	1.4 yrs	1.5 yrs	1.6 yrs
0	0.8	0.8	0.8	0.8	0.8	0.8	0.8
0.06	0.747	0.75	0.751	0.756	0.752	0.753	0.755
0.12	0.695	0.701	0.703	0.711	0.705	0.707	0.71
0.18	0.643	0.652	0.655	0.667	0.658	0.661	0.665
0.24	0.593	0.604	0.608	0.624	0.612	0.616	0.621
0.3	0.544	0.558	0.562	0.582	0.567	0.572	0.578
0.36	0.496	0.512	0.518	0.54	0.523	0.529	0.536
0.42	0.45	0.469	0.475	0.5	0.481	0.488	0.495
0.48	0.407	0.427	0.434	0.461	0.44	0.448	0.456
0.54	0.366	0.387	0.394	0.424	0.401	0.409	0.418
0.6	0.327	0.349	0.357	0.388	0.364	0.373	0.382
0.66	0.291	0.313	0.321	0.354	0.329	0.338	0.348
0.72	0.257	0.28	0.288	0.322	0.296	0.305	0.315
0.78	0.226	0.249	0.257	0.292	0.265	0.274	0.285
0.84	0.198	0.221	0.229	0.263	0.237	0.246	0.256
0.9	0.172	0.194	0.202	0.236	0.21	0.219	0.23
0.96	0.149	0.17	0.178	0.212	0.186	0.195	0.205
1.02	0.128	0.149	0.156	0.189	0.164	0.172	0.182
1.08	0.11	0.129	0.136	0.168	0.143	0.151	0.161
1.14	0.093	0.111	0.118	0.148	0.125	0.133	0.142
1.2	0.079	0.096	0.102	0.131	0.108	0.116	0.125
1.26	0.066	0.082	0.088	0.114	0.094	0.101	0.109
1.32	0.055	0.07	0.075	0.1	0.08	0.087	0.095
1.38	0.046	0.059	0.064	0.087	0.069	0.075	0.082
1.44	0.038	0.05	0.054	0.075	0.059	0.064	0.071
1.5	0.031	0.041	0.045	0.065	0.05	0.055	0.061
1.56	0.026	0.035	0.038	0.056	0.042	0.046	0.052

Table E.6. Life-365 predictions for silica fume panels (% by wt of concrete).

	Panle 8		Panel 9		Panel 10	
Depth	0.7 yrs	1.3 yrs	0.4 yrs	0.7 yrs	0.9 yrs	0.7 yrs
0	0.8	0.8	0.8	0.8	0.8	0.8
0.06	0.714	0.732	0.695	0.715	0.722	0.714
0.12	0.63	0.665	0.593	0.631	0.646	0.63
0.18	0.548	0.6	0.497	0.55	0.572	0.548
0.24	0.471	0.537	0.408	0.473	0.501	0.471
0.3	0.4	0.476	0.328	0.402	0.434	0.4
0.36	0.334	0.419	0.258	0.337	0.372	0.334
0.42	0.276	0.365	0.199	0.278	0.315	0.276
0.48	0.224	0.316	0.15	0.227	0.264	0.224
0.54	0.18	0.271	0.111	0.182	0.218	0.18
0.6	0.142	0.23	0.08	0.144	0.179	0.142
0.66	0.11	0.194	0.057	0.112	0.144	0.11
0.72	0.085	0.162	0.039	0.086	0.115	0.085
0.78	0.064	0.134	0.026	0.065	0.091	0.064
0.84	0.047	0.11	0.017	0.049	0.071	0.047
0.9	0.035	0.089	0.011	0.036	0.054	0.035
0.96	0.025	0.071	0.007	0.026	0.041	0.025
1.02	0.018	0.057	0.004	0.018	0.031	0.018
1.08	0.012	0.045	0.003	0.013	0.023	0.012
1.14	0.009	0.035	0.002	0.009	0.017	0.009
1.2	0.006	0.027	0.001	0.006	0.012	0.006
1.26	0.004	0.021	0.001	0.004	0.009	0.004
1.32	0.003	0.016	0	0.003	0.006	0.003
1.38	0.002	0.012	0	0.002	0.004	0.002
1.44	0.001	0.009	0	0.001	0.003	0.001
1.5	0.001	0.006	0	0.001	0.002	0.001
1.56	0	0.005	0	0	0.001	0

APPENDIX F
CHLORIDE CONCENTRATION DATA FROM PHASE II

Table F.1. Chloride concentration for mixtures C1 and C2 (% by wt of cement).

Cycles	C1	C2
0	0.021	0.032
3	0.426	0.028
5	0.228	0.075
7	0.991	1.053
16	1.487	3.476
16	1.045817	2.215
25	2.838645	
32		3.217
32		3.692
32		3.376
32		2.690
32		3.903

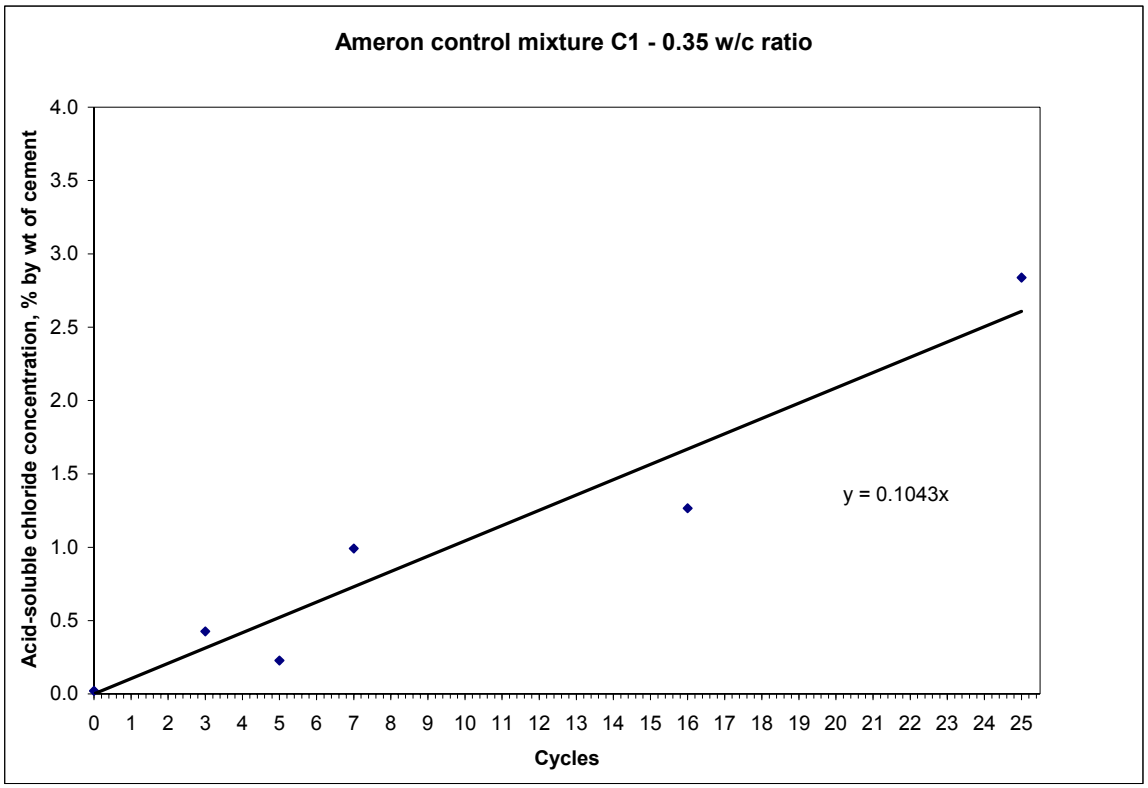

Figure F.1. Chloride concentration vs. cycle length for mixture C1.

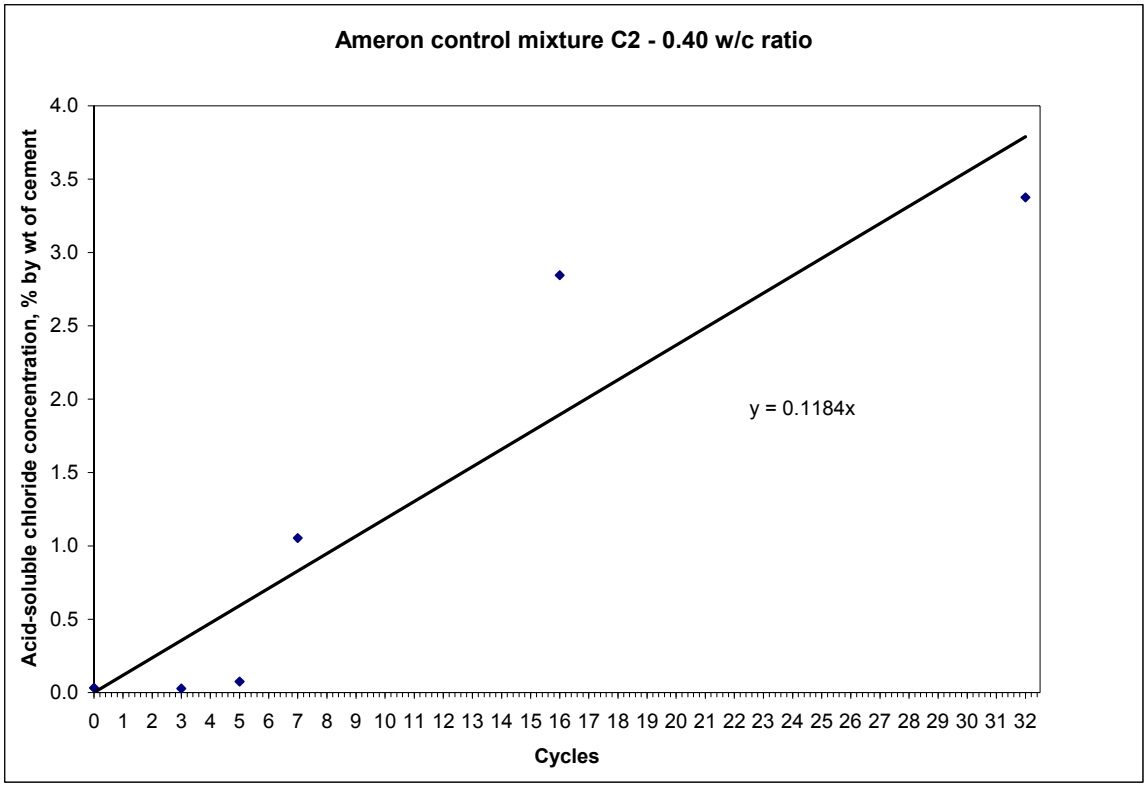

Figure F.2. Chloride concentration vs. cycle length for mixture C2

Table F.2. Chloride concentration for D4 and D5 (% by wt of cement).

Cycles	D4	D5
0	0.050	0.045
3	0.284	0.648
4	0.695	0.432
6	1.053	1.106

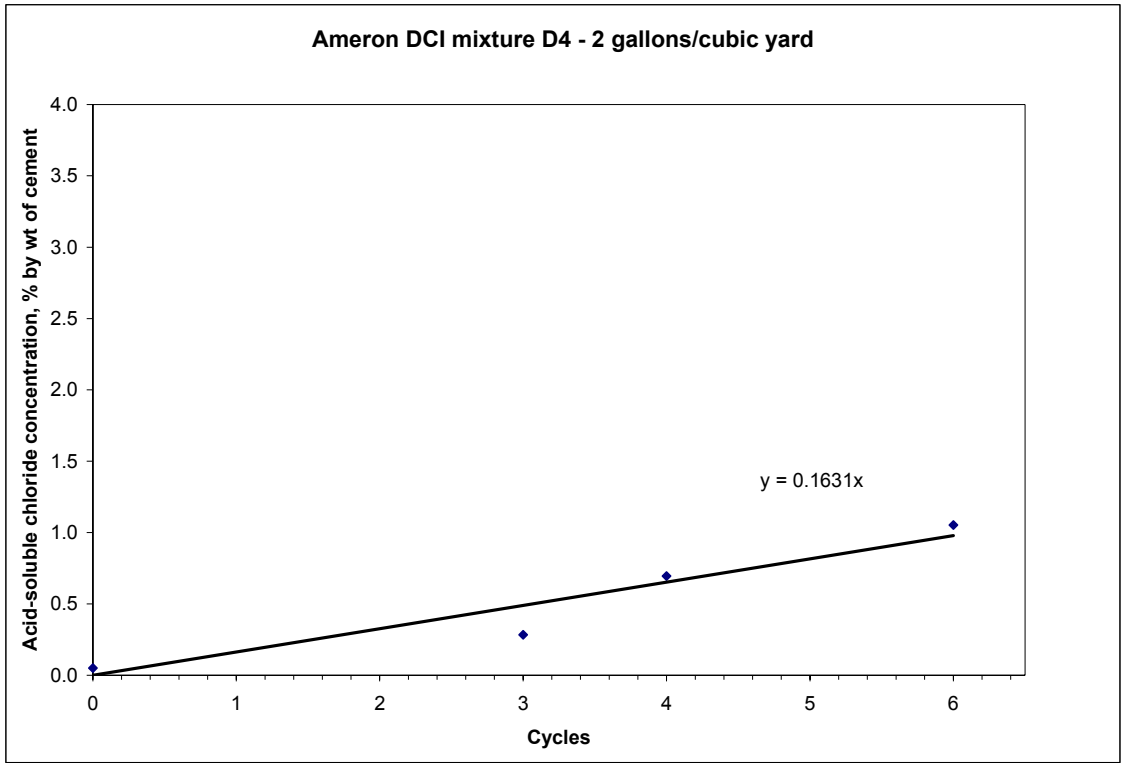

Figure F3. Chloride concentration vs. cycle length for mixture D4.

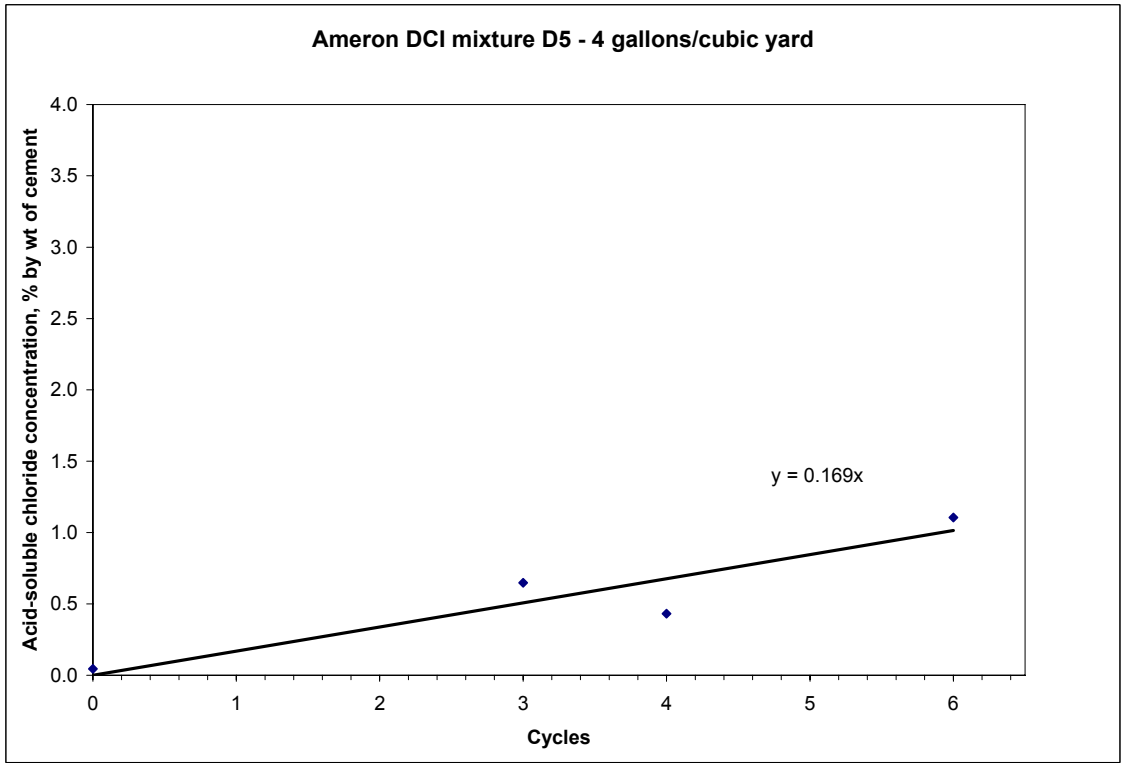

Figure F4. Chloride concentration vs. cycle length for mixture D5.

Table F.3. Chloride concentration for mixture RHE2 (% by wt of cement).

Cycles	%
0	0.041
2	0.259
4	0.660
6	0.808

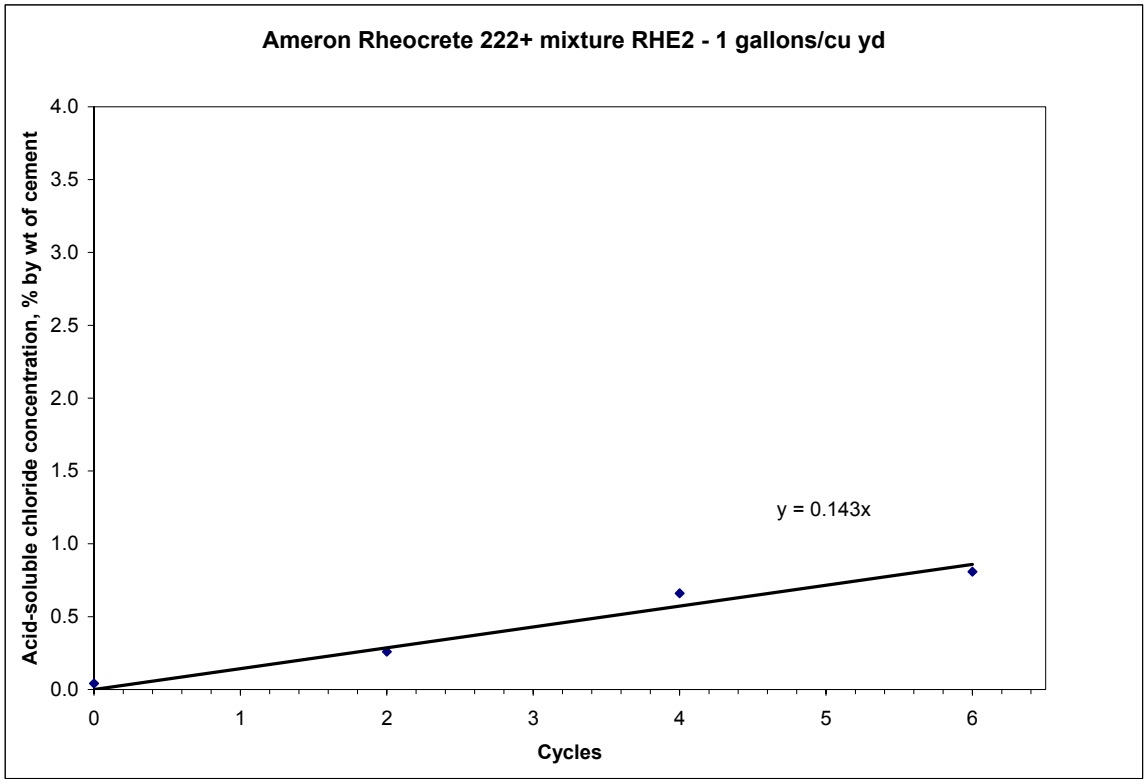

Figure F5. Chloride concentration vs. cycle length for mixture RHE2.

Table F.4. Chloride concentration for mixture FER2 (% by wt of cement).

Cycles	%
0	0.034
3	0.169
4	0.728
6	0.908
18	2.058

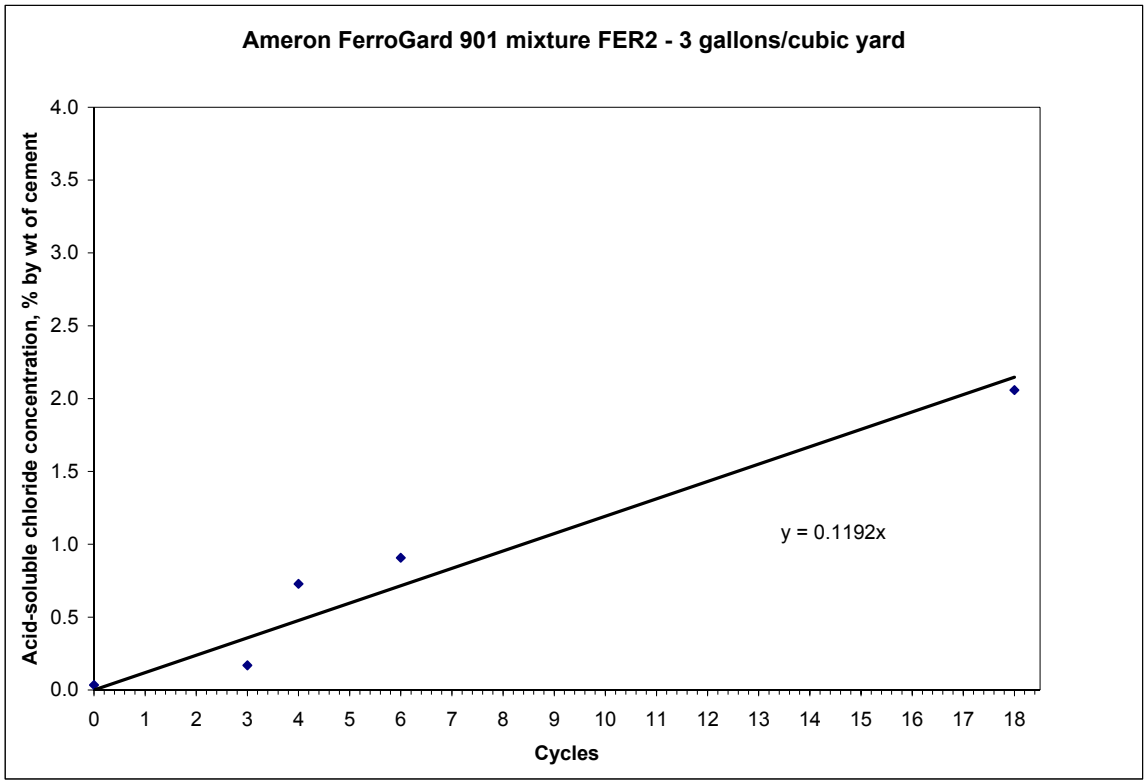

Figure F6. Chloride concentration vs. cycle length for mixture FER2.

Table F.5. Chloride concentration for mixture L5 (% by wt of cement).

Cycles	%
0	0.028
2	0.311
4	0.8741
6	0.944

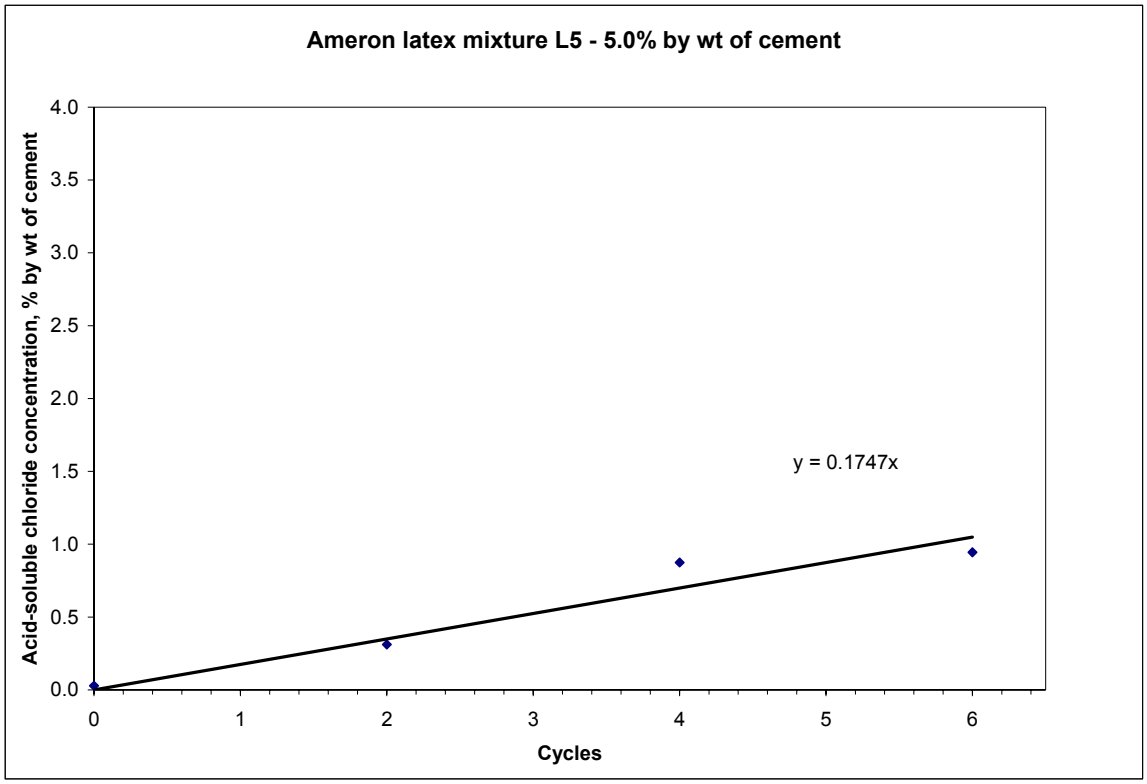

Figure F7. Chloride concentration vs. cycle length for mixture L5.

Table F.6. Chloride concentration for mixture SF2 (% by wt of cement).

Cycles	%
0	0.057
3	0.278
4	0.345
6	0.360

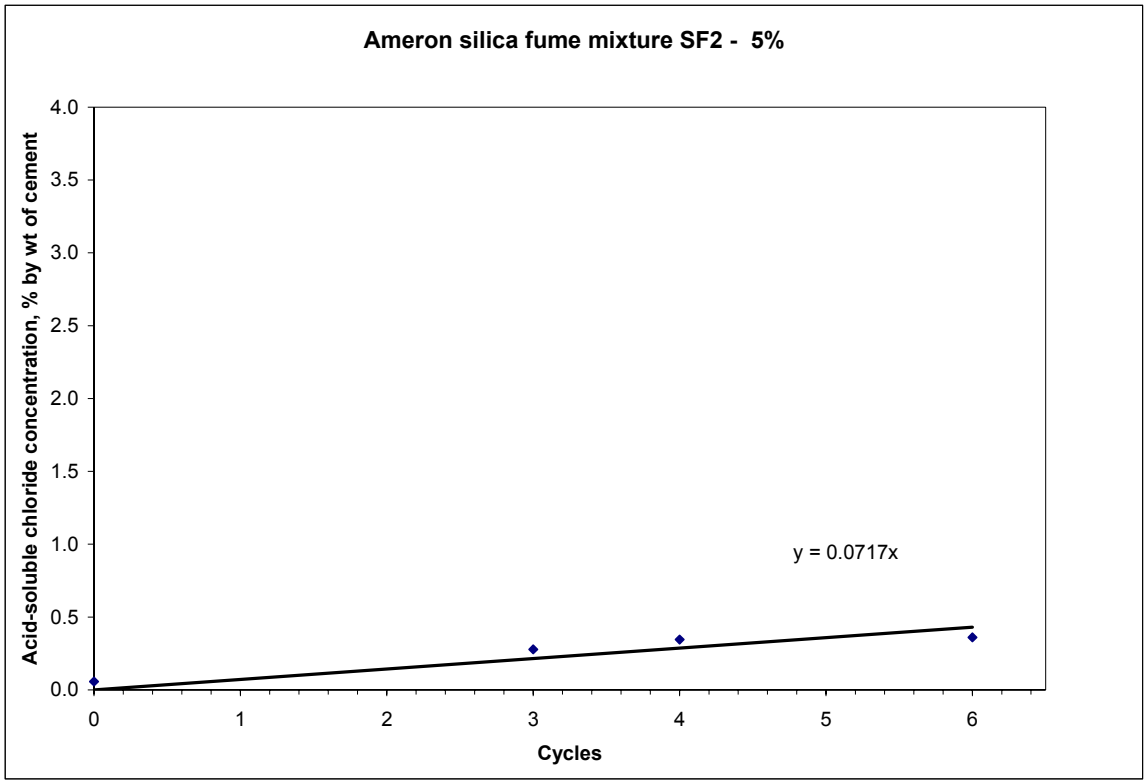

Figure F8. Chloride concentration vs. cycle length for mixture SF2.

ASTM STANDARDS

ASTM C 39 *Standard Test Method for Compressive Strength of Cylindrical Concrete Specimens*

ASTM C 127 *Standard Test Method for Density, Relative Density (Specific Gravity), and Absorption of Coarse Aggregate*

ASTM C 128 *Standard Test Method for Density, Relative Density (Specific Gravity), and Absorption of Fine Aggregate*

ASTM C 143 *Standard Test Method for Slump of Hydraulic Cement Concrete*

ASTM C 150 *Standard Specification for Portland Cement*

ASTM C 192 *Standard Practice for Making and Curing Concrete Test Specimens in the Laboratory*

ASTM C 231 *Standard Test Method for Air Content of Freshly Mixed Concrete by the Pressure Method*

ASTM C 469 *Standard Test Method for Static Modulus of Elasticity and Poisson's Ratio of Concrete in Compression*

ASTM C 470 *Standard Specification for Molds for Forming Concrete Test Cylinders Vertically*

ASTM C 494 *Standard Specification for Chemical Admixtures for Concrete Type C - Accelerating Admixture*

ASTM C 617 *Standard Practice for Capping Cylindrical Concrete Specimens*

ASTM C 618 *Standard Specification for Coal Fly Ash and Raw or Calcined Natural Pozzolan for Use as a Mineral Admixture in Concrete*

ASTM C 876 *Standard Test Method for Half-Cell Potentials of Uncoated Reinforcing Steel in Concrete*

ASTM C 1152 *Standard Test Method for Acid-Soluble Chloride in Mortar and Concrete*

ASTM G 59 *Standard Test Method for Conducting Potentiodynamic Polarization Resistance Measurements*

ASTM G 109 *Standard Test Method for Determining the Effects of Chemical Admixtures on the Corrosion of Embedded Steel Reinforcement in Concrete Exposed to Chloride Environments*

REFERENCES

ACI Committee 201, (1991). "Guide to Durable Concrete, " *Durable Concrete – Designing, Specifying, and Constructing for Durable Concrete*, ACI 201.2R-92, SBM-4 (94), American Concrete Institute, pp. 3-41.

ACI Committee 222, (1989). "Corrosion of Metals in Concrete," *Durable Concrete – Designing, Specifying, and Constructing for Durable Concrete*, ACI 222R-89, SBM-4 (94), American Concrete Institute, pp. 70-99.

ACI Committee 222, (2003). *Design and Construction Practices to Mitigate Corrosion of Reinforcement in Concrete Structures*, ACI 222.3R-03, American Concrete Institute.

ACI Committee 318, (1999). *Building Code Requirements for Reinforced Concrete*.

Al-Tayyib, A.J., and Khan, M.S., (1988). "Corrosion Rate Measurements of Reinforcing Steel in Concrete by Electrochemical Techniques," *ACI Materials Journal*, Vol. 85. No. 3, pp. 172-177.

ASTM, (2000). *Annual Book of ASTM Standards*.

Bola, M., and Newtson, C.M., (2000). *Field Evaluation of Corrosion in Reinforced Concrete Structures in Marine Environment*, Research Report UHM/CE/00-01, Department of Civil and Environmental Engineering, University of Hawaii at Manoa.

Bungey, J.H., and Millard, S.G., (1996). *Testing of Concrete in Structures 3rd Edition*.

Cather, R., Figg, J.W., Marsden, A.F., and O'Brien, T.P., (1984). "Improvements to the Figg method for determining the air permeability of concrete," *Magazine of Concrete Research*, Vol. 36, No. 129, pp. 241-245.

Corrosion Doctors, (2004). http://www.corrosion-doctors.org/References/Potential.htm.

Dhir, R.K., Hewlett, P.C., Byars, E.A., and Shaaban, I.G., (1995). "A new technique for measuring the air permeability of near-surface concrete," *Magazine of Concrete Research*, Vol. 47, No. 171, pp. 167-171.

Dhir, R.K., Jones, M.R., and McCarthy, M.J., (1991). "Measurement of reinforcement corrosion in concrete structures," *Concrete – Journal of the Concrete Society*, Vol. 25, No. 1, pp. 15-19.

EPA, (2002). *Test Methods for Evaluating Solid Wastes, Physical/Chemical Methods*, SW-846, Environmental Protection Agency, August 2002.

Figg, J.W., (1973). "Methods of measuring the air and water permeability of concrete," *Magazine of Concrete Research*, Vol. 25, No. 85, pp. 213-219.

FHWA, (2001). *Corrosion Costs and Preventative Strategies in the United States*, Publication No. FHWA-RD-01-156, Federal Highway Administration.

Fraczek, J., (1987). "A Review of Electrochemical Principles as Applied to Corrosion of Steel in a Concrete or Grout Environment," *Corrosion, Concrete, and Chlorides Steel Corrosion in Concrete: Causes and Restraints*, SP-102, American Concrete Institute, Detroit, pp. 13-24.

Gaynor, R., (1987). "Understanding Chloride Percentages," *Corrosion, Concrete, and Chlorides Steel Corrosion in Concrete: Causes and Restraints*, SP-102, American Concrete Institute, Detroit, pp. 161-174.

Grace Construction Products, (2002). "Daracem 19," Technical Data Sheet.

Grace Construction Products, (2003). "Darex II AEA," Technical Data Sheet.

Grace Construction Products, (2003). "DCI," Technical Data Sheet.

Hime, W., Erlin, B., (1987). "Some Chemical and Physical Aspects of Phenomena Associated with Chloride-Induced Corrosion," *Corrosion, Concrete, and Chlorides Steel Corrosion in Concrete: Causes and Restraints*, SP-102, American Concrete Institute, Detroit, pp. 1-12.

Hope, B.B., and Ip, A.K.C., (1987). "Chloride Corrosion Threshold in Concrete," *ACI Materials Journal*, Vol. 84, No. 4, pp.306-314.

James Instruments, Inc., (1998). *Poroscope Plus*, Technical Data Sheet.

Keck, R. H., (2001). "Improving Concrete Durability with Cementitious Materials," *Concrete International*, Vol. 23, No. 9, pp.47-51.

Kosmatka, S.H., and Panarese, W.C., (1994). *Design and Control of Concrete Mixtures*, Portland Cement Association (PCA), pp. 84-90.

Kryton, (2003). "KIM – Krystol Internal Membrane Waterproofing Admixture for Concrete," Technical Data Sheet.

Manning, D.G., (1992). "Reflections on Steel Corrosion in Concrete," *Durability of Concrete G.M. Idorn International Symposium*, SP-131, American Concrete Institute, pp. 321-338.

Master Builders, Inc., (2002). "Rheocrete 222+ Organic corrosion inhibitor," Technical Data Sheet.

Master Builders, Inc., (2002). "Rheocrete CNI calcium nitrite-based corrosion inhibitor," Technical Data Sheet.

Mehta, P.K., (1991). "Durability of Concrete – Fifty Years of Progress?," *Durability of Concrete Second International Conference*, SP-126, American Concrete Institute, pp. 1-31.

Nmai, C.K., Farrington, S.A., and Bobrowski, G.S., (1992). "Organic-Based Corrosion-Inhibiting Admixtures for Reinforced Concrete," *Concrete International: Design and Construction*, Vol. 14, No. 4, pp. 45-51.

NOAA, (2004). *Tides Online*, National Oceanic and Atmospheric Administration, http://tidesonline.nos.noaa.gov/.

Ohama, Y., (1987). "Principle of Latex Modification and Some Typical Properties of Latex-Modified Mortars and Concretes," *ACI Materials Journal*, Vol. 84, No. 6, pp. 511-518.

Okunaga, G. J., Robertson, I. N., and Newtson, C., (2004). *Laboratory Study of Concrete Produced With Admixtures Intended To Inhibit Corrosion*, Research Report UHM/CEE/05-05, Department of Civil and Environmental Engineering, University of Hawaii at Manoa.

Pham, P.A., and Newtson, C.M., (2001). *Properties of Concrete Produced With Admixtures Intended To Inhibit Corrosion*, Research Report UHM/CE/01-01, Department of Civil and Environmental Engineering, University of Hawaii at Manoa.

Sharp, J.V., Figg, J.W., and Leeming, M.B., (1988). "The Assessment of Corrosion of the Reinforcement in Marine Concrete by Electrochemical and Other Methods," *Concrete in Marine Environment Proceedings – Second International Conference*, SP-109, American Concrete Institute, pp. 105-125.

Sika Corporation, (1998). "Sika FerroGard 901: Corrosion Inhibiting Admixture," Technical Data Sheet.

Silica Fume Association, (2001). *Life-365 Service Life Prediction Model*, Users' Manual.

Violetta, B., (2002). "Life-365 Service Life Prediction Model," *Concrete International*, vol. 24, issue 12, pp. 53-57.

Xypex Chemical Corporation, (2002). "Xypex Admix C-2000NF," Technical Data Sheet.

Yokota, H., and Buenfeld, N.R., (2004). "Predicting the Life of Reinforced Concrete Structures in Marine Areas," *Proceedings of the 14th International Offshore and Polar Engineering Conference ISOPE-2004*, Vol. 4, pp. 257-262.